DOE/RL/12089-T2

NOAA Technical Memorandum ERL WPL-211

# A FIELD EVALUATION OF REMOTE SENSOR MEASUREMENTS OF WIND, TEMPERATURE, AND MOISTURE FOR ARM INTEGRATED SOUNDING SYSTEM RESEARCH


B.E. Martner
E.R. Westwater
R.G. Strauch
B.B. Stankov
D.B. Wuertz
W.L. Ecklund (*)
K.S. Gage (*)
D.A. Carter (*)
J.B. Snider
J.C. Churnside
J.A. Shaw
K.P. Moran
J.C. Reynolds

Wave Propagation Laboratory
and Aeronomy Laboratory (*)
Boulder, Colorado

October 1991


## DISCLAIMER

This report was prepared as an account of work sponsored by an agency of the United States Government. Neither the United States Government nor any agency thereof, nor any of their employees, makes any warranty, express or implied, or assumes any legal liability or responsibility for the accuracy, completeness, or usefulness of any information, apparatus, product, or process disclosed, or represents that its use would not infringe privately owned rights. Reference herein to any specific commercial product, process, or service by trade name, trademark, manufacturer, or otherwise does not necessarily constitute or imply its endorsement, recommendation, or favoring by the United States Government or any agency thereof. The views and opinions of authors expressed herein do not necessarily state or reflect those of the United States Government or any agency thereof.

MASTER

DISTRIBUTION OF THIS DOCUMENT IS UNLIMITED

## CONTENTS


**ABSTRACT** ..... iv

**1. INTRODUCTION** ..... 1

**2. FIELD OPERATIONS** ..... 2

**3. DATA STATUS** ..... 6

**4. INSTRUMENTATION** ..... 7
- 4.1. Wind Profilers and RASS ..... 7
- 4.2. Microwave Radiometers ..... 15
- 4.3. Infrared Radiometers ..... 15
- 4.4. Ceilometers ..... 17
- 4.5. Fourier-transform InfraRed Sounder ..... 17

**5. REMOTE SENSOR PERFORMANCE** ..... 17
- 5.1. RASS ..... 17
  - 5.1.1. RASS Height Coverage ..... 19
  - 5.1.2. RASS Accuracy ..... 25
- 5.2. Wind Profilers ..... 31
- 5.3. Microwave Radiometers ..... 40

**6. RECOMMENDATIONS FOR ARM CART SITES** ..... 44
- 6.1. Wind Profilers ..... 44
  - 6.1.1. Boundary Layer 915 MHz Wind Profiler ... 44
  - 6.1.2. 50 MHz Wind Profiler ..... 45
- 6.2. RASS ..... 45
- 6.3. Microwave Radiometers and complementary instruments ..... 45
- 6.4. Instrument modeling ..... 47

**ACKNOWLEDGEMENTS** ..... 48

**REFERENCES** ..... 49

**APPENDIX A. FIRS** ..... 53

**APPENDIX B. DATA PRODUCTS FOR SELECTED IOPS** ..... 58
- B.1. IOP#3 - Variable cloudiness ..... 58
- B.2. IOP#4 - Cold frontal rain ..... 77
- B.3. IOP#5 - Clear skies ..... 94

# A FIELD EVALUATION OF REMOTE SENSOR MEASUREMENTS OF WIND, TEMPERATURE, AND MOISTURE FOR ARM INTEGRATED SOUNDING SYSTEM RESEARCH

B.E. Martner, E.R. Westwater, R.G. Strauch, B.B. Stankov, D.B. Wuertz, W.L. Ecklund, K.S. Gage, D.A. Carter, J.B. Snider, J.C. Churnside, J.A. Shaw, K.P. Moran, and J.C. Reynolds

**ABSTRACT.** Remote sensing systems were operated in Colorado in February and March 1991 to obtain detailed profiles of the kinematic and thermodynamic structure of the atmosphere for the U.S. Department of Energy's Atmospheric Radiation Measurement (ARM) research program. The instruments included wind profilers, Radio Acoustic Sounding Systems (RASS), microwave and infrared radiometers, an infrared spectrometer, ceilometers, radiosondes, surface meteorological stations, and other equipment. A mesoscale data assimilation model will be used to combine the data into dynamically consistent four-dimensional fields as part of an integrated data assimilation sounding system.

This report evaluates the performance of the NOAA remote sensors used in the 1991 field data collection. These included five different wind profilers, each equipped with RASS capability for temperature profiling, and microwave radiometers for measurements of path-integrated water vapor and liquid water content. The design and initial testing of a Fourier-transform InfraRed Sounder (FIRS) for humidity profiling is also described. The ranges of height coverage and measurement accuracies for each wind profiler/RASS are examined. Specific recommendations for optimizing the design and configuration of similar instruments are made for the ARM Cloud And Radiation Testbed (CART) sites, based on results of the 1991 field work and earlier tests. Examples of routine processed data products are presented for three intensive operating period studies to further illustrate the remote sensors' capabilities.

# 1. INTRODUCTION

The U.S. Department of Energy's Atmospheric Radiation Measurement (ARM) program seeks to improve general circulation models (GCMs) for predicting global and regional climate changes that will be caused by the increasing concentrations of greenhouse gases in the atmosphere. The program's primary emphasis is on improving radiative transfer aspects of GCMs through a combined measurements and modeling approach. Remote sensing will play a central role in the measurements facet of the program, which will attempt to accurately assess all features of the atmosphere that significantly influence the radiative budget at a few climatically strategic sites (DOE, 1990). Long-term continuous measurements of the atmospheric structure and radiative fluxes will be conducted at these sites, known as Cloud And Radiation Testbeds (CART).

The ARM goals are ambitious and its schedule is demanding. The first CART is scheduled to begin phased-in operations in 1992. Many of the instruments proposed for use in CART operations represent emerging technology and exist only as specialized research prototypes. Therefore, an important preparatory step for ARM was an intensive field project in Colorado in 1991 to assess the suitability and readiness of instruments and techniques for profiling the thermodynamic and kinematic structure of the troposphere and lower stratosphere. The field work was designed to provide ARM with a head start by gathering practical information for the design and operation of the CART sites. Additional longer term research, also fundamental to ARM goals, will use 1991 data to design an optimized combination of diverse profiling instruments and to extrapolate single-site data to dynamically consistent, four-dimensional fields at GCM sub-grid scales using a data assimilation mesoscale model. The result will be an integrated system for atmospheric profiling tailored to ARM's requirements. The research is being conducted by a cooperative partnership that includes the National Oceanic and Atmospheric Administration's (NOAA) Wave Propagation Laboratory (WPL) and Aeronomy Laboratory (AL), the National Center for Atmospheric Research (NCAR), and the University of Wisconsin (UW). An overview of the research plan is given by Dabberdt et al. (1991).

This report summarizes measurements obtained with the NOAA remote sensors during the 1991 field project and evaluates the performance of these instruments. Recommendations for CART instrumentation are presented, based on the results of the field project and the considerable experience of NOAA scientists and engineers with designing and operating these instruments and their predecessors. The research is ongoing and the results are not final, but the urgency of the ARM schedule requires preliminary assessments and recommendations at this time.

The important task of integrating measurements from all the instruments into a cohesive and dynamically consistent, four dimensional data set is an ongoing cooperative endeavor of the

NOAA/NCAR/UW research. The measurements obtained by the ARM Colorado field experiment and related concurrent field projects provide a rich data set for testing the integration techniques.

## 2. FIELD OPERATIONS

The first quarter of 1991 was an extremely active time for atmospheric measurements in the Denver area. As shown in Table 1, four projects were conducted with overlapping schedules and area domains between mid-January and mid-April. This report addresses the research conducted for the ARM Integrated Data Assimilation Sounding System (ARM/IDASS), which is referred to here as ARM-91 for brevity. Most of its instrumentation was located at the WPL Platteville site northeast of Denver, Colorado, with additional instruments at other locations, as shown in Fig. 1.

The ARM-91 field work was conducted during February and March within the more extensive Winter Icing and Storms Project (WISP) experimental area, which is shown in Fig. 2 (Politovich, 1991). Close coordination was maintained between these two projects, and arrangements have been made for exchanging data that may be useful to scientists of both experiments. The second Cloud Lidar and Radar Exploratory Test (CLARET-II) was another ARM project conducted during this period at the WPL Erie-1 site north of Denver. The ARM-91 project focused on thermodynamic and kinematic profiling measurements, whereas CLARET-II emphasized observations of clouds and their radiative effects. In addition, the Atmospheric Studies in COmplex Terrain (ASCOT) program conducted a winter validation field experiment in the Denver area. Together, these projects represented an unprecedented concentration of instrumentation for profiling the structure of the atmosphere.

Many of the instruments in the ARM-91 project, such as the wind profilers and radiometers, were designed to obtain continuous measurements with little or no operator intervention. Others, such as the radiosonde systems, require operator attention and consume expendables; these instruments must be operated in an episodic manner to conserve labor and money. Therefore, ARM-91 operations used a strategy of continuous, unattended operation for some sensors, and short (about 24-36 h) intensive operating periods (IOPs) for all instruments.

ARM-91 conducted full operations for one month beginning on 15 February 1991. Seven IOPs were declared during this period (Table 2). The IOPs included a wide variety of weather, ranging from snow and rain showers to variable cloudiness to clear skies. However, the NOAA remote sensors operated continuously except for down time for maintenance, calibrations, and unscheduled problems. Many of the NOAA instruments were operated from mid-January to mid-April and their data are archived for that entire period. Most

**Table 1.** Field Projects Conducted in Denver Area in Early 1991

**ARM/IDASS "ARM-91"** (Atmospheric Radiation Measurement/Integrated Data Assimilation and Sounding System) research

Purpose: field test an ad-hoc integrated sounding system and evaluate its performance for the design of ARM Cloud And Radiation Testbed (CART) sites

Period: 15FEB91-15MAR91
Area: Platteville site (primarily)
Data Catalog: of NOAA data only, available from NOAA/WPL

**ARM/CLARET-II** (Cloud Lidar And Radar Exploratory Test)

Purpose: obtain measurements of non-precipitating stratiform clouds with combinations of remote sensors and evaluate the clouds' radiational effects

Period: 15FEB91-31MAR91
Area: Erie-1 site
Data Catalog: available from NOAA/WPL

**WISP-91** (Winter Icing & Storms Project)

Purpose: study the meteorological conditions which produce hazardous aircraft icing, and conduct basic research on winter storms

Period: 15JAN91 - 31MAR91
Area: Northern Colorado plains adjacent to the Front Range
Data Catalog: Available from NCAR/RAP

**ASCOT-91** (Atmospheric Studies in COmplex Terrain)

Purpose: study local nocturnal flows from canyons and slopes and transport and dispersion around Rocky Flats

Period: intensive period: 3FEB91-19FEB91
Front Range Air Quality Study: 15JAN91-20APR91
Area: Front Range and plains centered around Rocky Flats
Data Catalog: Available from TRC, Inc.

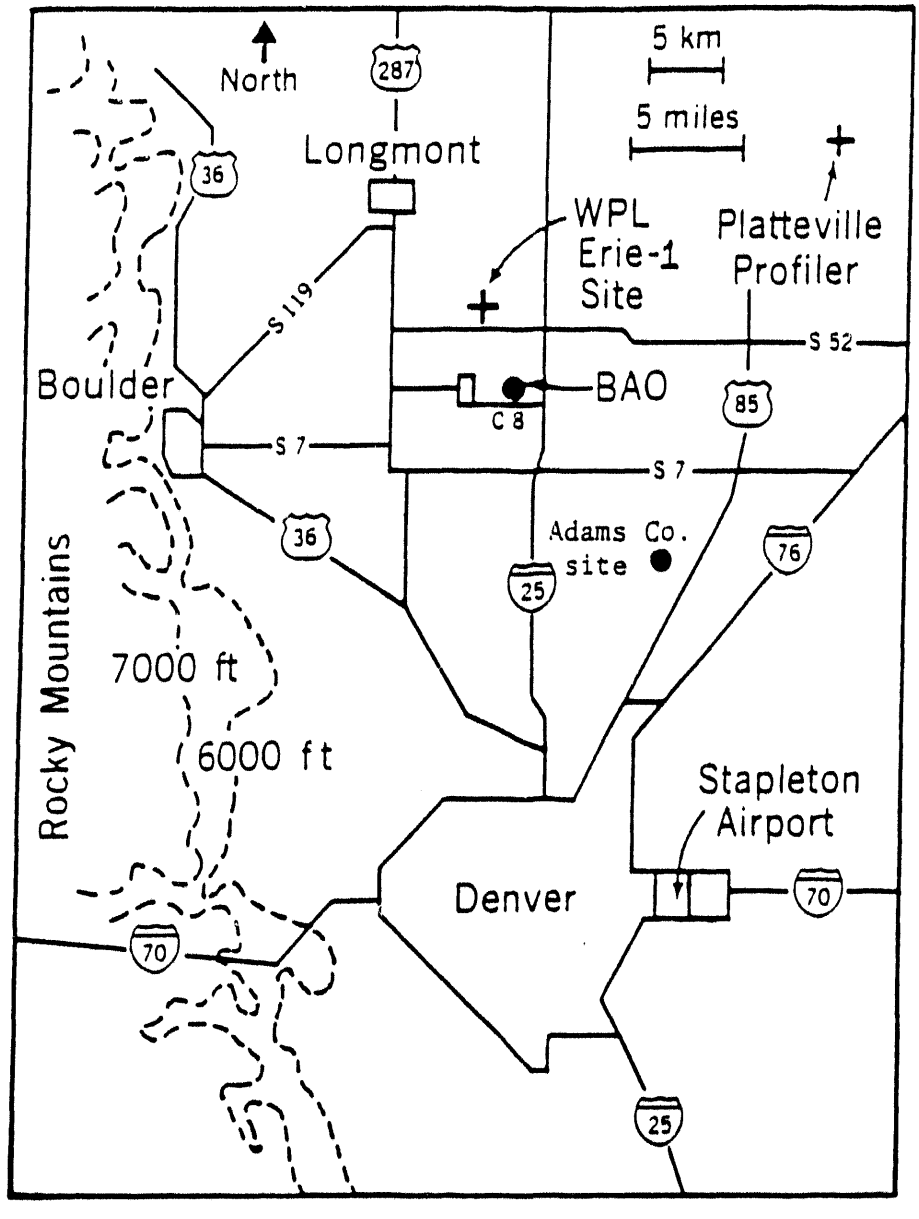


Figure 1. Map of the locations of instrumentation used in the ARM-91 field project. Platteville was the primary site; other instruments were located at Stapleton Airport, Erie-1, and Adams County.

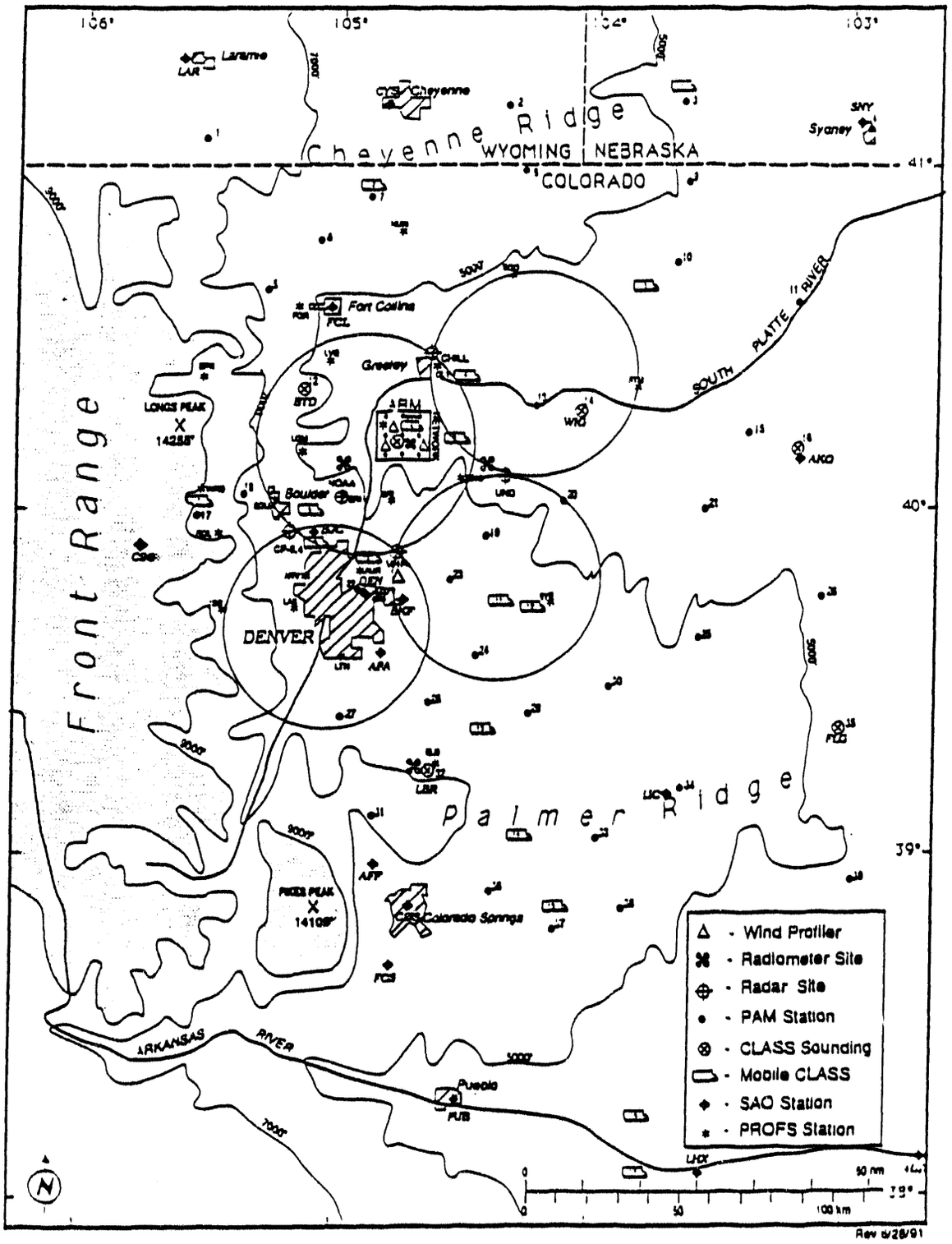


Figure 2. Map of instrumentation used in the WISP-91 field experiment. The concentration of ARM instruments at Platteville is shown by the square box northeast of Denver (courtesy of NCAR Research Applications Program).

data examined in this report are based on the complete period of data collection, not just the IOPs. WPL's routinely processed data products for three of the IOPs are presented in Appendix B.

**Table 2.** ARM-91 Intensive Operating Periods

------- 15 February 1991 - 16 March 1991 -------

1. 17 FEB (1200 GMT) - 19 FEB (0100 GMT)
   variable cloudiness (with WISP)

2. 24 FEB (1200 GMT) - 25 FEB (1300 GMT)
   light snow (with WISP)

3. 28 FEB (0300 GMT) - 1 MAR (0400 GMT)
   clear sky turning to broken and overcast

4. 5 MAR (1800 GMT) - 7 MAR (0100 GMT)
   cold front rain to variable cloudiness (with WISP)

5. 8 MAR (2100 GMT) - 9 MAR (2200 GMT)
   clear sky

6. 11 MAR (2100 GMT) - 12 MAR (2200 GMT)
   cold front showers, then clear (with WISP)

7. 14 MAR (1200 GMT) - 16 MAR (0300 GMT)
   variable low and high clouds (with WISP)

## 3. DATA STATUS

An inventory of measurements obtained with the NOAA instruments in ARM-91 is available from WPL, as is a similar inventory for the CLARET-II experiment. These catalogs document the time periods when data were recorded by each NOAA instrument.

Currently, the data from the NOAA remote sensors are archived locally at WPL and AL. Following the field experiment, various quality checks and post-processing refinements were applied to the data. All WPL wind profiler data were been processed with an automated editing algorithm that recognizes and removes outliers (Wuertz and Weber, 1989). The AL data archive includes Doppler spectra measurements recorded on optical disks. The microwave radiometer data were reprocessed to remove periods when the data were contaminated by the presence of liquid water on the reflector surfaces (Stankov et al., 1991).

The edited data sets are now being provided to NCAR for inclusion in the comprehensive ARM-91 data archive. NCAR scientists will reformat the data and place it on the Mass Storage System of the NCAR Cray computer. Both netCDF and ASCII format versions of the data will then be available, through NCAR, to all participants of ARM and WISP (Martin, 1991).

## 4. INSTRUMENTATION

The primary instruments operated for ARM-91 are listed in Table 3. Together, the instruments represent an ad hoc, integrated data sounding system composed of available research components. It is a prelude to the more extensive and sophisticated CART site systems. This report is concerned with evaluating the performance of the NOAA remote sensors and offering recommendations concerning the design and use of similar instruments at CART sites. Instruments operated by NCAR and UW are not discussed here. ARM-91 was the first experiment where three different frequency wind profilers were operated side by side for comparison. Each of these profilers at Platteville was specially equipped for ARM with Radio Acoustic Sounding System (RASS) capability for measuring profiles of virtual temperature. The data allow the accuracies and ranges of height coverage to be examined for the individual profilers and for combinations of them. Different microwave radiometers were also operated side by side at the Platteville site and the data have provided valuable verification of their measurements. Additional NOAA remote sensors operated at Denver's Stapleton Airport, Erie, Roggens, Adams County, and Elbert also provided useful information for designing an optimum ensemble of instruments for the CART sites.

### 4.1. Wind Profilers and RASS

Wind profilers are Doppler radars designed primarily for measuring winds in the clear atmosphere by using wavelengths longer than those employed by "weather" radars. These profilers are able to sense atmospheric motions by detecting signals backscattered from refractive index perturbations created by turbulence on scales of half of the radar wavelength. These eddies drift with the mean wind speed and their translational velocity therefore provides a direct measure of the wind.

The RASS combines acoustic sources with wind profilers to obtain measurements of the profile of virtual temperature. The wind profiler's Doppler radar measures the speed of refractive index perturbations induced by the acoustic waves (approximately matched with the radar's half-wavelength) as they ascend at the local speed of sound, which is directly related to the virtual temperature at each height.

**Table 3.** Primary Instruments Operated for ARM-91

* = primary systems addressed in this report

**At Platteville:**

* 50 MHz wind profiler (NOAA/WPL)
* +RASS (NOAA/WPL)

* 404 MHz "UNISYS" wind profiler (NOAA/FSL)
* +RASS (NOAA/WPL)

* 915 MHz "boundary layer" wind profiler (NOAA/AL)
* +RASS (NOAA/AL)

* microwave radiometer (NOAA/WPL)

other radiometers (Jet Propulsion Lab)

High resolution Interferometer Sounder (Univ. Wisconsin)

CLASS radiosondes (NCAR/SSSF)

ASTER (NCAR/SSSF)

Doppler sodar (NCAR/SSSF)

PAM surface mesonet stations (NCAR/SSSF)

ceilometer (NWS)

**At Denver Stapleton Airport:**

* 915 MHz wind profiler (NOAA/WPL)
* +RASS (NOAA/WPL)

**At Erie-1 site:**

* 404 MHz RASS system (NOAA/WPL)

**At Adams County:**

* 915 MHz "boundary layer" wind profiler (NOAA/WPL)
* +RASS (NOAA/WPL)

**On-going field work (after WISP/ARM-91):**

- 915 MHz wind profiler/RASS comparisons with BAO tower
- Field tests of Fourier InfraRed Sounder (FIRS)

Balsey and Gage (1982) reviewed design consideration for wind profilers and showed that different frequencies have advantages and limitations. Thus, a combination of profilers using different frequencies may be required to maximize the availability of wind and temperature profile data for a wide range of heights and conditions. ARM-91 used three different frequencies to obtain overlapping height coverage and differing vertical resolutions. These included a VHF system of 50 MHz ($\lambda$ = 6.0 m), and UHF systems of 404 MHz (75 cm) and 915 MHz (33 cm).

WPL operated wind profiler systems equipped with RASS at Platteville, Denver's Stapleton Airport, and Erie. The basic characteristics and operating parameters for these systems are shown in Tables 4-7. One of the systems was a NOAA Wind Profiler Demonstration unit manufactured by Unisys, Inc., and operated by the NOAA Forecast Systems Laboratory (FSL) as part of a 31-station network emerging across the central United States. WPL added RASS capability to this profiler for the ARM research. For each of these systems, the speed of the RASS acoustic waves and the vertical wind were not simultaneously measured.

The Aeronomy Laboratory installed and operated a small 915 MHz "boundary layer" wind profiler (Ecklund et al., 1988) at Platteville and equipped it with RASS capability. This profiler used a fixed beam flat microstrip antenna (approximately 2 m x 2 m) on a mechanical positioner. Basic parameters for this system are given in Table 8. The profiler used a single height resolution of 100 m for ARM-91, although resolutions of 60 m have also been used on this profiler. In addition to the winter observations, the same system was used for summertime observations at Platteville.

The AL boundary layer profiler was operated with new software which switches between wind and temperature profiling and uses a new RASS technique. This technique, described by Angevine et al. (1991), uses a 2048 point Fast Fourier Transform to measure both the acoustically generated signals at the local speed of sound as well as the simultaneous vertical wind speed. This allowed the observed sound speed to be corrected by the observed vertical wind speed. This correction reduces the variance in the derived temperatures. In addition to recording two averaged wind and temperature profiles per hour, all of the basic 30-s average Doppler spectra for each height were recorded on optical disk. The spectra are useful for post-processing refinement of the wind and temperature measurements and for examination of other parameters such as signal-to-noise profiles and hydrometeor fall-speed profiles.

**Table 4.** 50 MHz Wind Profiler/RASS at Platteville

System Characteristics

**Wind Profiler:**

Frequency: 49.82 MHz (VHF)

Wavelength: 6.0 m

Antenna size: 10,000 $m^2$

Beamwidth (1 way): 3°

Mean power: 200 W

Sampling time (1 profile): 1 min

**RASS:**

Acoustic frequency: 110 Hz

Beamwidth (1 way): 60°

Acoustic power: 2400 W (total electrical input)

Operating parameters for ARM-91

| | Recorded Observations | No. of Profiles Averaged | Typical Range (AGL) | Resolution |
|---|---|---|---|---|
| horizontal winds | 1 per hour | 12 | 1.8 - 8.4 km<br>& 4.2 - 17.3 km | 300 m<br>870 m |
| vertical winds | 1 per hour | 12 | 1.85-12.7 km | 350 m |
| virtual temperature | 1 per hour | 6 | 2 - 6 km | 300 m |

**Table 5.** 404 MHz Wind Profiler/RASS at Platteville

The 404 MHz Unisys wind profiler at Platteville is one of the NOAA Demonstration Network profiling radars which are being installed at 31 locations across the central United States. The wind data are processed and archived by the NOAA Forecast Systems Laboratory. The NOAA Wave Propagation Laboratory added RASS capability to this wind profiler for the ARM-91 project.

System Characteristics

**Wind Profiler:**

Frequency: 404 MHz (VHF)

Wavelength: 0.74 m

Antenna size: 170 $m^2$

Beamwidth (1 way): 4°

Mean power: 2220 W

Sampling time (1 profile): 1 min

**RASS:**

Acoustic frequency: 900 Hz

Beamwidth (1 way): 18°

Acoustic power: 125 W (total electrical input)

Operating parameters during ARM-91

| | Recorded Observations | Profiles Averaged | Typical Range (AGL) | Resolution |
|---|---|---|---|---|
| horizontal winds | 1 per hour | 12 | 0.5 - 16.5 km | 250 m |
| virtual temperature | 2 per hour | 1 | 0.5 - 3.5 km | 250 m |

**Table 6.** 404 MHz Wind Profiler/RASS At Erie-1

WPL operated a 404 MHz RASS system at the Erie-1 site to obtain profiles of virtual temperature. Horizontal winds were not measured with this system which only used a vertical beam. This research system is much less sensitive than the NOAA Demonstration Network 404 MHz systems such as the one at Platteville.

System Characteristics

**Wind Profiler:**

Frequency: 404.37 MHz (UHF)

Wavelength: 0.74 cm

Antenna size: 57 $m^2$

Beamwidth (1 way): 6°

Mean power: 45 W

Sampling time (1 profile): 30 s

**RASS:**

Acoustic freq.: 900 Hz

Beamwidth (1 way): 19°

Acoustic power: 125 W (total electrical input)

Operating parameters for ARM-91

| | Recorded Observations | No. of Profiles Averaged | Typical Range (AGL) | Resolution |
|---|---|---|---|---|
| virtual temperature and vertical wind | 1 per 3 hours | 6 | 0.4-2.5 km | 200 m |
| | 1 per hour for special events | 2 | | |

**Table 7.** 915 MHz Wind Profiler/RASS at Denver Stapleton Airport

WPL continued its long-term operation of a high power 915 MHz wind profiler with RASS capability at Stapleton Airport for ARM-91. This system uses a more powerful transmitter, and a larger and different style antenna than is employed in the "boundary layer" 915 MHz profilers, such as the one operated at Platteville by the AL. It therefore produces wind and virtual temperature profiles which extend to greater heights than the boundary layer profiler, but the minimum measurement height is also higher.

System Characteristics

**Wind Profiler:**

Frequency: 915 MHz (UHF)

Wavelength: 0.33 m

Antenna size: 100 $m^2$

Beamwidth (1 way): 2°

Mean power: 145 W

Sampling time (1 profile): 1 min

**RASS:**

Acoustic frequency: 2000 Hz

Beamwidth (1 way): 8°

Acoustic power: 200 W (total electrical input)

Operating parameters for ARM

| | Recorded Observations | No. of Profiles Averaged | Typical Range (AGL) | Resolution |
|---|---|---|---|---|
| horizontal & vertical winds | 3 per hour | 12 | 0.3-6.5 km | 200 m |
| virtual temperature | 1 per hour, 3/hr for special events | 6 | 0.3-1.5 km | 150 m |

**Table 8.** 915 Mhz Wind Profiler/RASS at Platteville

The NOAA Aeronomy Laboratory installed and operated a small 915 MHz "boundary layer" wind profiler with RASS capability at Platteville for ARM-91. The 915 MHz profiler was operated with a new software program which switches between wind profiling and temperature profiling and use a new RASS technique. The new RASS method uses a 2048 point Fast Fourier Transform to observe both the acoustically generated signals at the local speed of sound as well as the simultaneous vertical wind speed in the same volume.

System Characteristics

| **Wind Profiler:** | **RASS:** |
|---|---|
| Frequency: 915 MHz (UHF) | Acoustic Freq.: 2000 Hz |
| Wavelength: 0.33 m | Acoustic power: 50 W (total electrical input) |
| Antenna Size: 4 $m^2$ | |
| Beamwidth (1 way): 9° | |
| Mean Power: 7 W | |
| Sampling time (1 profile): 30 s | |
| Spectral points: 64 (winds), 2048 (temperature) | |

Operating Parameters for ARM-91

| | |
|---|---|
| sampling vertical spacing: | 100 m |
| horizontal & vertical winds: | 2 profiles per hour from 25 minute consensus (30 s spectra recorded) |
| temperature: | 2 profiles per hour from 5 minute consensus |

## 4.2. Microwave Radiometers

WPL operated three dual-channel microwave radiometers during the ARM-91 and WISP-91 experiments. The dual-channel instruments, located at Platteville, Denver, and Elbert measure downwelling radiation in the zenith-direction at 20.6 and 31.65 GHz. The emission at 20.6 GHz is more sensitive to water vapor; the emission at 31.65 GHz is more sensitive to cloud liquid water. From a simple retrieval algorithm, precipitable water vapor (PWV) and integrated cloud liquid water (CLW) are derived (Hogg et al., 1983). Similar radiometers of independent design were also operated at Platteville during ARM-91 by the Jet Propulsion Laboratory (Keihm, 1991).

The WPL radiometers operated continuously during the period 15 January to 31 March, and provided high-quality data, except for occasional periods they suffered performance degradations from melting snow and ice on the reflector surfaces. Data presented in this report have been edited to remove these effects. In addition, data missing because of communication outages were transferred from backup recorders at the field sites to the WPL central data base.

The microwave receivers are enclosed in shelters whose internal temperatures are strictly controlled. The offset paraboloid antennas of the radiometers view, through a window that is nearly transparent to microwave radiation, a flat reflector located outside the instrument shelter. This reflector is oriented at 45° and thus reflects zenith radiation onto the offset paraboloid. A schematic view of the radiometer antenna arrangement is shown in Fig. 3. The major characteristics of the dual-channel radiometer are given in Table 9.

WPL also operated a three-channel steerable instrument at Roggins (15 January to 13 February) and at Erie (18 February to 2 April) for the WISP and CLARET-II experiments. The characteristics of this instrument are similar to those given in Table 9, except that it also has a 90 GHz channel for more accurate measurement of small amounts of liquid. At Roggins, the instrument was operated in the zenith-viewing mode. Much of the time at Erie, the radiometer scanned in synchronization with a WPL dual-wavelength radar system (Martner et al., 1991).

## 4.3. Infrared Radiometers

Two infrared radiometers were operated by WPL during the experiment: one at Denver and one at Elbert. The instruments use Barnes PRT-5 systems with custom optical filters (9.95-11.43 $\mu$m) and 2° fields of view (Shaw, 1991). These instruments have been a very reliable source of information about clouds, and, when supplemented by microwave radiometers, they can measure cloud-base temperature of optically thick liquid-bearing clouds to within 1°C.

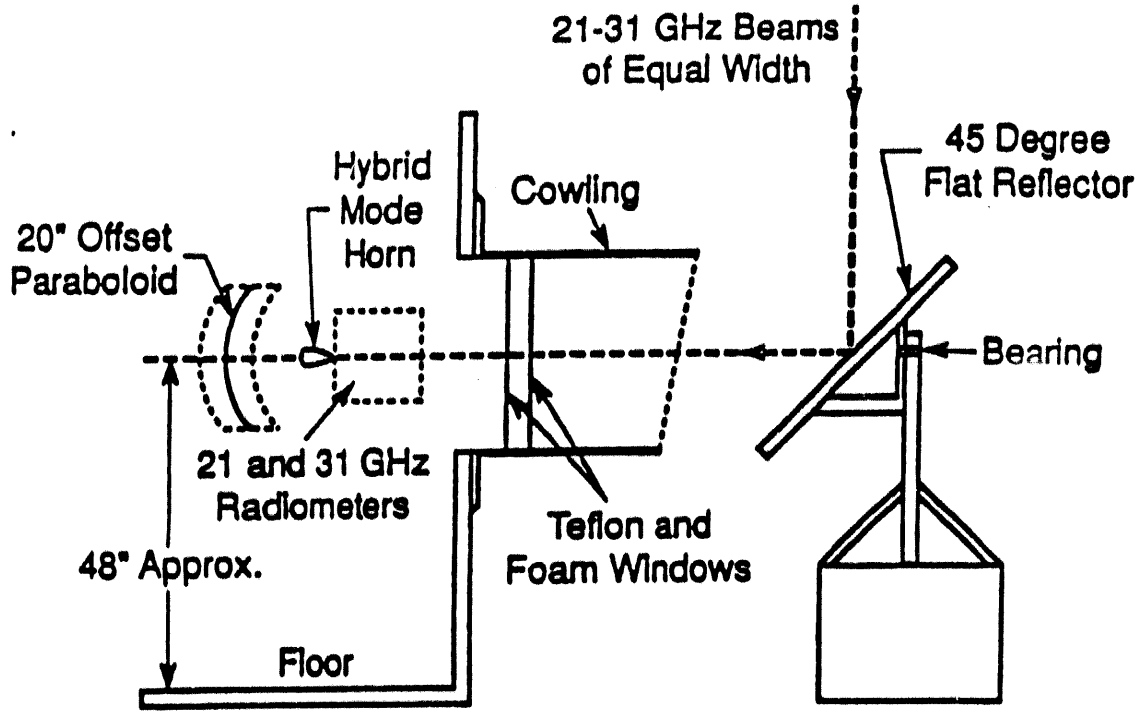


Figure 3. Schematic of WPL dual-channel microwave radiometers.

**Table 9.** Characteristics of WPL Dual-channel Radiometers

| | |
|---|---|
| Operating frequencies (wavelengths) | 20.6 and 31.65 GHz (1.46 and 0.95 cm) |
| Viewing | Zenith |
| Antenna half-power beam width | 2.5° (Denver)<br>5.0° (Platteville, Erie) |
| Total bandwidth (double side band) | 1 GHz |
| Integration time | 2 min |
| Radiometric sensitivity (for 2-min integration time) | 0.05 K, rms |
| Estimated absolute radiometric accuracy | 0.75 K |

### 4.4 Ceilometers

The National Weather Service (NWS) routinely operates a lidar ceilometer at Denver; a similar instrument was operated at Platteville for ARM-91 from 15 February to 31 March. This instrument provides cloud base height every 30 s with an accuracy of about 50 m up to an altitude of 3.7 km. Joint operation of the ceilometer and infrared radiometer at Denver has shown excellent agreement between the instruments, except when the radiometer senses clouds that are above the operating range of the lidar ceilometer.

### 4.5. Fourier Transform Infrared Sounder (FIRS)

Remote sensing of humidity profiles has proven to be a very difficult problem. One promising new technique for this task uses infrared spectrometers. These instruments obtain highly resolved measurements of atmospheric emissions across the infrared spectrum and convert these using retrieval techniques to render profiles of temperature, water vapor, and other gases. One such instrument, the High-resolution Interferometer Sounder (HIS), was operated by UW at Platteville during ARM-91. A similar instrument, called a Fourier-transform InfraRed Sounder (FIRS) is being developed for ARM by WPL. Its design is described in detail in Appendix A, and its field performance will be reported in the future.

## 5. REMOTE SENSOR PERFORMANCE

Evaluating the performance of the research-grade remote sensors used in ARM-91 basically involves assessments of accuracies and height coverage, rather than studies of factors such as mean time between failures (which are more appropriate for operational systems). For some of the sensors, such as most of the wind profilers and microwave radiometers, earlier tests and several years of research operations have established this kind of performance information with confidence. For others, such as the UHF RASS, these are some of the first extensive assessments. A special effort is made in this section to combine and summarize performance information of earlier studies and the ARM-91 results.

### 5.1. RASS

As described in the previous section, WPL operated four RASS and the Aeronomy Laboratory operated one during the ARM-91 field experiment. The RASS principles are well understood (May et al., 1990) and the technique used to implement RASS on wind profiler radars has been described previously (Strauch et al., 1988). Implementation of RASS on the NOAA wind profiler demonstration network radars has been successfully demonstrated (Moran et al.,

1991b) and the accuracy of RASS has been established by comparisons with radiosondes (May et al., 1989).

For this experiment the WPL RASS systems used the offset frequency method that allows the profiler radar to observe the Doppler shift of the speed of sound ($C_s$) near 320 m $s^{-1}$, but while doing so, it cannot also measure the vertical wind (w) near zero velocity. Thus, simultaneous measurements of the speed of sound and vertical wind were not possible. Therefore, in the analysis of the RASS data, the effect of vertical wind has been neglected. After the experiment, the WPL research radars at Platteville (50 MHz), Erie (404 MHz), and Stapleton (915 MHz - high power) were all equipped with new PC-based data systems, developed by the Aeronomy Laboratory, that allow simultaneous measurement of $C_s$ and w. The processors do this by performing 2048-point Fourier transforms over a Nyquist velocity interval of about ± 400 m $s^{-1}$, as explained by Angevine et al. (1991). This enables the radar to measure the spectra of both signals with good frequency resolution. Therefore, the effects of vertical wind can henceforth be corrected for in the WPL RASS signals. It was found previously (May et al., 1989) that the largest RASS errors occurred with vertical winds associated with gravity waves. The major limitation with the new PC system is that it can handle only 14 heights, a limitation that can be removed with digital signal processing (DSP) boards with more memory. As a result of successful test demonstrations, including the ARM-91 experiment, RASS capability will be added in 1992 to the NOAA Demonstration Network profiler at Platteville by the manufacturer, Unisys, Inc. Although the technique used will be different from the long transform method, the result should be the same: both $C_s$ and w can be measured simultaneously with good resolution.

The vertical wind correction can sometimes be made by using the vertical wind measurements made before and after the RASS measurements. However, the 915 MHz and 404 MHz RASS are lower tropospheric measurement systems where complex boundary layer flows usually require simultaneous measurements. In contrast, RASS measurements at 50 MHz extend well above the boundary layer and, when gravity waves with periods longer than the observation time of the radar are observed, the vertical wind correction can be made with the nearest measurement in time.

The correction required for vertical wind implies that RASS measurements are limited during precipitation to nonconvective situations. The reason for this is that the radar reflectivity of precipitation particles dominates clear air radar reflectivity for UHF frequencies, so the observed mean vertical Doppler velocity is the mean fall speed of the particles. This can vary from less than 1 m $s^{-1}$ (snow and light rain) to greater than 7 m $s^{-1}$ in heavy rain and even higher velocities in hail. Thus, any automated vertical velocity correction scheme must be able to recognize when precipitation echoes are present so that the

vertical correction is not used. The vertical wind must then be assumed to be zero, which restricts UHF RASS to nonconvective precipitation. Although the 50 MHz profilers do not always observe rain echoes, care must also be used in precipitation because these radars can detect rain in some cases.

### 5.1.1. RASS height coverage

Of particular interest to instrument designers is the altitude coverage of the various RASS systems. We examined the height coverage during ARM-91 for all five RASS, and the results are consistent with those obtained in preliminary studies in 1988 (May et al., 1989). Temperature height coverage statistics for each system from the present experiment are shown in Fig. 4.

For the 50 MHz system, coverage started about 2.1 km above ground level (AGL) and extended to above 6 km, where data were reported about 50% of the time. With this system the height coverage is determined primarily by the horizontal winds (which advect the acoustic waves away from the antenna), the size of the vertically pointing radar antenna (100 m x 100 m), and the placement of the acoustic sources, shown in Fig. 5.

Figure 4 also shows the NOAA network 404 MHz (Unisys) RASS height coverage for February and March 1991. The first measurement height is 500 m AGL (the same as for wind measurements), and the coverage extends to about 3.5 km at 50% availability. Note that this radar was inoperative for about 2 weeks during the experiment; the height statistics are computed for those times the radar was operating. For this radar, acoustic attenuation can be a significant limitation. Therefore, somewhat higher coverage is expected in seasons and locations where acoustic attenuation is reduced by higher humidities. Nonetheless, the results have been favorable enough to prompt the installation of RASS on five network profilers by the end of 1992. One will be at Platteville and two in the central United States, probably in Oklahoma or Kansas. Perhaps the greatest limitation with this radar is the lack of a high-resolution boundary layer mode. The best height resolution is about 350 m, which is too coarse to resolve many temperature inversions.

Figure 4 also shows RASS results for another 404 MHz WPL research profiler at Erie, whose sensitivity is about 20 dB less than the NOAA network profiler. In this case, RASS data start about 400 m AGL and extend to about 2 km half of the time. The height resolution used was 200 m, but the radar is capable of 100 m resolution. Note the fall-off in coverage for the first height, which is caused by radar recovery time.

The "high-power" 915 MHz RASS at Denver's Stapleton Airport had height coverage that is also shown in Figure 4. Here the minimum height is about 200 m AGL, with coverage to about 1.5 km

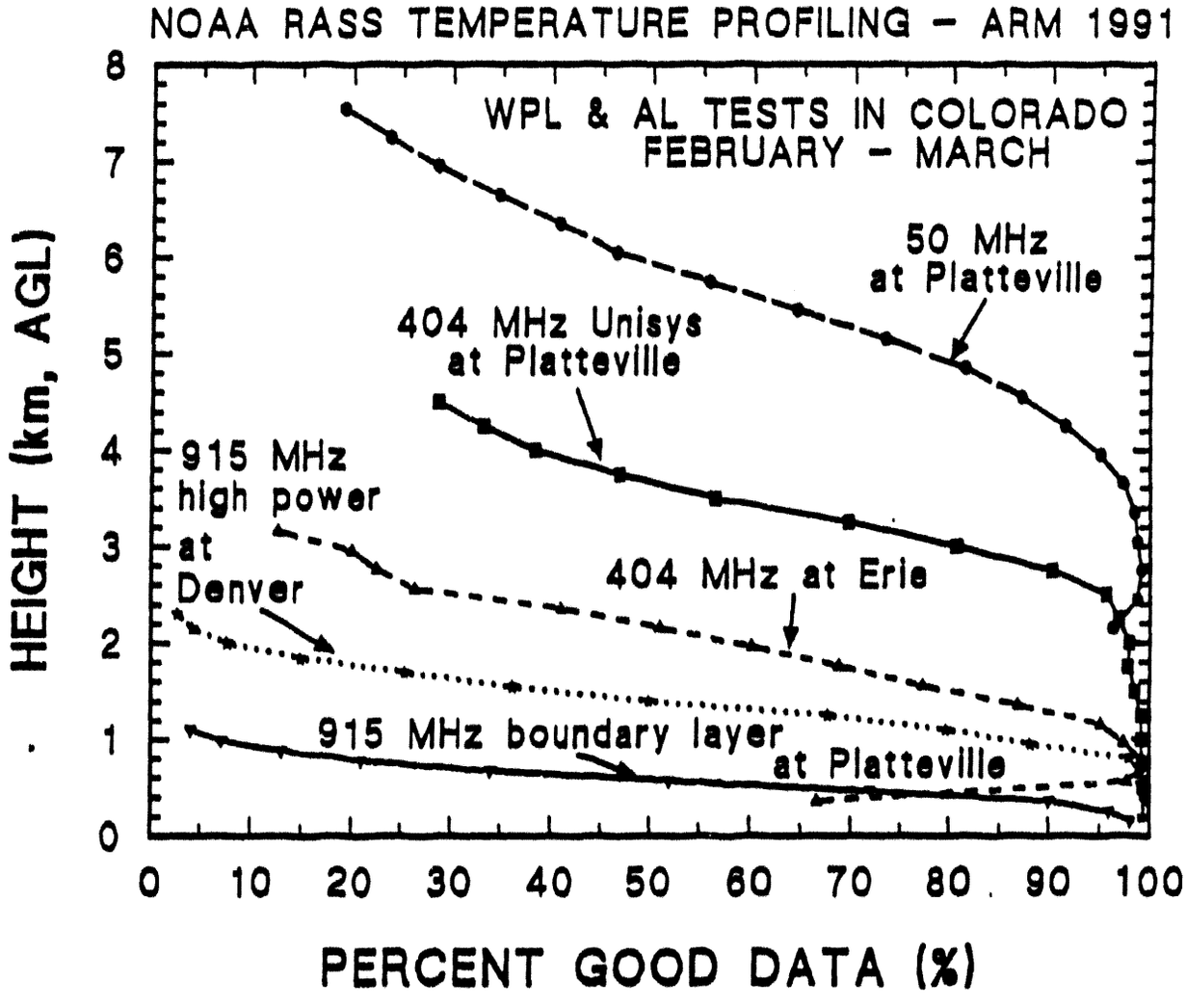


Figure 4. Height coverage statistics for temperature measurements obtained with five RASS operated by NOAA in Colorado during ARM-91. The curves show the percent of time that the measurements extended to the indicated heights.

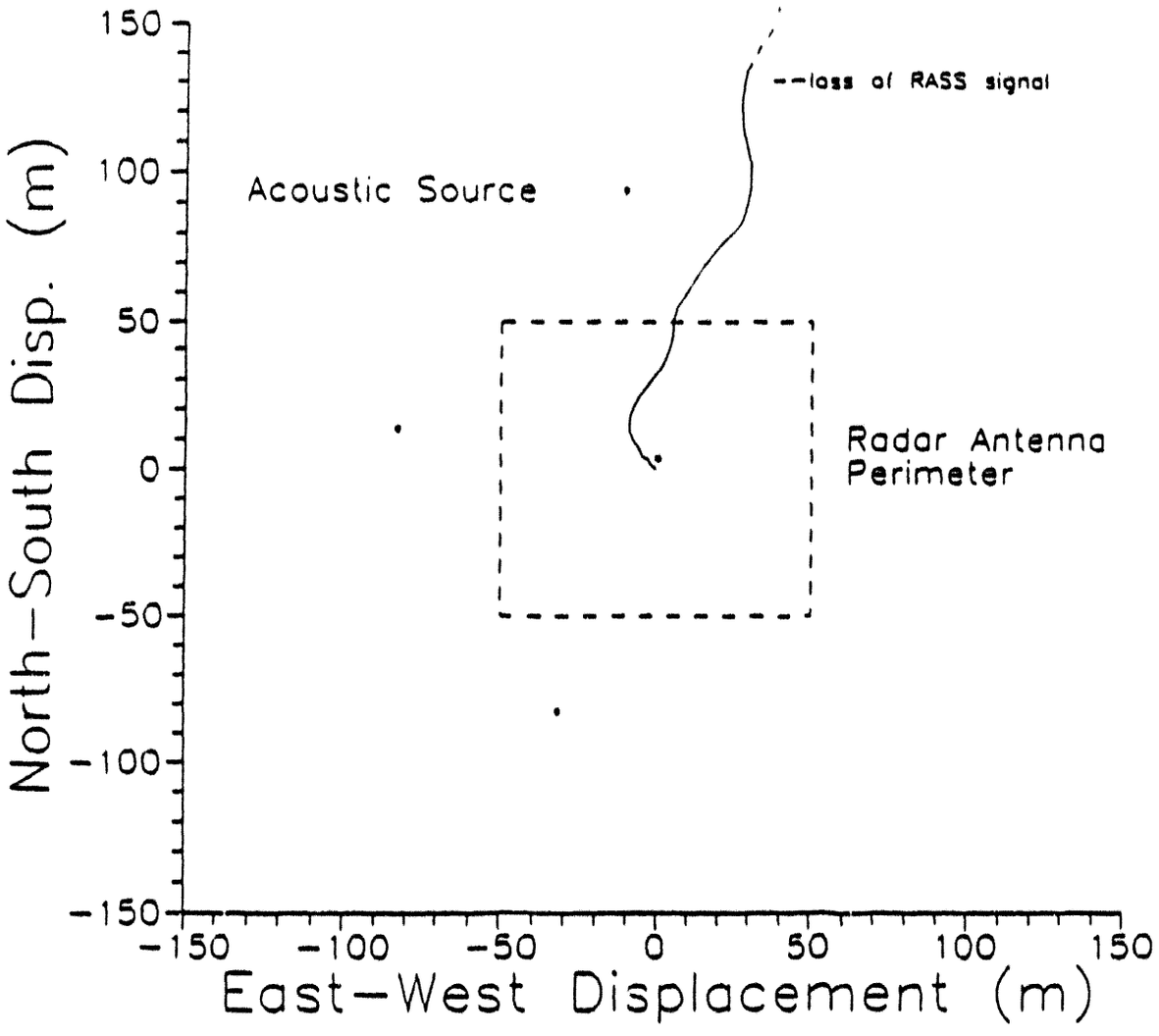


Figure 5. Location of acoustic sources (*) for the 50 MHz RASS. Solid line shows the optimum location for an acoustic source as a function of height for a measured profile of northeasterly winds. Height increases outward from the antenna along the line. Signal loss occurs when no fixed source is within one radar antenna radius of optimum source location.

AGL about 50% of the time. Height resolution was 150 m, although the radar can be operated with 100 m resolution or better. This 915 MHz system should not be confused with the much smaller "boundary layer" systems of the same frequency that are now becoming available commercially. The Stapleton 915 system has a much larger antenna (100 $m^2$ versus about 4 $m^2$), and much greater transmitted average power (145 W versus about 10 W) than the boundary layer systems such as the one operated at Platteville by the Aeronomy Laboratory. Nevertheless, the RASS height coverage is not greatly different for the two systems. This is because acoustic attenuation, which is typically 20 dB $km^{-1}$, and can be as great as 45 dB $km^{-1}$ in very dry conditions, often dominates other height-limiting factors at this frequency.

The Aeronomy Laboratory's boundary layer 915 MHz profiler RASS coverage was severely limited by acoustic attenuation and strong low-level winds during ARM-91. Most often temperature data were obtained only to about 0.5 or 0.6 km AGL with occasional coverage extending to about 1.0 km (Fig. 4). The height coverage could have been improved by a better deployment of the acoustic sources with regard to positions and increased drive power to the speakers. Height coverage in summer conditions at Platteville was substantially better than during the winter ARM-91 experiment (Fig. 6).

The acoustic sources for all of the UHF RASS were similar: four or five acoustic transducers located around the radar antenna (about one antenna diameter from the center) with one source located northwest (the typical upwind direction) of the radar antenna by about one radar antenna diameter from the edge. Each acoustic source was excited with about 25 W electrical input (near 900 Hz for the 405 MHz profilers) or 40 W (near 2 kHz for WPL 915 MHz profiler). The four acoustic transducers used for the 50 MHz RASS (shown in Fig. 5) each had 600 W electrical input near 100 Hz. The AL 915 MHz RASS sound source consisted of four speakers equally spaced around the antenna perimeter; all were driven by a single amplifier with 50 W total electrical output. The audio modulation was generated by a DSP card installed in the PC-based profiler. The modulation consisted of 25 ms sine wave segments randomly switched in frequency (phase continuous) over the required frequency range near 2000 Hz.

Figure 7 summarizes the height coverage statistics for all five RASS operated during ARM-91. Regions of height overlaps and gaps for different combinations of RASS are easy to examine in this diagram. As previously discussed, the upper height limits are primarily determined by strong winds aloft for the 50 MHz system and by acoustic attenuation for the higher frequency systems. From this diagram we note that the usual temperature coverage which could be obtained with a combined 915/50 MHz RASS would extend from about 0.2 to 6.0 km AGL (and even higher in light winds). However, there would also usually be a data gap

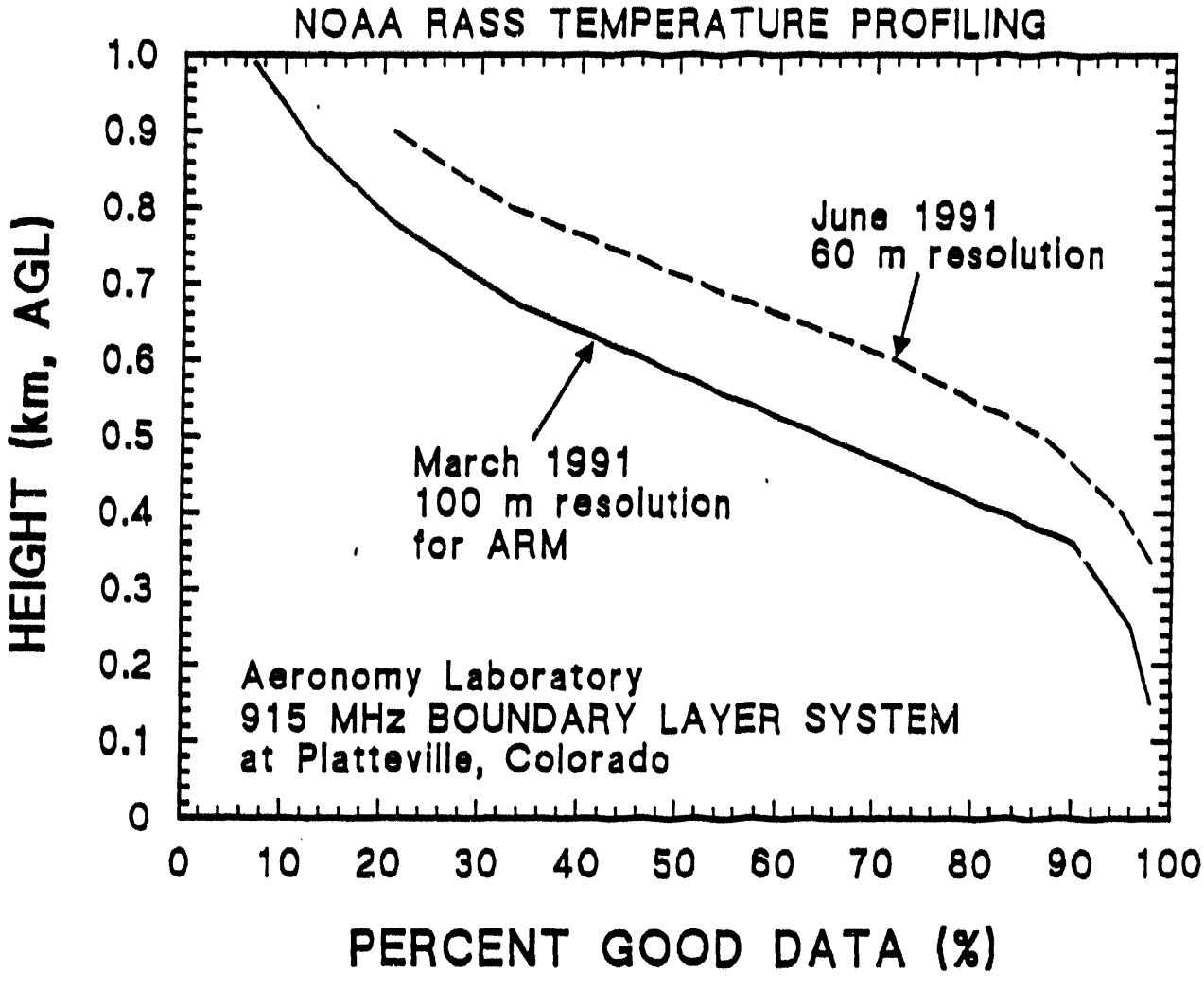


Figure 6. Height coverage statistics for temperature measurements obtained with the AL boundary layer 915 MHz RASS in winter (solid line) for ARM-91 and in summer (dashed line).

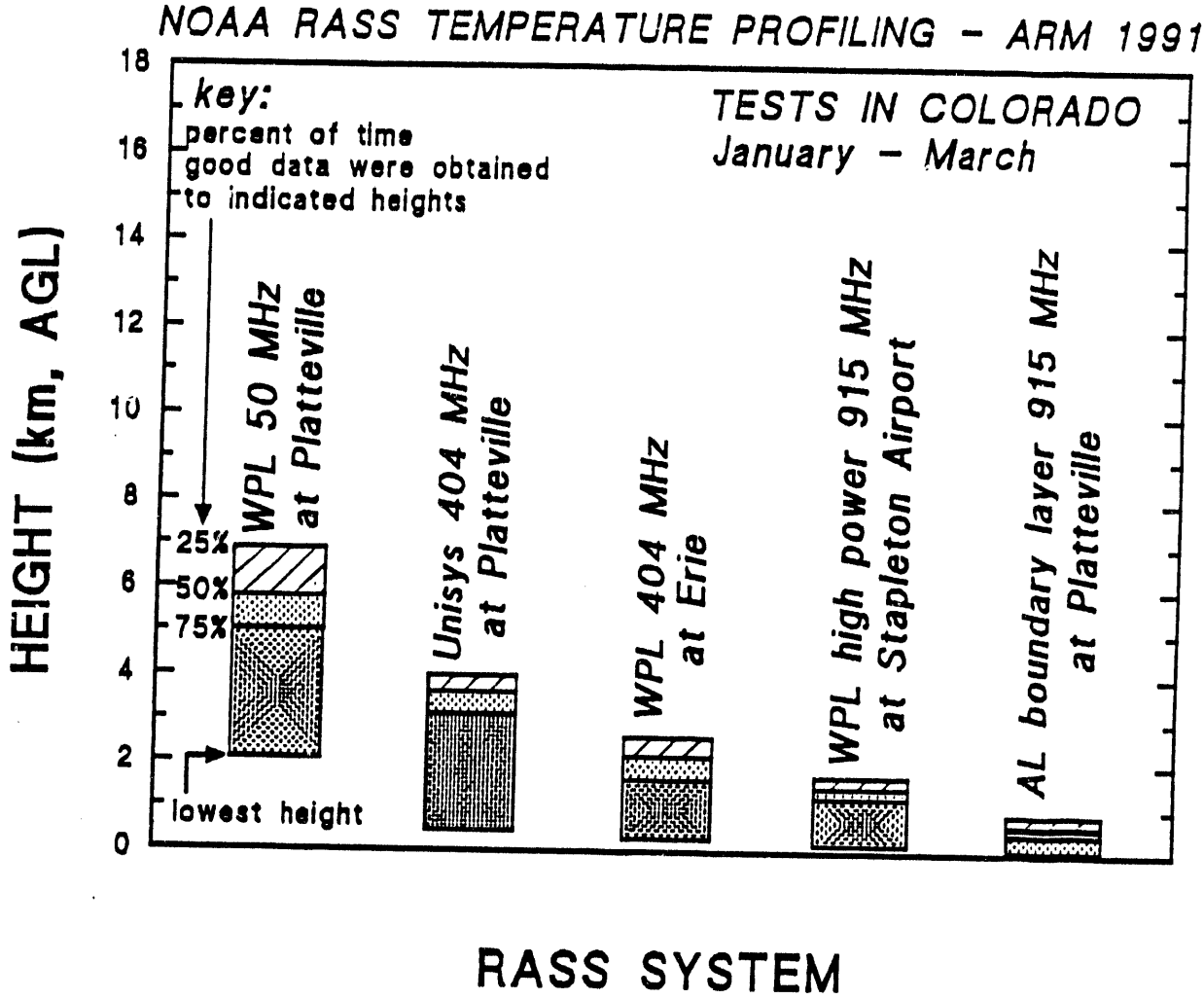


Figure 7. Summary of height coverage statistics of temperature measurements obtained in ARM-91 with five RASS operated by NOAA in Colorado. For comparison purposes, the vertical scale is the same as that used in Fig. 16 for wind data.

from about 0.7 to 2.1 km for this combination. It may be possible to reduce or eliminate this gap by lowering the 2.1 km minimum height of the 50 MHz system with a bistatic antenna configuration. A separate receiving antenna would eliminate the need for a T/R switch with its associated transients, would be much less susceptible to transient ringing on the large antenna, and would be less likely to saturate from nearby ground clutter echoes. This idea will be tested at Platteville. It should also be noted that other researchers have succeeded in reducing the minimum height of a VHF system to below 1 km using a small (10 m x 10 m) antenna (Crochet et al., 1991).

### 5.1.2. RASS accuracy

Figure 8 shows a comparison of simultaneous virtual temperature profiles measured by various RASS systems with radiosonde data from the ARM-91 experiment. The impressive agreement is reiterated in additional similar plots from the ARM-91 IOPs shown in Appendix B.

May et al. (1989) conducted detailed comparisons of RASS virtual temperature measurements with radiosondes using the 915 MHz profiler at Denver's Stapleton Airport. RMS differences of about 1°C were obtained during a variety of meteorological conditions. Figure 9 shows data from this study. Of particular note are the lines of data points showing temperatures too warm and too cold. These outliers were primarily from two comparisons made when significant vertical wind was present (as verified by profiler's vertical wind measurements). Even without the vertical wind correction the RMS difference was about 1°C; data obtained when vertical wind was negligible showed a much lower RMS difference. When the vertical wind correction is made we expect RMS differences between RASS and radiosonde to be about 0.5°C. This is similar to the RMS temperature differences between radiosondes themselves (Hoehne, 1980).

Figure 10 shows a comparison between the virtual temperature measured with a 404 MHz and a 50 MHz RASS. The offset of the best fit line indicates that the height calibration of one (or both) of the systems was incorrect. The 404 MHz radar has been calibrated using a delay line and its calibration should be accurate to within 60 m. The mean and RMS differences (after correction for the height offset) are shown in Fig. 11. In both figures, data from the lowest height of the 50 MHz system may have greater errors because of the radar recovery time. RMS differences of about 0.5°C are observed. Figure 12 shows a comparison of the 404 MHz network profiler with 12 Cross-chain Loran Atmospheric Sounding System (CLASS) radiosondes launched by NCAR on 15 March 1991 during an ARM IOP. With no height correction, the RMS difference in the two instruments is 0.9°C. There appears to be a bias at the coldest measurement points;

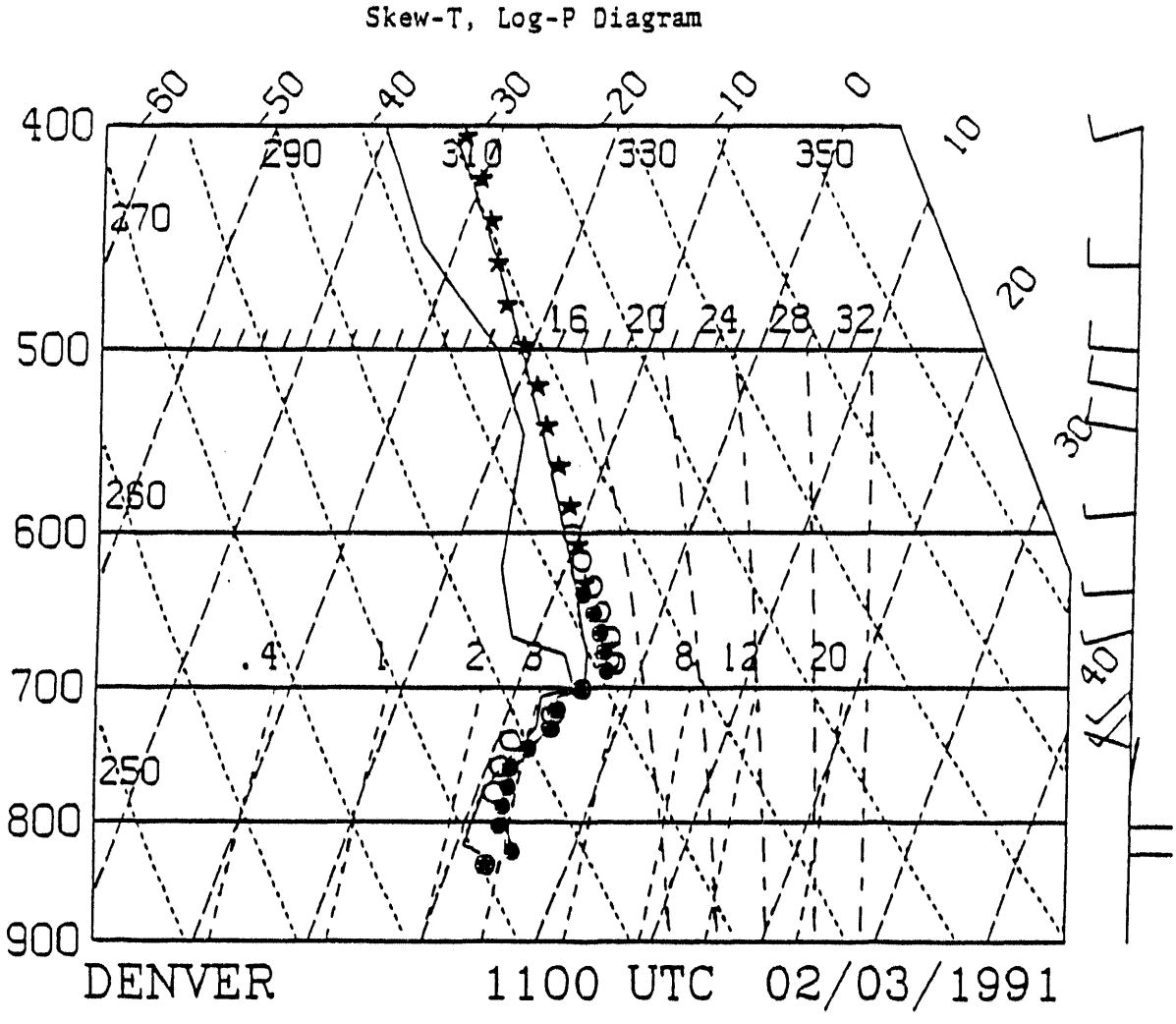


Figure 8. Example comparison of temperature profiles measured by various RASS (points) with NWS radiosonde temperature and dew point profiles (solid lines).

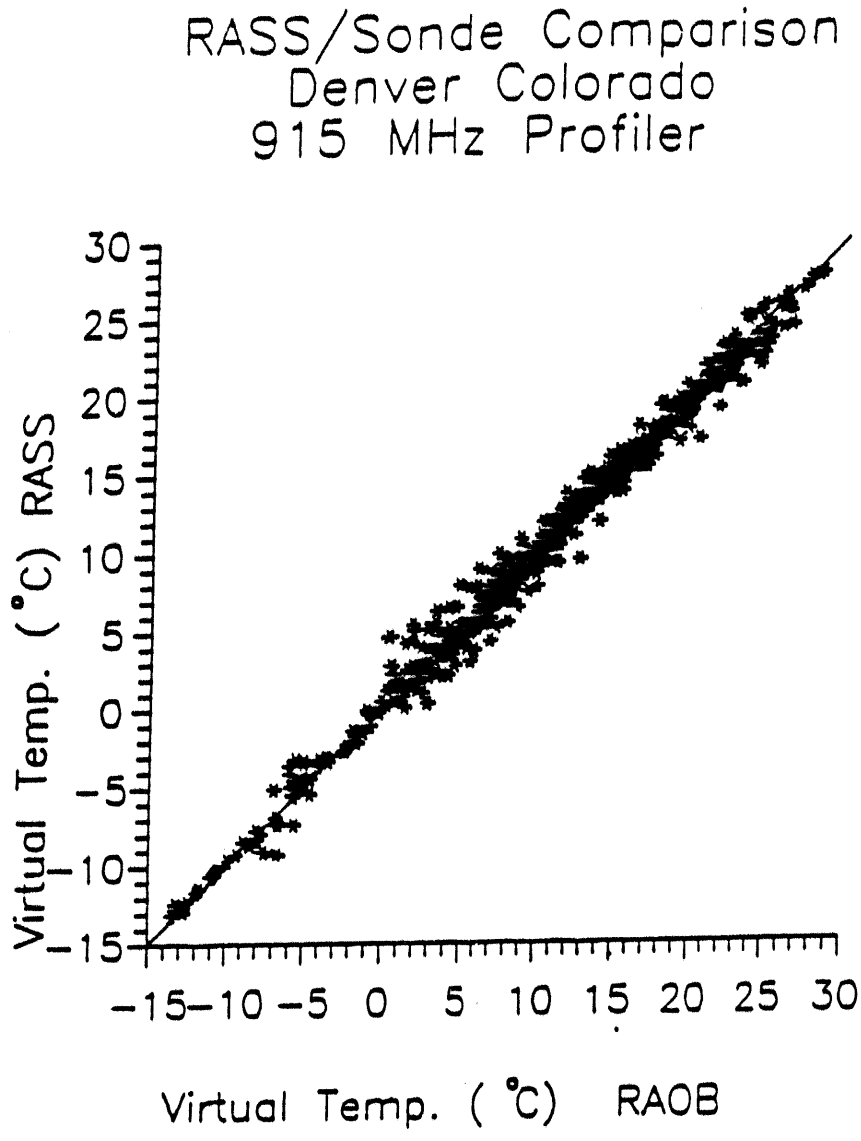


Figure 9. Virtual temperatures measured by radiosondes and by RASS using the Denver 915 MHz wind profiler. The results of about 50 soundings are included in this figure with an overall RMS difference of about 1.0°C.

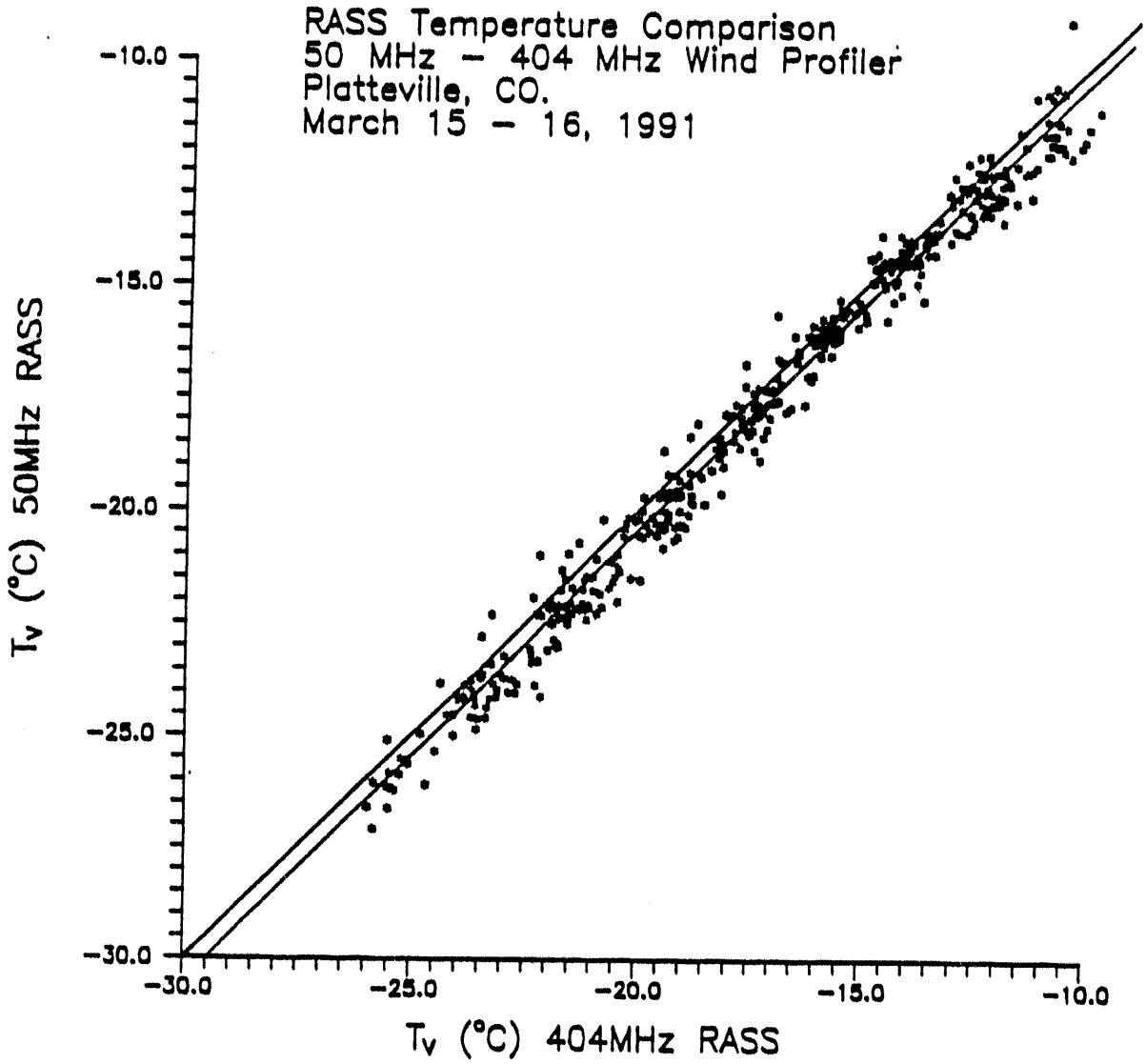


Figure 10. Virtual temperatures measured by 50 MHz RASS and 404 MHz RASS. Measurements are compared at nearest height and time.

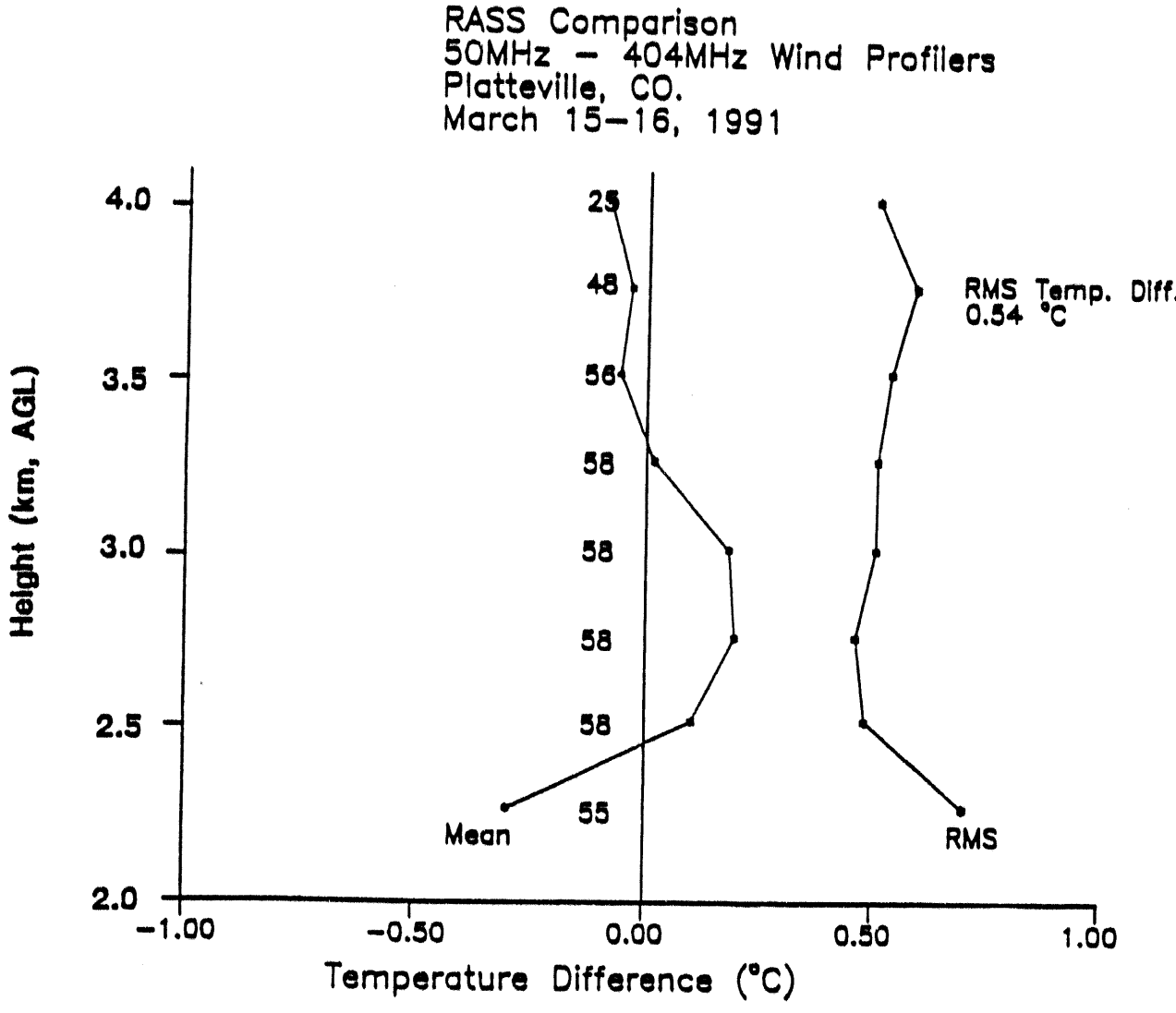


Figure 11. Mean and RMS temperature difference of 50 MHz RASS and 404 MHz RASS measurements after correcting for height offset. The number of data points for each height are shown left of the zero difference line.

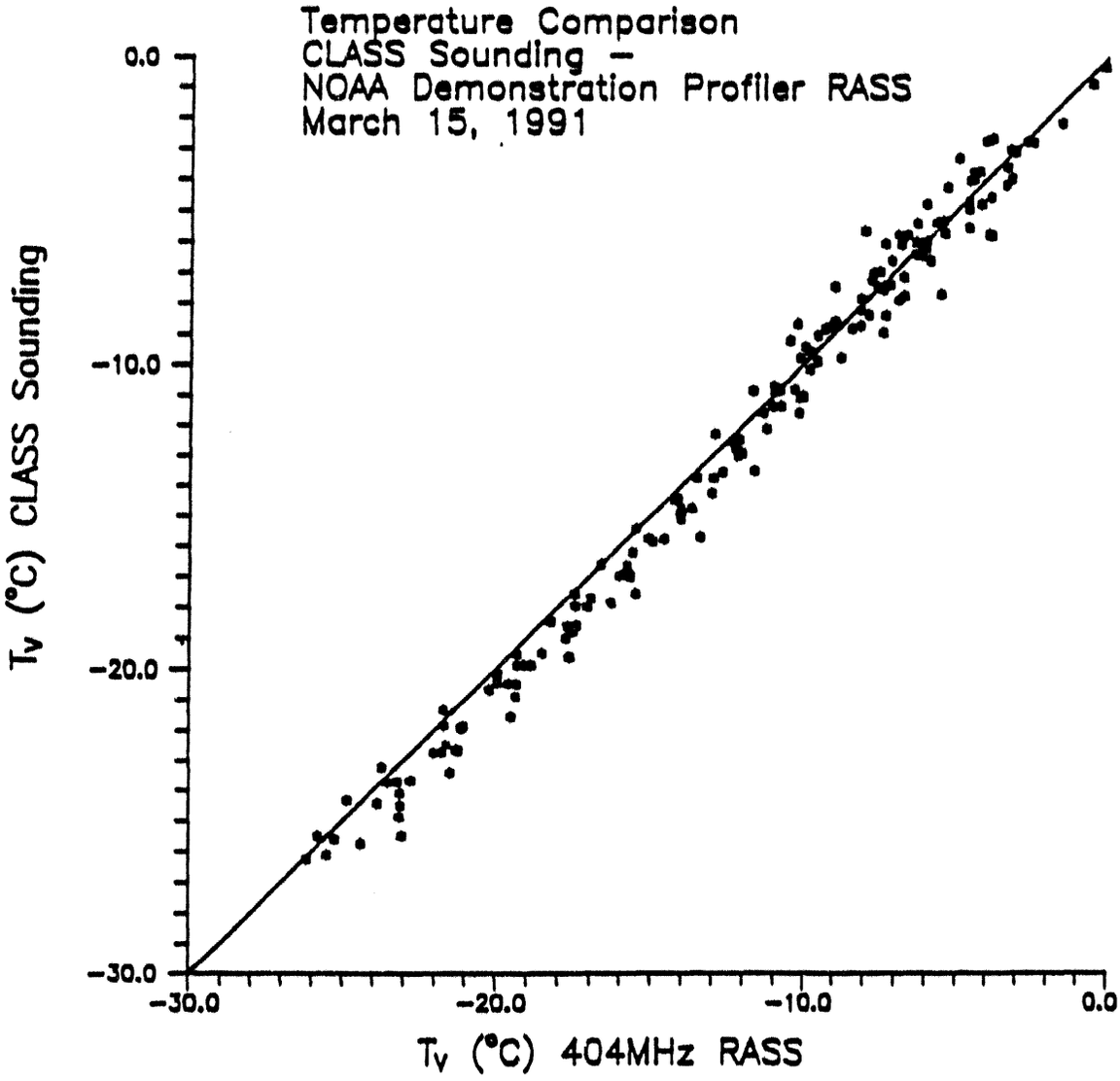


Figure 12. Virtual temperatures measured by CLASS radiosondes and 404 MHz RASS. Data taken for 12 soundings show an RMS difference of 0.9°C.

however, these points were measured when the radiosonde packages had drifted farthest from the radar. The warmer points were obtained close to the radar and no bias is evident.

Figure 13 illustrates a second cause of temperature differences when comparing RASS and radiosondes. The height resolution of the 404 MHz profiler is too coarse to resolve the temperature structure between 3.0 and 3.5 km, illustrating the need for a high-resolution boundary layer mode for this radar. This type of inversion is resolved very well by the 915 MHz profilers with 100-150 m height resolution, but the measurements are generally limited to below 1 km for the boundary layer 915 MHz systems.

During the next year WPL and AL will study the accuracy of RASS with vertical wind corrections. Improved algorithms will be developed to recognize and deal with precipitation effects. Just as with wind profilers, the accuracy and limitations of RASS will gradually become firmly established as the technology is more widely utilized. The ARM-91 measurements have provided a large step foreward in this assessment process.

## 5.2. Wind Profilers

Wind measurements were obtained in ARM-91 with the same NOAA wind profiler systems mentioned in the RASS performance section. Unlike RASS, however, wind profiler performance has been examined in detail in several earlier studies. The wind measurement height coverage is documented by Frisch et al. (1986) for various profilers, and by Weber et al. (1990) for the NOAA Demonstration Network (Unisys) profilers. Reinking (1991) discusses performance of a boundary layer 915 MHz profiler that used three 1 m x 2 m antennas in winter conditions. Wind data height coverage statistics reconstructed from these studies are shown in Figs. 14-15. Figure 16 summarizes these data and can be used to examine regions of overlap and gaps for various combinations of profilers.

As more of the 31 network profilers come on line, their height coverage will quickly become better established. These radars will provide hourly wind profiles from 0.5 to 9.25 km AGL with 375 m resolution and from 7.5 km to 16.25 km AGL with 1000 m resolution a very high percentage of time. Because their sensitivity is higher than the WPL 50 MHz profiler at Platteville, these radars do not experience data loss because of low signal-to-noise ratio in the laminar flow of jet streams nearly as often as does the 50 MHz profiler. Figure 17 illustrates a case where the 50 MHz system had such a dropout, whereas the 404 MHz system shown in Fig. 18 did not. The 404 MHz profiler will not have adequate sensitivity to measure winds in every meteorological situation, but the performance to date

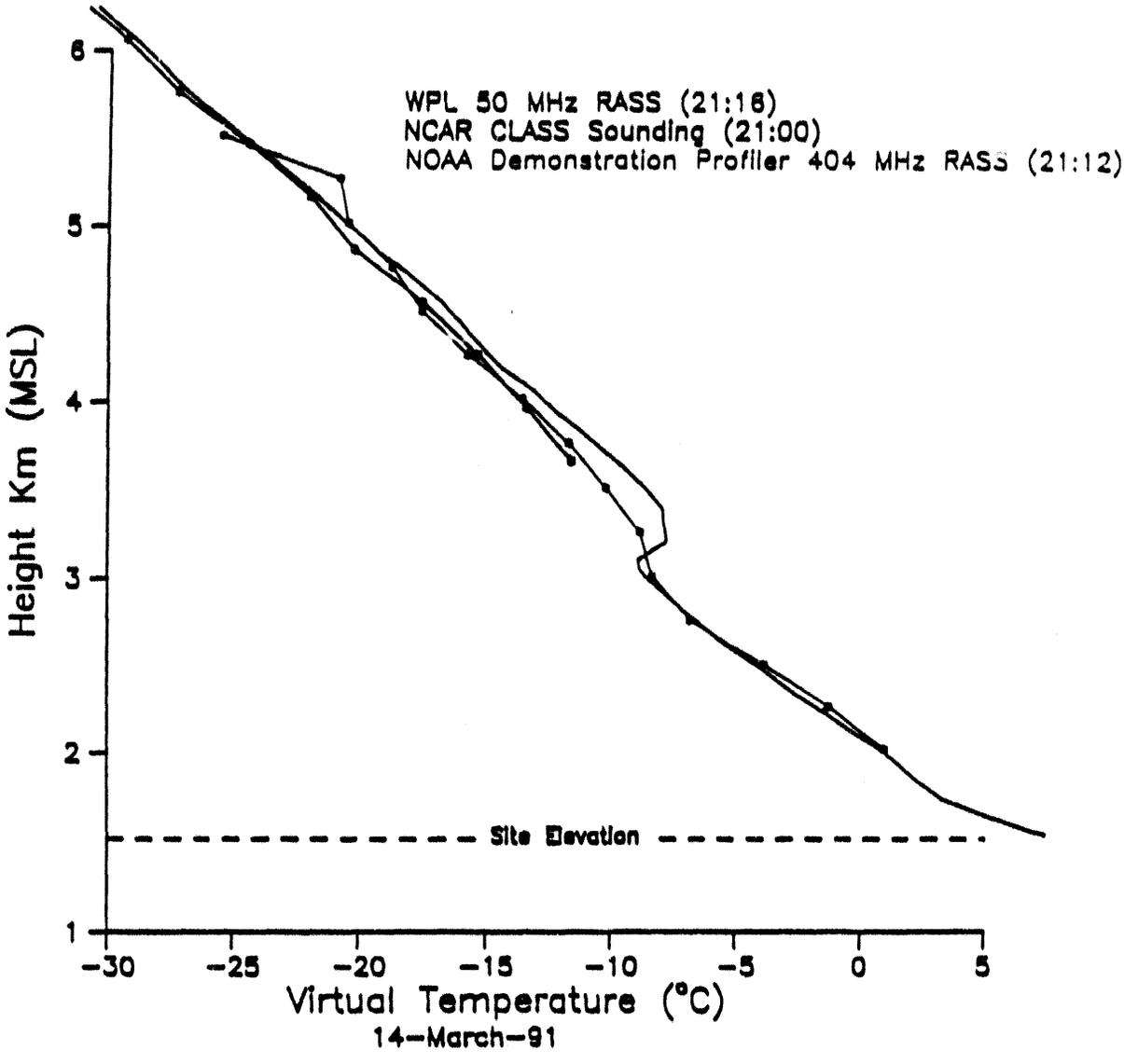


Figure 13. Virtual temperature profile measured by CLASS radiosonde (solid line) and RASS (*) of 50 MHz and 404 MHz.

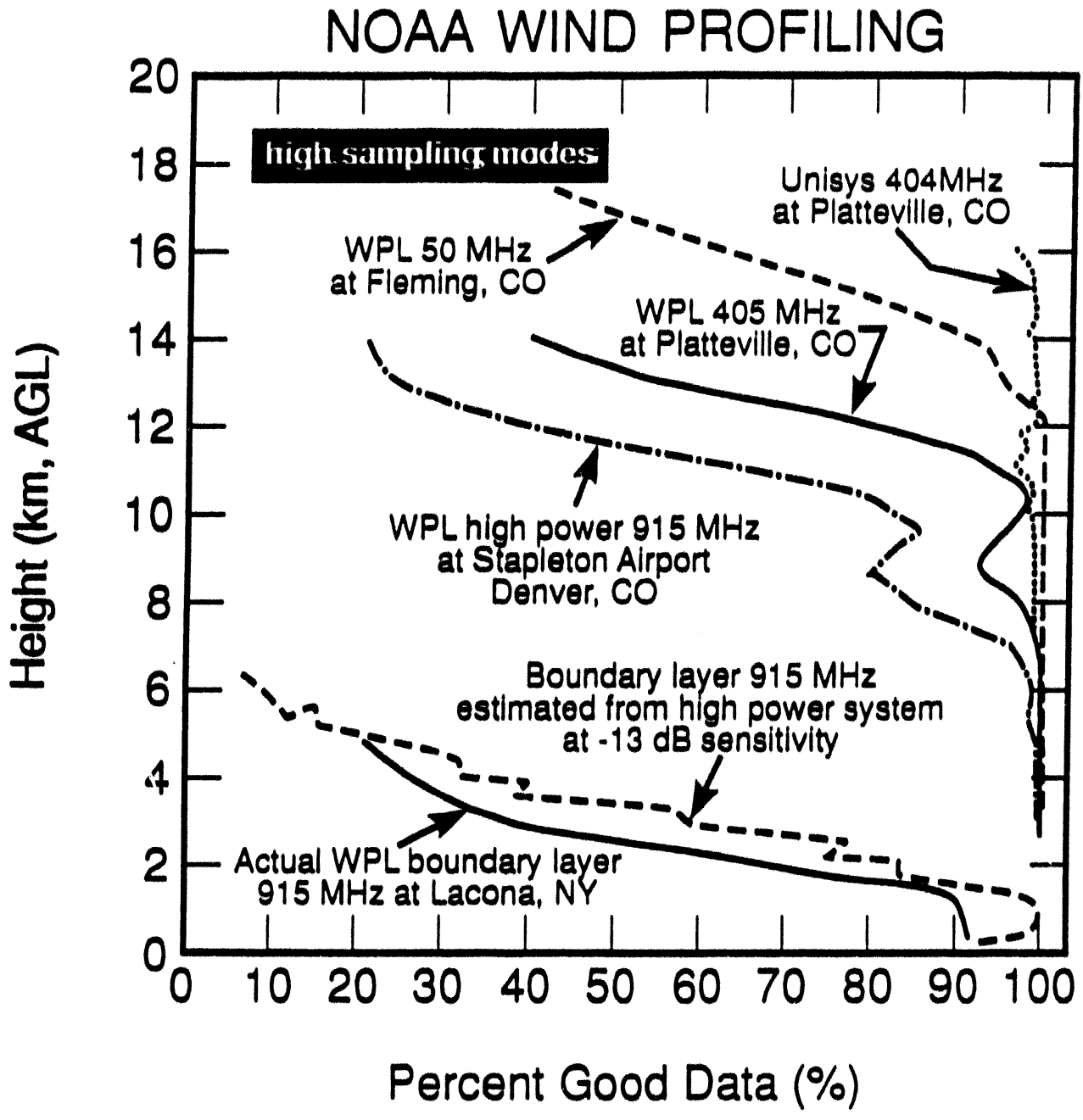


Figure 14. Statistics of height coverage of wind measurements obtained with wind profilers operated by NOAA in the high-altitude sampling mode. Data for the WPL 50 MHz, 405 MHz, and high-power 915 MHz systems are from Frisch et al., (1986). The Unisys 404 MHz data are from Weber et al., (1990). The WPL boundary layer 915 MHz data are from Reinking (1991). Years, seasons and duration of data collection varied.

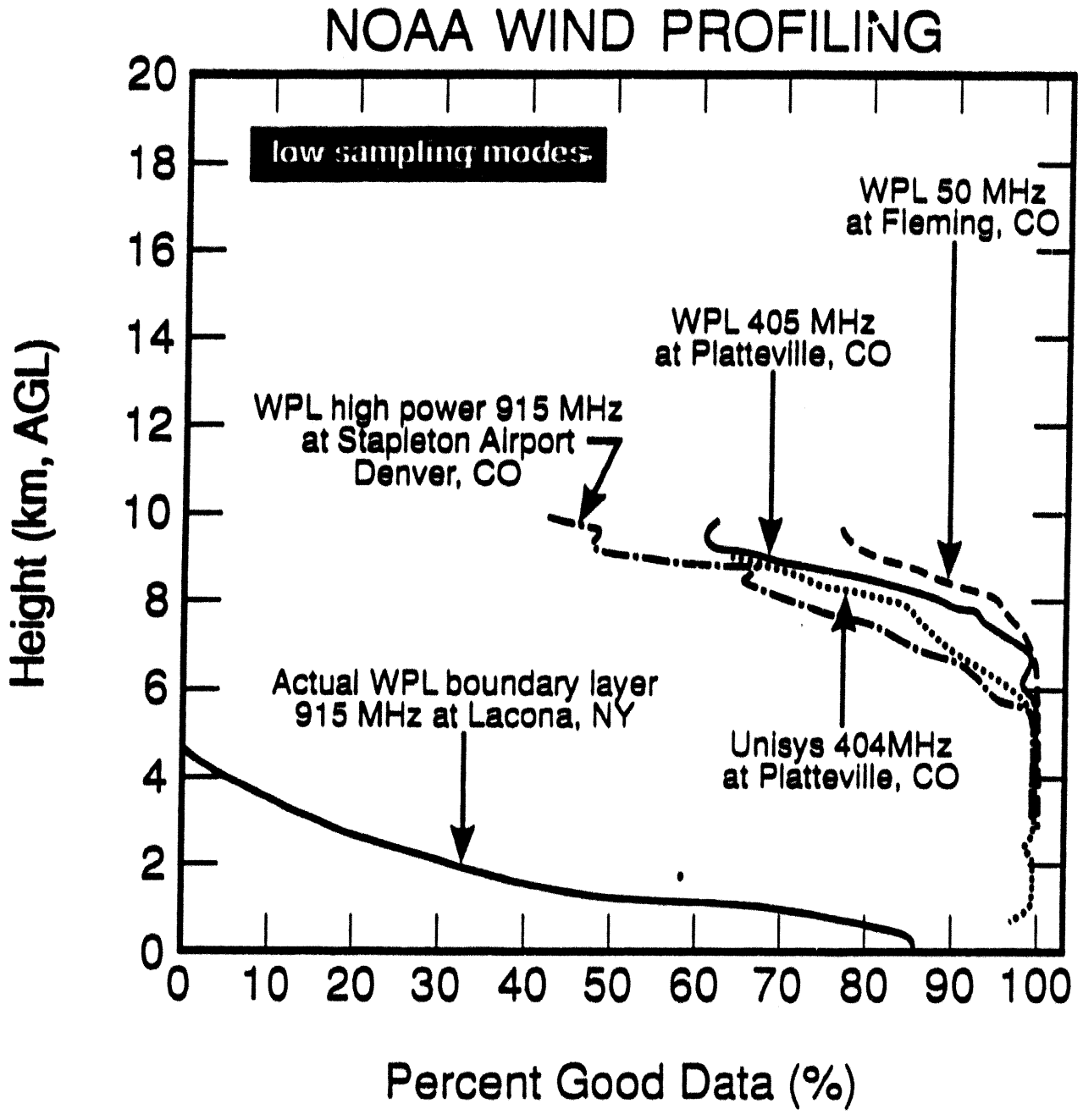


Figure 15. As in Fig. 14, except for the low-altitude sampling modes of the wind profilers.

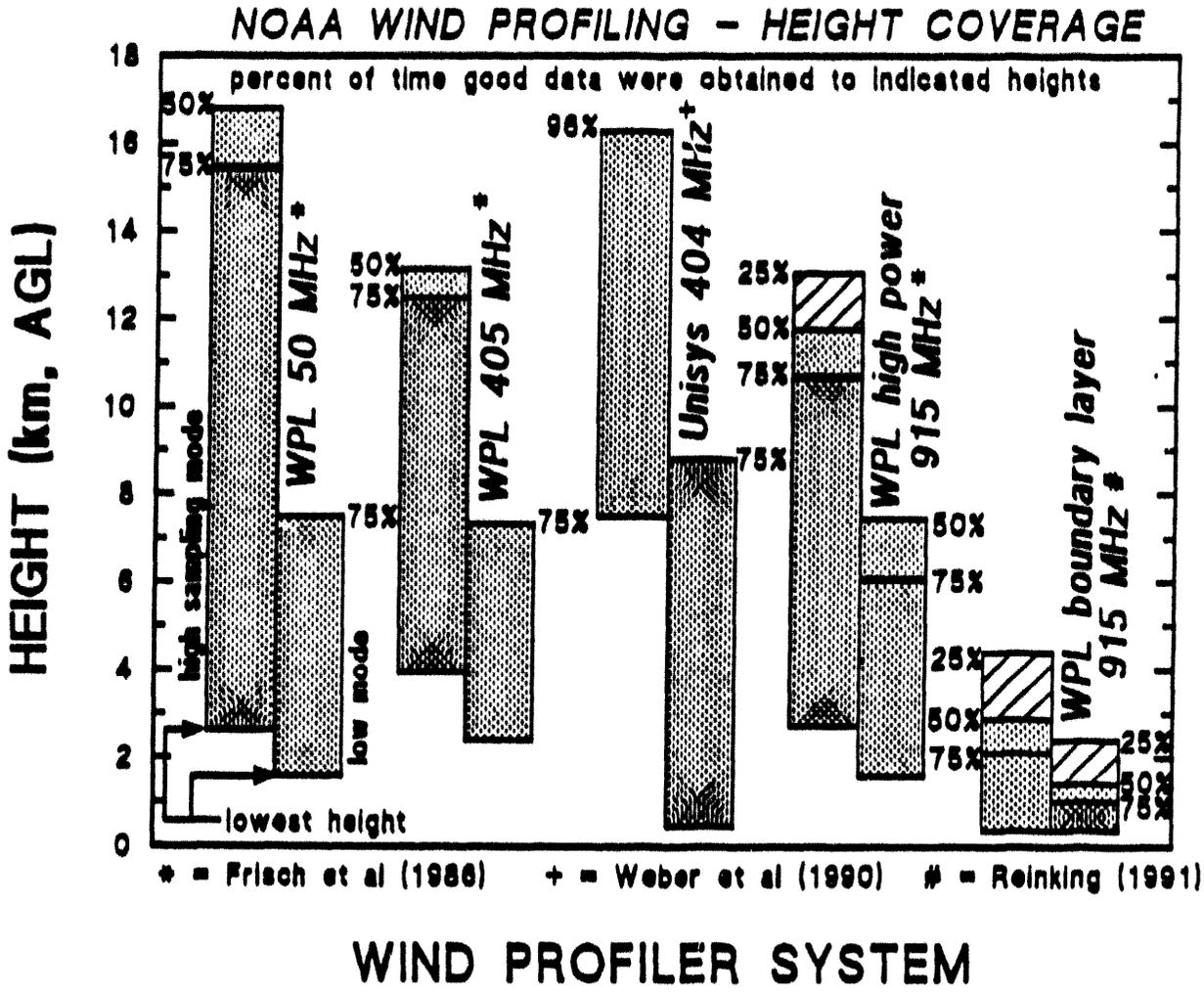


Figure 16. Summary of height coverage statistics for wind measurements obtained with wind profilers operated by NOAA in high altitude and low altitude sampling modes. All data were obtained in Colorado except for the 915 MHz boundary layer system data, which are from New York. Years, seasons, and duration of data collection varied from system to system.

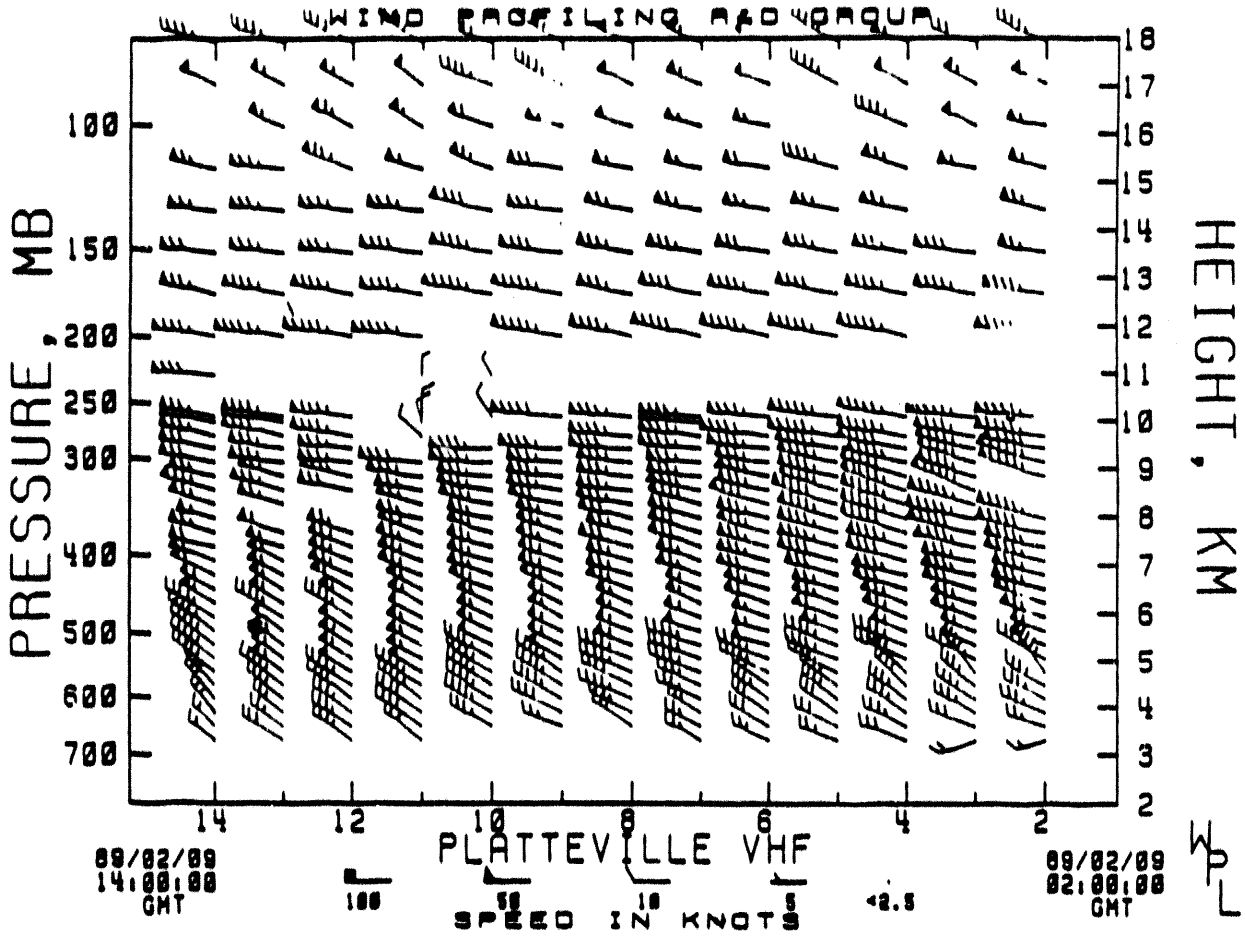


Figure 17. Hourly wind profiles measured by 50 MHz radar showing signal dropout in the jet core near 11 km. Hourly average speeds are shown in units of knots.

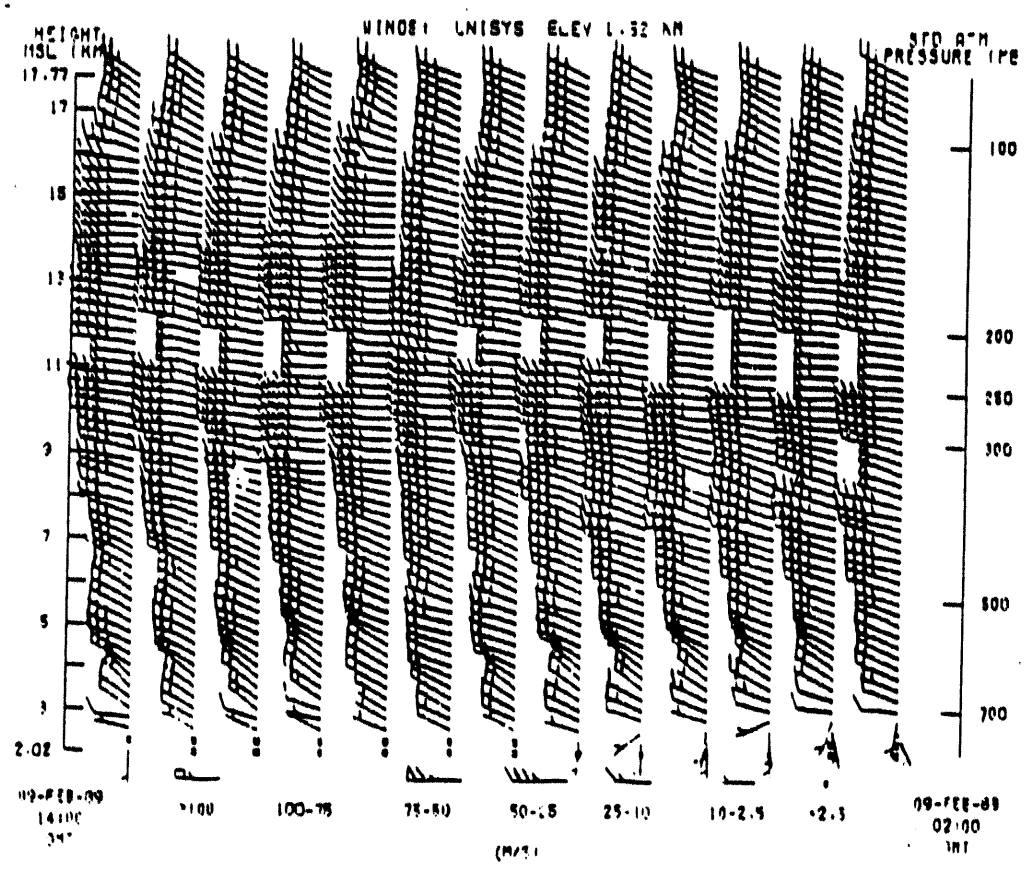


Figure 18. Same time period shown in Fig. 17, but these data were measured by the Unisys 404 MHz radar and do not have a dropout. Speeds are shown in m $s^{-1}$.

indicates the sensitivity is about as predicted and about as desired for most meteorological purposes. Experience based on ARM-91 and earlier studies suggests optimized 50 MHz profilers for CART sites would need about 7 dB more sensitivity than that of the WPL 50 MHz profiler at Platteville. The Platteville 50 MHz profiler has a 50 m x 50 m antenna for horizontal wind measurements with about 200 W average transmitted power. A radar with the same antenna and 1 kW average power, or a radar with a 70 m x 70 m antenna and about 500 W average power, should be installed at the first CART site.

Experience with 915 MHz boundary layer profilers shows that these radars will not always measure winds to the minimum height of the 50 MHz systems, though they will much of the time. Moran et al. (1991b) show comparisons of various UHF wind profilers for lower tropospheric measurements. Using the 915 MHz profiler at Stapleton Airport as a test system, the performance of lower sensitivity systems can be evaluated. Figure 19 shows a test case. A boundary layer radar with 2 m x 2 m antenna panels would approach the performance shown on the curve labeled -13 dB. This curve is reproduced on Fig. 14 for comparison with other profilers.

The AL boundary layer 915 MHz profiler at Platteville had limited sensitivity in ARM-91 because it was designed primarily for work in the tropics where atmospheric reflectivity is higher. There were some periods during the ARM winter experiment when the wind data extended only to 500 m AGL. However, depending on atmospheric conditions, there were also frequent occasions when measurements reached to several kilometers. Ground clutter problems at Platteville were caused by wires strung between tall towers. The wires swayed in the wind and increased the spectral width of the return near zero velocity. This made it difficult to obtain good wind measurements in the lowest levels when surface winds were strong. Similar problems were encountered with another boundary layer 915 MHz profiler in New York described by Reinking (1991). Clutter reduction fences designed to combat this problem have shown some success (Russell and Jordan, 1991). The height coverage of boundary layer wind profilers is significantly better in warmer and more humid climates, as shown for example by Neff et al. (1991) for central California where summer wind measurements usually extended to 4 km AGL.

The accuracy of wind profilers has been reported by Strauch et al. (1987), Wuertz et al. (1988), and Weber and Wuertz (1990). We have not attempted to duplicate these studies for the ARM-91 field experiment. Being satisfied with the accuracies established in the earlier studies for these same profilers, we have archived the 1991 WPL profiler data after editing to remove outliers, using a time-height continuity algorithm developed by Wuertz and Weber (1989).

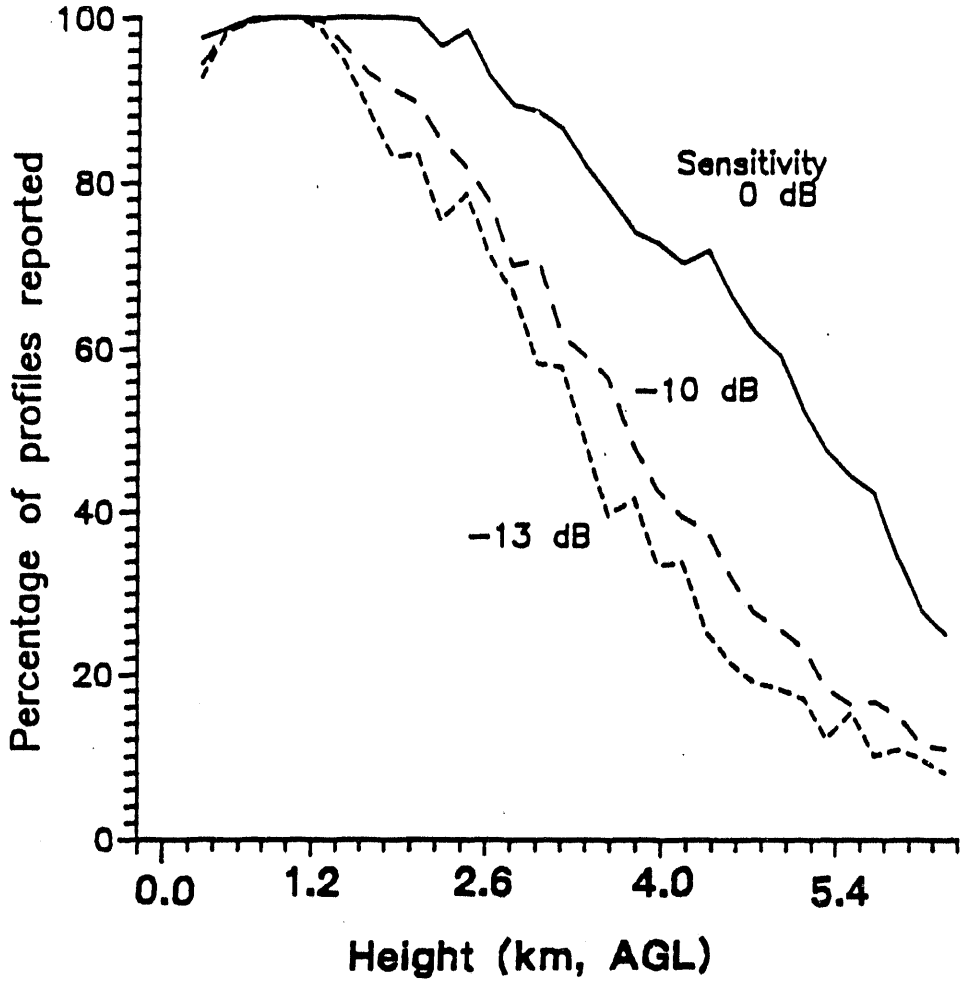


Figure 19. Height coverage of wind measurements with a 915 MHz profiler with normal sensitivity and with reduced sensitivity. During each hour the radar measured winds with normal sensitivity and with average power decreased by 10 and 13 dB. The percentage of time that a 20-min average wind was reported to a given height is plotted for the three conditions (250 events each).

## 5.3 Microwave Radiometers

Figure 20 shows time-series plots of precipitable water vapor measured by the WPL microwave radiometers, annotated for comparison, with collocated measurements by routine NWS radiosondes and NCAR radiosondes for one of the ARM-91 IOPs. The agreement is excellent and the figure illustrates the vastly superior temporal resolution (2 min) of the radiometer measurements. Similarly impressive comparisons are shown for other IOPs in Appendix B.

Westwater et al. (1985b) showed that precipitable water vapor measured with the WPL radiometers had an RMS difference of only 1.7 mm from NWS radiosondes, based on a full year of data at Denver. An important feature of ARM-91 was the frequent launching (every 3 h or more often) of NCAR's CLASS rawinsondes at Platteville during IOPs. The WISP experiment also frequently launched CLASS sondes near the Elbert radiometer site. The CLASS uses a different humidity sensor and routinely records data with finer vertical resolution than the NWS sondes. In preliminary comparisons for ARM-91 at Platteville, the precipitable water vapor measurement differences between the WPL microwave radiometer and the CLASS sondes appear to be smaller than for the earlier comparisons with NWS radiosondes (Fig. 21). During the period of 15 February to 31 March, RMS differences were 1.1 mm; this approaches the 0.7 mm RMS error theoretical accuracy of the radiometers. (For these comparisons, the CLASS surface humidity data appear to be erroneous in sub-freezing conditions, and were replaced with surface humidity measurements made by WPL instruments at the radiometer sites.) A comprehensive and more precise comparison is being made for the entire ARM-91 and WISP-91 sets of radiosonde data at all three radiometer sites. Similar comparisons of integrated liquid water content of clouds are not possible because the balloon-borne NWS and CLASS sondes do not have a liquid water sensor. The accuracies and comparisons are summarized in Table 10.

Of course, the vapor and liquid contents are derived from the radiometer's basic measurement of brightness temperature for the detected frequencies. Keihm (1991) shows that the brightness temperatures measured by the WPL and Jet Propulsion Laboratory radiometers at Platteville during ARM-91 agreed within 0.1°K for clear sky conditions.

The radiometers do suffer data contamination when liquid water from rain or melted snow accumulates on the reflector viewing surfaces. This can be a problem for unattended operations and occurred on about 11% of the hours at Platteville during ARM-91 IOPs as shown in Table 11. Strategies to remedy this problem are being tested at WPL (Stankov et al., 1991).

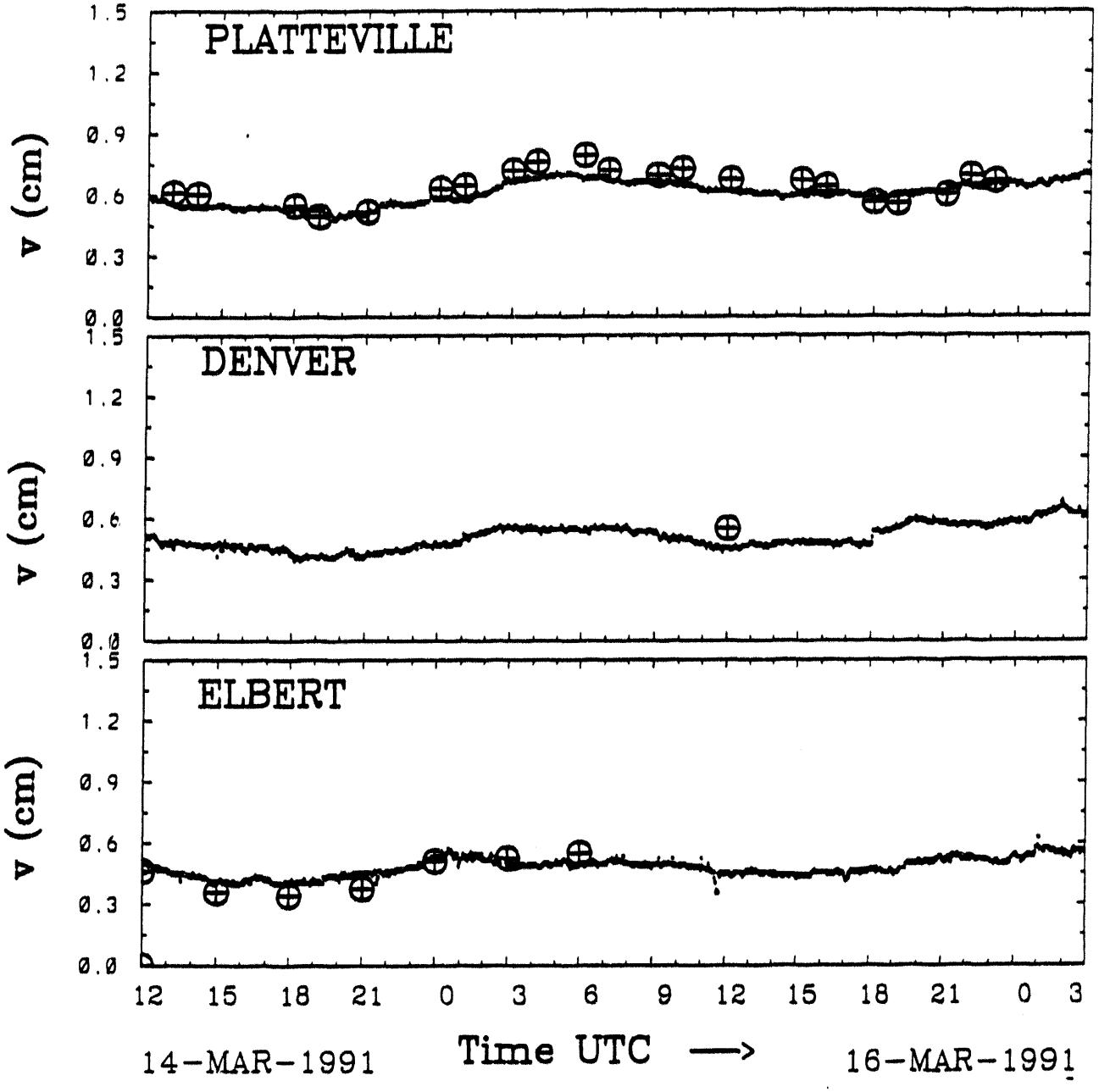


Figure 20. Precipitable water vapor measured by WPL's microwave radiometers (small dots) and computed from radiosonde data (circled crosses) at three sites during an ARM-91 IOP.

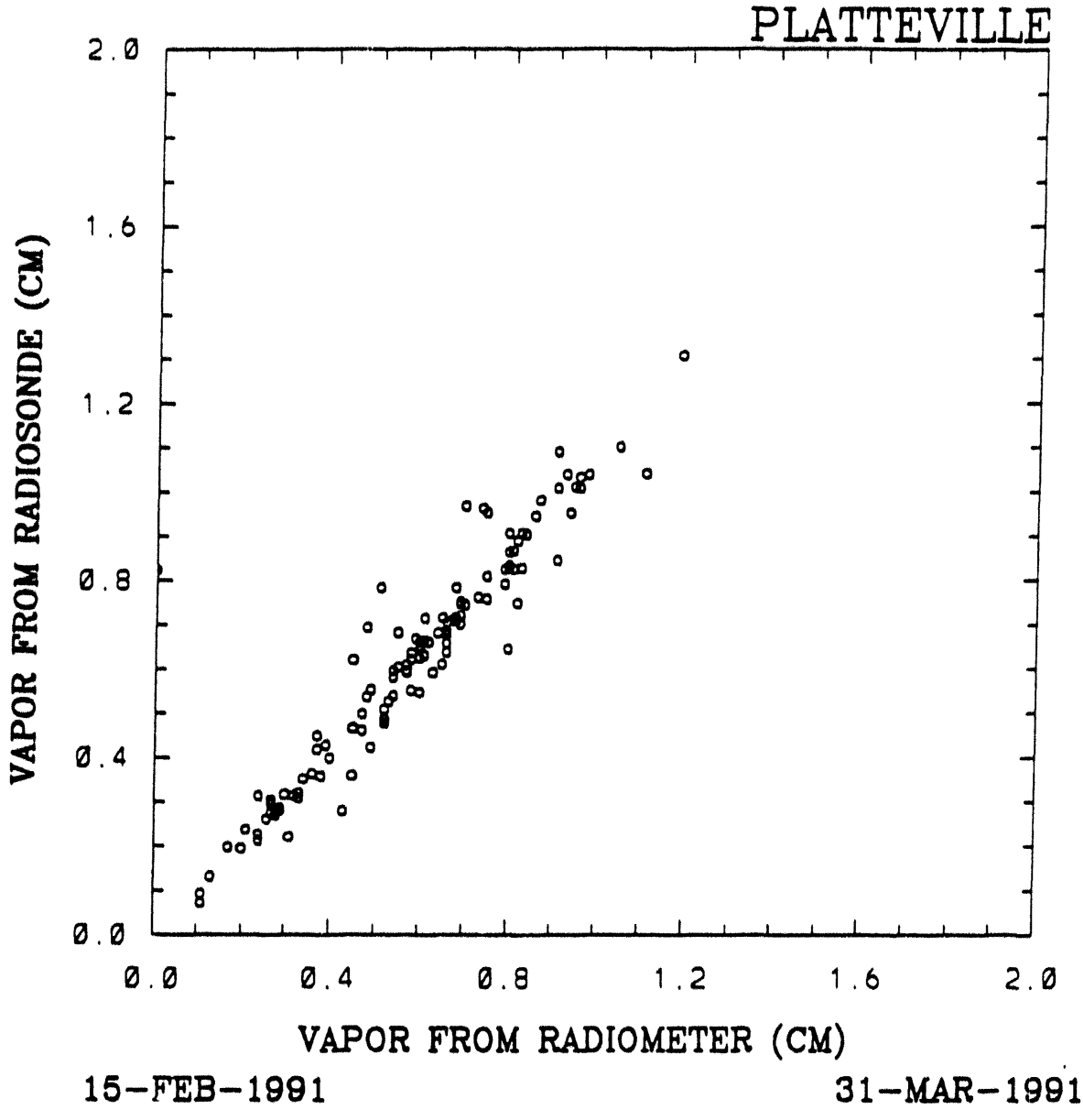


Figure 21. Preliminary comparison of precipitable water vapor measured by microwave radiometer and computed from CLASS radiosondes for launches at Platteville. Radiometer data are averages for the first 16 min of the hour during which a sonde was launched. Data include 121 sonde launches for ARM and WISP from 15 February to 31 March 1991.

Table 10. RMS accuracy of WPL Dual-channel Radiometers in Inferring Precipitable Water Vapor (PWV) and Integrated Cloud Liquid Water (CLW)

| | PWV (mm) | CLW (mm) |
|---|---|---|
| Theoretical absolute accuracy | 0.7 | 0.03 |
| Measured absolute accuracy, RMS difference: | | |
| from NWS radiosondes | 1.7 | ---- |
| from CLASS at Platteville | 1.1 | ---- |
| Sensitivity (2-min integration time) | 0.07 | 0.005 |

Table 11. Radiometer Data Losses During ARM-91 IOPs

| | | Platteville | | Denver | | Elbert | |
|---|---|---|---|---|---|---|---|
| Period | Hours | C | E | C | E | C | E |
| 17 Feb. 12 UTC<br>19 Feb. 12 UTC | 42 | 0.09 | 62.7 | 0.00 | 6.40 | 0.00 | 3.97 |
| 24 Feb. 12 UTC<br>25 Feb. 12 UTC | 24 | 0.00 | 0.73 | 0.00 | 1.37 | 0.00 | 2.30 |
| 28 Feb. 12 UTC<br>1 Mar. 12 UTC | 34 | 0.00 | 4.13 | 0.27 | 4.87 | 0.00 | 3.17 |
| 5 Mar. 12 UTC<br>7 Mar. 12 UTC | 30 | 0.07 | 5.17 | 1.27 | 9.23 | 0.00 | 4.87 |
| 8 Mar. 12 UTC<br>9 Mar. 12 UTC | 24 | 0.00 | 2.27 | 0.00 | 0.80 | 0.00 | 1.30 |
| 11 Mar. 12 UTC<br>12 Mar. 12 UTC | 24 | 0.00 | 4.27 | 0.00 | 4.93 | 0.00 | 4.83 |
| 14 Mar. 12 UTC<br>16 Mar. 12 UTC | 39 | 0.00 | 0.70 | 0.00 | 1.67 | 0.00 | 3.23 |
| All IOPs (hrs) | 217 | 0.16 | 23.54 | 1.54 | 29.27 | 0.00 | 23.67 |
| (percent) | 100 | 0.07 | 10.85 | 0.71 | 13.49 | 0.00 | 10.91 |

C = Communication outage, E = Editing removal of spurious data

## 6. RECOMMENDATIONS FOR ARM CART SITES

Based on preliminary results from the ARM-91 field experiment and lessons acquired from years of experience with remote sensors, we offer here some recommendations to DOE for the design and implementation of certain profiling equipment. The suggestions are confined to the NOAA remote sensors used for wind, temperature, and moisture measurements which were studied in the WPL & AL research for ARM. The recommendations do not cover remote sensors such as lidars and millimeter radars that are specifically intended for monitoring clouds, aerosols, and radiatively important trace gases. These are subjects for other ARM research projects. The integration of profiling data from various diverse instruments is a longer term topic of the ongoing cooperative research with NCAR and UW that will be reported later.

The ARM-91 results indicate a 404 MHz Unisys-type wind profiler with RASS capability could provide excellent height coverage for wind and temperature profiling, except in the lowest (and possibly crucial) 500 m layer of the atmosphere. Problems with frequency allocation, however, may prevent wider use of such a system (Barth, 1989). Since DOE has already chosen to use 50 MHz and 915 MHz systems at the first CART site, we confine our profiler/RASS recommendations to features and characteristics that these systems should have at a U.S. Southern Plains location. The recommendations take account of the short time allowed for deploying operational systems at the first CART. Different recommendations may be appropriate for CARTs in other climates or for longer lead times.

### 6.1. Wind Profilers

#### 6.1.a. Boundary layer 915 MHz wind profiler

A "standard" version of this system can be procured from private industry. We recommend that the sensitivity of the standard profiler be increased to allow measurement of wind profiles from near the surface to the lowest height measured by the 50 MHz radar for a higher percentage of time. Increased sensitivity can be obtained most economically by adding pulse compression and a larger antenna; doing both would give this radar a comfortable margin for sensitivity. However, based on time considerations, it is recommended that pulse compression be added at a later date. There are a variety of antenna choices. A 3 m x 3 m phased array is recommended over separate antennas for each pointing direction because more than three pointing directions would be desirable to test heat and momentum flux measurement concepts as well as to measure wind profiles in more complex dynamical regimes. The larger antenna also helps RASS

height coverage. The radar should operate with at least two height resolution modes, 100 and 300 m. Data measured in the two modes should have significant height overlap. Therefore, we recommend the purchase of the standard 915 MHz profiler, but it should be equipped with a 3 m x 3 m phased array antenna; pulse compression should be added when it is developed.

### 6.1.b. 50 MHz wind profiler

The 50 MHz profiler is not a commercial product so care must be exercised in the procurement process to obtain a truly operational system. We recommend a 70 m x 70 m antenna with at least 0.5 kW average power to obtain the sensitivity desired to measure winds into the lower stratosphere. A two-mode radar range resolution system with significant height overlap should be procured with resolution of 300 m to 10 km altitude and 1 km resolution to 20 km altitude. The data processor/radar controller should be the same as that used in the 915 MHz systems. Other radar hardware must be based on existing 50 MHz systems if the radar is to be ready in 1992.

## 6.2. RASS

Automated RASS control and data processing of the type used by the Aeronomy Laboratory at Platteville are built into the 915 MHz standard boundary layer wind profiler that is available commercially. This will allow RASS temperatures to be corrected by the simultaneous measurement of the vertical air speed. Multiple acoustic sound sources are recommended for this system to achieve good height coverage in various wind conditions. These sources are available commercially for 915 MHz RASS. They are based on sodar designs. Sound baffles must be specified. We recommend that at least five acoustic sources be procured with the 915 MHz radar, and at least one of these should be mobile. We expect that improved height coverage will be attained if an acoustic source is positioned upwind (based on the measured wind profiles), though this has not been tested. Acoustic power should be at least 25 W (continuous) for each source.

The 50 MHz RASS should be able to measure at least 24 heights. This requires a change in the type of data processor used on WPL's unit, which is limited to 14 heights. (The range gates could also be stepped.) At least three acoustic sources are recommended, and one of these should be mobile. The radar antenna for the vertical beam should be 70 m x 70 m or larger. Acoustic power should be at least 200 W (continuous) for each source.

## 6.3. Microwave Radiometers and Complementary Instruments

Measurements of PWV during both clear and cloudy conditions may be important for CART development because (a) PWV can be

inserted into dynamic assimilation models to derive water vapor profiles; (b) PWV can be combined with other sensors (RASS, FIRS, ceilometers, and millimeter-wavelength radars) to derive profiles during cloudy conditions; (c) PWV can be used between special radiosonde launches to derive time series of water vapor profiles; (d) PWV is of intrinsic interest in radiative transfer parameterization; and (e) the coarse vertical resolution of radiometrically inferred profiles alone may be adequate for many kinds of radiative transfer calculations.

Since CLW is also commonly used in cloud radiative transfer parameterization, its unique measurement by microwave radiometers may be useful for radiative transfer studies. For example, CLW measurements were extremely valuable in the FIRE stratus cloud experiments. If CLW is used in combination with cloud measurements made by active sensors, such as lidars or short-wavelength microwave radars, at least crude profile information can be derived (Shaw, 1991).

WPL's microwave radiometers have been successful in accurately measuring PWV and CLW because (a) they are accurately calibrated; (b) their calibration is stable over periods of weeks; and (c) they have equal beamwidths at both operating frequencies, which allows the same atmospheric volume to be observed simultaneously at both frequencies. Also, since significant water vapor and cloud changes occur over periods of a few minutes, a sampling interval of less than 5 min is highly recommended.

In terms of CART deployment, we recommend that dual-channel radiometers be placed at five locations around a site: one at the central location, and four around the perimeter. At the central site, the radiometer could be used as a valuable supplement to other sensors that are being considered for deployment, such as RASS, microwave radars, Raman lidars, infrared spectrometer or interferometer devices such as the UW HIS and the WPL FIRS. At perimeter locations, the dual-channel radiometers, in addition to measuring PWV and CLW, could be operated with 915 MHz boundary layer profilers to derive horizontal water vapor fluxes, following the techniques of Uttal et al. (1990). At the central location, we recommend that all the potential water vapor and cloud sensing instruments be collocated, such that all-weather water vapor profiles can be derived from measurements of an integrated system. We also believe that the combination of dual-channel radiometers, ceilometers, and FIRS to derive water vapor profiles should be seriously considered for perimeter locations. This could be a low-cost extension to an expensive Raman lidar system at a central facility.

WPL now has about 2 years of experience with the simultaneous operation of NWS lidar ceilometers and WPL infrared

radiometers. Usually, these instruments provide complementary information on cloud base height and cloud base temperature. However, the upper altitude range of the NWS ceilometer is about 3.7 km. In many cases, we have observed cloud signatures with the infrared radiometer from clouds that are above the upper range of the lidar. We suggest, since many CART activities are focused on the radiative properties of clouds, that a vertically pointing, low-cost lidar that will probe to at least 10 km AGL, would be a valuable addition to CART instrumentation. Another instrument that could provide extremely valuable cloud information is a vertically pointing 8 mm wavelength radar, which could supplement a lidar for cloud-base measurements, but could also measure most cloud tops and the height characteristics of multiple layer clouds. Unlike lidars, such a radar is not blocked by liquid water clouds and can operate in precipitation. If such an instrument could be built at a reasonable cost, it would have a large impact on future cloud studies.

RASS-derived temperature profiles will have a minimum range below which a temperature measurement will not be possible. This lowest range is about 100 m, 300 m, and 2.0 km for 915 MHz, 404 MHz, and 50 MHz systems, respectively. The temperature profile in this radiatively important region from the surface to about 500 m could be accurately be reconstructed from FIRS-type measurements. It is recommended that combined RASS/FIRS temperature profiling be tested and evaluated. FIRS radiances might also be used to control the quality of wind-contaminated RASS data.

It is also clear that, even with 50 MHz Profilers, RASS-derived temperatures will be limited at upper altitudes to ranges of about 7 km AGL. To derive profiles above these altitudes, several remote sensing techniques, combined with four-dimensional data assimilation modeling, may be required. Reflectivity profiles from 50 MHz profilers have been used to derive tropopause height (Gage and Green, 1979); measurements of tropopause height, in turn, can be combined with RASS to derive upper altitude temperature profiles. In addition, soundings from polar orbiting satellites can add useful upper-altitude thermal information (Westwater et al., 1985b; Schroeder et al., 1991). We recommend the development of algorithms to combine these available additional sources of information.

## 6.4. Instrument Modeling

The evaluations of the NOAA remote sensors reported here have relied almost entirely on empirical methods. Instrument behavioral models offer another complementary approach to the problem. An accurate model can be used to theoretically define an instrument's capabilities and provide valuable quantitative predictions of how it should perform in untested environmental

conditions. Instrument models can also quantify the relative importance of various hardware and environmental factors for specified conditions. Modeling of microwave radiometers is relatively advanced. It has led to the optimum choice of operating frequencies for PVW and CLW measurements, and has influenced the development of profile retrieval algorithms for these instruments.

In examining the height coverage limitations of the much more complex RASS, it is clear that several factors are important including radar transmitter power, acoustic power, speaker locations, antenna size, wind speed, and acoustic attenuation. RASS operation has now been evaluated fairly well for Colorado conditions, but its performance in other climate regimes is largely unknown. Using RASS as an obvious example of need, we recommend that instrument system modeling, such as has been started by NOAA and DOE/ARM scientists, be pursued. When designing integrated systems for long-term operational use, as is intended for CART, it is desirable to have a model for each component instrument to help predict performance in various environmental and physical configurations.

## ACKNOWLEDGEMENTS

This research was sponsored by the Department of Energy's Atmospheric Radiation Measurement (ARM) program under contracts DE-AI06-91RL12090 and DE-AI06-91RL12092. The authors are grateful to ARM Instrument Team Leader Marv Wesely for his efforts to initiate this project. Numerous colleagues at NOAA/WPL, NOAA/AL, NCAR, and UW assisted with installing and operating the suite of instruments. Walt Dabberdt and Charlie Martin of NCAR provided essential help in planning and coordinating the field operations of the cooperative research. WISP Operations Directors Roy Rasmussen and Marcia Politovich helped forge the cooperative agreement between ARM and WISP and provided valuable operations support during the field project. In particular, WISP launched numerous NCAR CLASS sondes at several locations to support the ARM research. All CLASS data were provided by NCAR. The Platteville 404 MHz network wind profiler data were obtained from the NOAA/FSL. Meteorologists from FSL provided daily weather briefings for WISP, which were also useful for declaring the ARM operational periods.

## REFERENCES


Angevine, W.M., D.A. Carter, W.L. Ecklund, and K.S. Gage, 1991: A new technique for temperature profiling using RASS. Preprints, 25th Intl. Conf. on Radar Meteorolgy, Paris, France, Amer. Meteor. Soc., 241-244.

Balsey B.B., and K.S. Gage, 1982: On the use of radars for operational wind profiling. Bull. Amer. Meteor. Soc., 63, 1009-1018.

Barth, R., 1989: The matter of frequency. Profiler Forum, Sept., NOAA/ERL, Boulder, CO, 2-3.

Bedford R.E., C.K. Ma, Z. Chu, Y. Sun, and S. Chen, 1985: Emissivities of diffuse cavities 4: Isothermal and nonisothermal cylindro-inner-cones. Applied Optics, 24, 2971-2980.

Berry, K.H., 1981: Emissivity of a cylindrical blackbody cavity with a re-entrant cone end face. J. Phys., E 14, 629-632.

Chu Z., S. Chen, and H. Chen, 1980: Radiant emission characteristics of isothermal diffuse cylindrical-inner-cone cavities. J. Optical Soc. Amer., 70, 1270-1274.

Crochet, M., C. Bourdier, and E. Spano, 1991: VHF ST radar developments for low altitudes exploration of the atmosphere. Preprints, 5th SCOSTEP/URSI Workshop on Tech. and Scientific Aspects of MST Radar. URSI, Aberystwyth, Wales, 159-160.

Dabberdt, W.F., H.L. Cole, P. Hildebrand, T. Horst, Y.H. Kuo, C. Martin, K.S. Gage, W. Ecklund, R. Strauch, E.R. Westwater, and W.L. Smith, 1991: The integrated sounding system - a new observing system for mesoscale research. Preprints, 7th Symposium on Meteorological Observations and instrumentation, New Orleans, LA, Amer. Meteor. Soc., J128-133.

DOE, 1990: Atmospheric Radiation Measurement program plan. DOE/ER-0441, U.S. Dept. of Energy, Atmospheric and Climate Research Div., Washington, DC, 116 pp.

Ecklund, W.L., D.A. Carter, and B.B. Balsey, 1988: A UHF wind profiler for the boundary layer: Brief description and initial results. J. Atmos. & Oceanic. Tech. 5, 432-441.

Frisch, A.S., B.L. Weber, R.G. Strauch, D.A. Merritt, and K.P. Moran, 1986: The altitude coverage of the Colorado wind profilers at 50, 405, and 915 MHz. J. of Atmos. & Oceanic Tech., 3, 680-692.

Gage, K.S., and J.L. Green, 1979: Tropopause detection by partial specular reflection with very-high-frequency radar. Science, 203, 1238-1239.

Hoehne, W.E., 1980: Precision of National Weather Service upper air measurements. NOAA Tech. Memo., NWS T&ED-16, 23 pp.

Hogg, D.C., F.O. Guiraud, J.B. Snider, M.T. Decker, and E.R. Westwater, 1983: A steerable dual-channel microwave radiometer for measurement of water vapor and liquid water in the troposphere. J. Climate Appl. Meteor., 22, 789-806.

Keihm, S.J., 1991: Water vapor radiometer intercomparison experiment, Platteville, Colorado. Final Report, Jet Propulsion Lab., Calif. Inst. Tech., Pasadena, CA, 38 pp.

Martin, C.L., 1991: Summary of observations made during the WISP/ARM 1991 field program in support of the integrated data assimilation and sounding system development. Proc., Lower Tropospheric Profiling: Needs and Technologies, Boulder, CO, Amer., Meteor. Soc., 139-140.

Martner, B.E., R.A. Kropfli, L.E. Ash, and J.B. Snider, 1991: Progress report on analysis of differential attenuation radar data obtained during WISP-91. NOAA Tech. Memo., ERL/WPL, Boulder, CO, 43 pp (in press).

May, P.T., K.P. Moran, and R.G. Strauch, 1988: The altitude coverage of temperature measurements using RASS with wind profiler radars. , Geophysical Res. Letters, 15, 1381-1384.

May, P.T., K.P. Moran, and R.G. Strauch, 1989: The accuracy of RASS temperature soundings. J. of Appl. Meteor., 28, 1329-1335.

May, P.T., R.G. Strauch, K.P. Moran, and W.L. Ecklund, 1990: Temperature soundings by RASS with wind profiler radars. IEEE Trans. on Geoscience & Remote Sensing, 28, 19-28.

Moran, K.P., R.G. Strauch, B.L. Weber, and D.B. Wuertz, 1991a: Wind profilers for mid-tropospheric sounding systems. Proc. Symp. on Tropospheric Profiling: Needs and Technologies, Boulder, CO, Amer. Meteor. Soc. 53-55.

Moran, K.P., R.G. Strauch, D.B. Wuertz, and B.L. Weber, 1991b: Temperature measurements by RASS with a NOAA demonstration network profiler: first results. Proc. Symp. on Tropospheric Profiling: Needs and Technologies, Boulder, CO, Amer. Meteor. Soc., 91-92.

Neff, W., J. Jordan, J. Gaynor, D. Wolfe, W. Ecklund, D. Carter, and K. Gage, 1991: The use of 915 MHz wind profilers in complex terrain and region air quality studies. Preprints, 7th Symp. on Meteor. Observations and Instrumentation, New Orleans, LA, Amer. Meteor. Soc., J230-233.

Politovich, M.K., 1991: WISP seeks understanding of winter storms. ATD Observer, Summer, National Center for Atmospheric Research, Boulder, CO, 1-3.

Reinking, R.F. (ed.), 1991: Lake Ontario Winter Storms project final technical report. Kaman Science Corp., Colorado Springs, CO, 213 pp.

Revercomb, H.E., H. Buijs, H.B. Howell, D.D. LaPorte, W.L. Smith, and L.A. Sromovsky, 1988: Radiometric calibration of IR Fourier Transform spectrometers: Solution to a problem with the High-resolution Interferometer Sounder. Applied Optics, 27, 3210-3218.

Russell, C.A., and J.R. Jordan, 1991: Portable clutter fence for UHF wind profiling radar. Preprints, 7th Symp. on Meteor. Observations and Instrumentation, New Orleans, LA, Amer. Meteor. Soc., J152-156.

Schroeder, J.A., E.R. Westwater, P.T. May, and L.M. McMillin, 1991: Prospects for temperature sounding with satellite and ground-based RASS measurements. J. Atmos. & Oceanic Tech., 8, 506-513.

Shaw, J.A., 1991: Calibration of infrared radiometers for cloud-base temperature remote sensing: technique and error analysis, NOAA Tech. Memo. ERL WPL-207, 17 pp.

Stankov, B.B., J.B. Snider, E.R. Westwater, R.H. Beeler, L.S. Fedor, D. Hazen, J.A. Shaw, J. Reynolds, D.B. Wuertz, and R.L. Weber, 1991: Remote sensor observations during WISP91: The use of microwave radiometers, RASS, and lidar ceilometers for detection of aircraft icing conditions. NOAA Tech. Memo., ERL/WPL, Boulder, CO, 83 pp (in press).

Strauch, R.G., K.P. Moran, P.T. May, A.J. Bedard, Jr., and W.L. Ecklund, 1988: RASS temperature sounding techniques. NOAA Tech. Memo. ERL WPL-158, 12 pp.

Strauch, R.G., B.L. Weber, A.S. Frisch, C.G. Little, D.A. Merritt, K.P. Moran, and D.C. Welsh, 1987: The precision and relative accuracy of profiler wind measurements. J. Atmos. and Oceanic Tech., 4, 563-571.

Uttal, T., J.B. Snider, R.A. Kropfli, and B.W. Orr, 1990: A remote sensing method of measuring atmospheric water vapor fluxes: application to winter mountain storms. J. Appl. Meteor., 29, 22-34.

Velleman, P.F., and D.C. Hoaglin, 1981: Applications, Basics, and Computing of Exploratory Data Analysis. Duxbury Press, Boston, MA.

Weber, B.L., and D.B. Wuertz, 1990: Comparison of rawinsonde and wind profiler radar measurements. J. of Atmospheric and Oceanic Technology, 7, 157-174.

Weber, B.L., D.B. Wuertz, R.G. Strauch, D.A. Merritt, and K.P. Moran, 1990: Preliminary evaluation of the first NOAA Demonstration Network wind profiler. J. of Atmospheric and Oceanic Technology, 7, 909-918.

Westwater, E.R., M.T. Decker, and M.J. Falls, 1985a: Remote sensing of atmospheric water vapor by ground-based microwave radiometry. Moisture and Humidity: Measurement and Control in Science and Industry, Instrument Society of America, 259-268.

Westwater, E.R., W. Zhenhui, N.C. Grody, and L.M. McMillin, 1985b: Remote sensing of temperature profiles from a combination of observations from the satellite-based microwave sounding unit and the ground-based profiler. J. Atmos. & Oceanic Tech., 2, 97-109.

Wuertz, D.B. and B.L. Weber, 1989: Editing wind profiler measurements. NOAA Tech. Rpt., ERL 438-WPL 62, Boulder, CO, 78 pp.

Wuertz, D.B., B.L. Weber, R.G. Strauch, A.S. Frisch, C.G. Frisch, C.G. Little, D.A. Merritt, K.P. Moran, and D.C. Welsh, 1988: Effects of precipitation on UHF wind profiler measurements. J. of Atmos. & Oceanic Tech., 5, 450-465.

## APPENDIX A. FIRS

The WPL infrared spectrometer system is known as FIRS (Fourier-transform InfraRed Sounder). Its central component is a Michelson interferometer manufactured by Bomem, Inc. Figure A1 is a diagram of the system; the Michelson interferometer comprises a beam splitter (BS) and two corner-cube mirrors (CC). Scanning the mirrors to create a varying optical path difference between the beam splitter and corner-cube mirrors creates an interferogram that is equivalent to the autocorrelation of the input radiance; the Fourier transform of the interferogram is the emission power spectrum. As a dual-emission device, the spectrometer has two complementary input ports into which external sources emit thermal radiation. The detected signal is the difference of the radiation from the two external sources. At one port we have a liquid-nitrogen reference that provides the dynamic range to allow measurements of low-radiance sources. At the other port is a beam-steering mirror (M1) that selects one of three sources: the sky, a warm blackbody simulator (BB1), and a cold blackbody simulator (BB2). These three sources are viewed sequentially and the atmospheric-emission spectrum is calibrated from the spectra of the two blackbody simulators using a two-point complex calibration scheme (Revercomb et al., 1988).

Radiation from the interferometer is focused by off-axis parabolic mirrors (M3, M4), through a variable field stop (FS), onto a mercury-cadmium-tellurium detector (Det) with a peak detectivity ($D^*$) approximately equal to $1.8 \times 10^{10}$ cm $Hz^{1/2}$ $W^{-1}$ at 15.4 $\mu$m. The detector half-power cutoff wavelengths are roughly 6.5 $\mu$m and 20.8 $\mu$m. At locations where removal of alignment-critical optics is necessary to replace the window, we used ZnSe windows; in other, more accessible locations, we used KBr windows. Though the hygroscopic KBr windows will occasionally require replacement, their higher infrared transmissivity is desirable for low-radiance atmospheric measurements.

FIRS measures spectral radiance between 550 and 2000 $cm^{-1}$ (5.0-18.2 $\mu$m) with spectral resolution variable from 1 $cm^{-1}$ to 128 $cm^{-1}$. We anticipate operating the system usually at near-maximum spectral resolution to resolve the various temperature- and humidity-dependent emission features in the spectra. A variable-diameter field stop provides a variable full-angle field of view from 3.6 to 46 mrad. Normally, 35 mrad (2°) will be used to match the angular field of view of the WPL microwave and single-channel infrared radiometers so that the radiance from a common atmospheric volume will be measured with several complementary sensors.

Signal-to-noise ratios of about 1000 are achievable with 2-min integration times. Ground-based operation allows such long dwell times if the atmospheric remains thermodynamically stable during the measurement. If clouds are present, this will not be

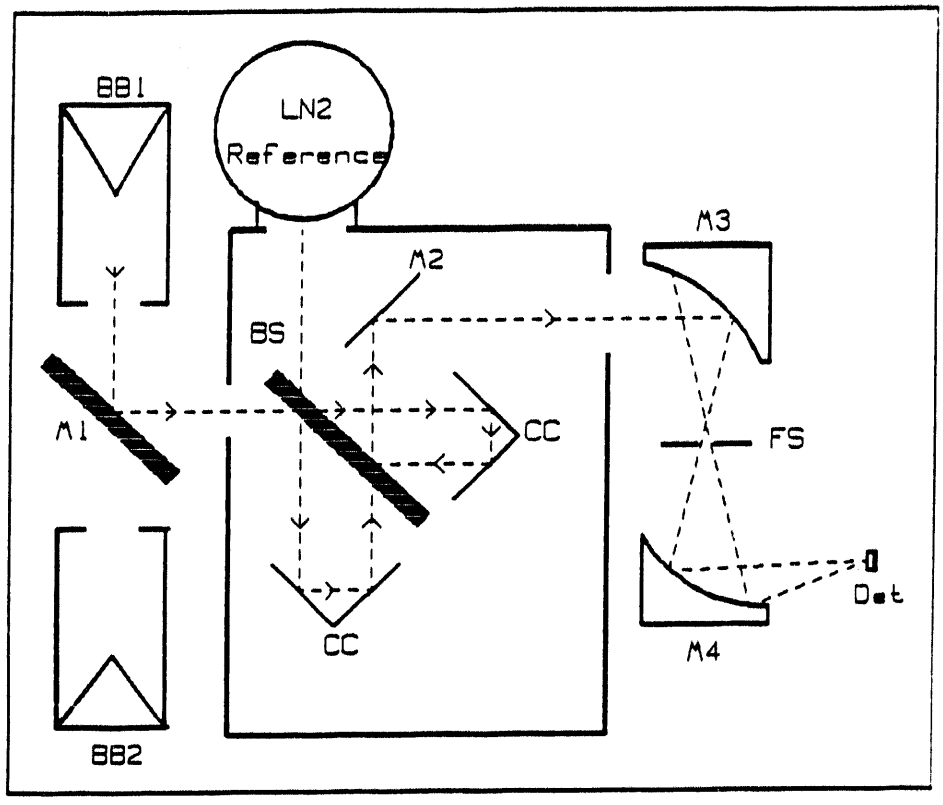


Figure A1. Diagram of the WPL FIRS system. See text for details.

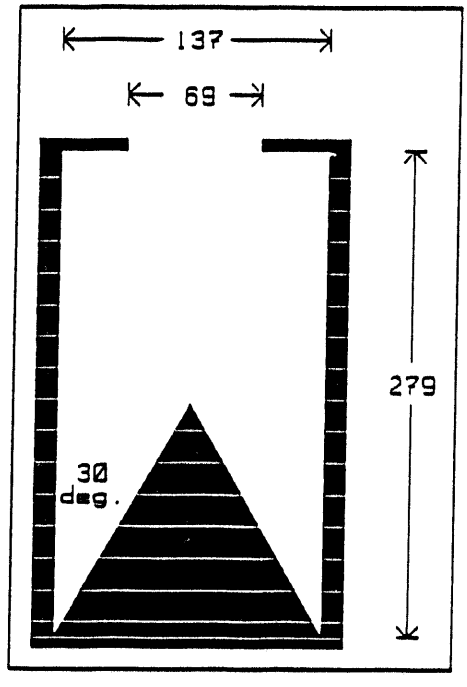


Figure A2. Inner-cone blackbody simulator geometry (dimensions in mm).

true, because clouds may drift in and out of the beam within two minutes. However, if clouds are present, other questions regarding the usefulness of FIRS for atmospheric profiling arise. We are studying the effects of clouds, especially cirrus, on FIRS measurements.

Absolute radiometric calibration will be necessary for retrieving accurate temperature and humidity information from atmospheric emission spectra. FIRS uses two calibration sources at near-ambient and liquid-nitrogen temperatures (~ +300 K and 77 K) to bracket the expected range of equivalent blackbody temperatures in atmospheric spectra. In order to obtain uniform, high-emissivity calibration sources, two black-anodized aluminum inner-cone cavities with annular lids shown in Figure A2 are incorporated (Bedford et al., 1985, Berry 1981, and Chu et al., 1980). Though these cavities are larger and heavier than flat-plate blackbody simulators, they have higher emissivity and less chance of reflecting interfering radiation into the instrument. Furthermore, weight and size are secondary concerns for ground-based operation. The cavities have a large thermal mass to reduce thermal gradients. We are studying the thermal stability of these cavities and will consider reconstructing them from copper if higher thermal conductivity is needed. Aluminum rather copper was chosen for the prototype cavities because it is easier to machine.

To determine the emissivity of our calibration cavities, we used the results of Bedford et al. (1985) for the dimensions indicated in Fig. A2. These results indicate that the effective emissivity on the surface of our inner cones varies from approximately 0.9994 at the base to 0.9985 at the cone's tip. With its widest field of view, our spectrometer sees only the top two-thirds of the inner cone; thus, the effective emissivity seen by the spectrometer varies between approximately 0.9990 and 0.9985. These results are for a perfectly isothermal cavity, so the actual emissivity of our cavities, though still high, is less ideal than these numbers suggest.

WPL is in the midst of implementing and evaluating an absolute radiometric calibration scheme for FIRS. The design goal for the FIRS calibration is to have an absolute error no greater than 1.0 K (WPL's microwave radiometers achieve this in the lower atmosphere). Absolute radiometric calibration requires determination of two unknown factors: the complex instrument-response function and the spectral radiance emitted by the optics. The radiance bias, or offset, caused by emission from the system is especially important in the measurement of weak-signal sources such as atmospheric emission. In other interferometer-spectrometer applications, where the source radiance is much greater than the instrument's self-emission, the offset can be neglected. The calibration technique being implementing will use complex spectra to compensate for both

magnitude and phase errors.

WPL has recently completed construction of the prototype FIRS system and we are beginning to examine data collected with it. Figure A3 shows a raw, uncalibrated emission spectrum of a clear sky collected with FIRS. Figure A4 is a spectrum taken soon afterward but with cirrus clouds in the beam. The cirrus clouds increase the radiance in the 1000-$cm^{-1}$ (10-$\mu$m) window region, but do not significantly affect other, more opaque spectral regions. The long-wave cutoff of the detector is evident below 700 $cm^{-1}$ (beyond 14.3 $\mu$m) in both spectra. Observable atmospheric emission features in Figures A3 and A4 include water-vapor emission from roughly 1250 to 2000 $cm^{-1}$ (5 to 8 $\mu$m), carbon dioxide emission in the 600-720 $cm^{-1}$ (14-16 $\mu$m) region, and water vapor emission again below 600 $cm^{-1}$ (above 17 $\mu$m). Also, the window region of 770 to 1100 $cm^{-1}$ (9-13 $\mu$m) is visible, with many small carbon dioxide and water vapor emission features enclosed within it.

Many carbon dioxide emission features have a strong temperature dependence, making them good temperature-sensing channels. Similarly, the numerous water vapor lines in the spectra provide humidity-profile information. For example, at some wavelengths, such as near 8 $\mu$m and 17 $\mu$m, water vapor emission (or absorption) is quite high (see Fig. A4), while at other wavelengths, such as near 9 $\mu$m, water-vapor emission is moderately low. Measurements of thermal emission at wavelengths with high emission are effectively measurements of water vapor near the ground for a ground-based sensor. Conversely, measurements of thermal emission at wavelengths with moderately low emission correspond to water vapor higher in the atmosphere. Many of the water vapor emission lines in the 9-11 $\mu$m window are weak enough that a measurement of their emission reflects column-integrated vapor amounts rather than the vapor density at any particular height. This is because the vapor in the lower atmosphere is not opaque, and therefore the sensor "sees" a small contribution from the water vapor at all heights within the beam. This explanation, though not precise, describes the concept of how thermal emission spectra are used to derive profiles of water vapor and temperature.

As soon as the FIRS system and calibration technique are completely operational, WPL will begin testing various techniques of retrieving atmospheric profiles from its spectra. We are studying FIRS spectra of laboratory sources and of the atmosphere in order to implement and evaluate the radiometric calibration. Calibration methods and the overall system design will be refined, as necessary. The effects of clouds on FIRS spectra and profiles will be studied using the complementary suite of sensors available at WPL, including microwave and infrared radiometers, radars, lidars, and radiosondes. Unattended and continuous operation of FIRS is a longer term goal.

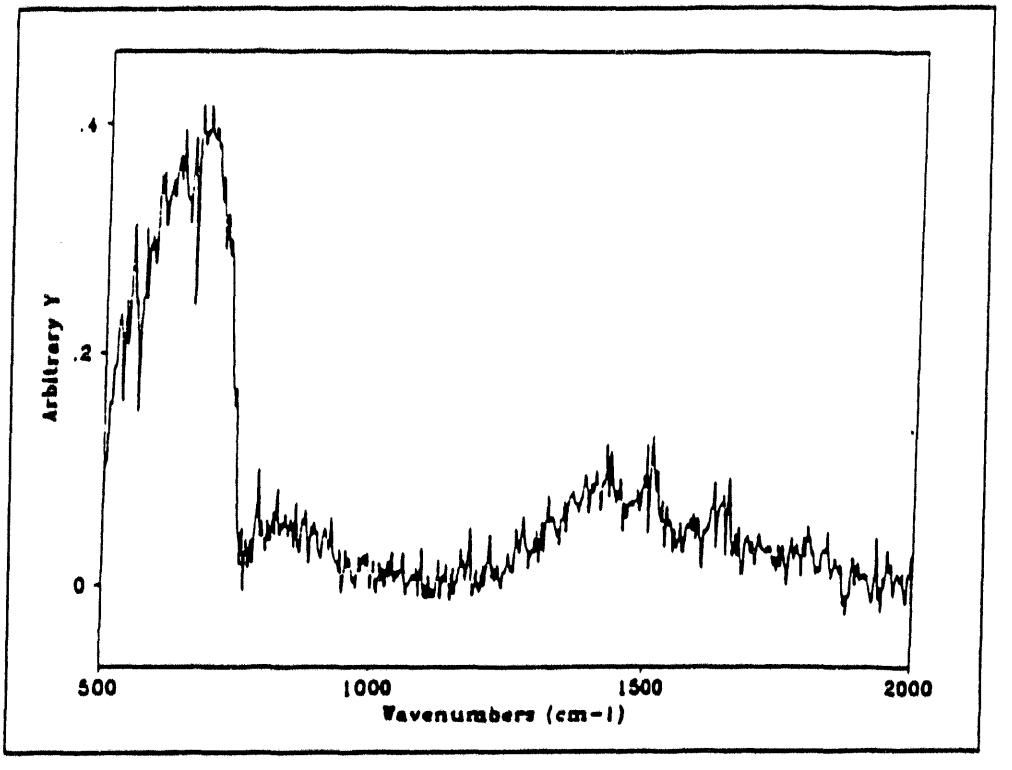


Figure A3. Example of the infrared emission spectrum measured by FIRS for a clear atmosphere.

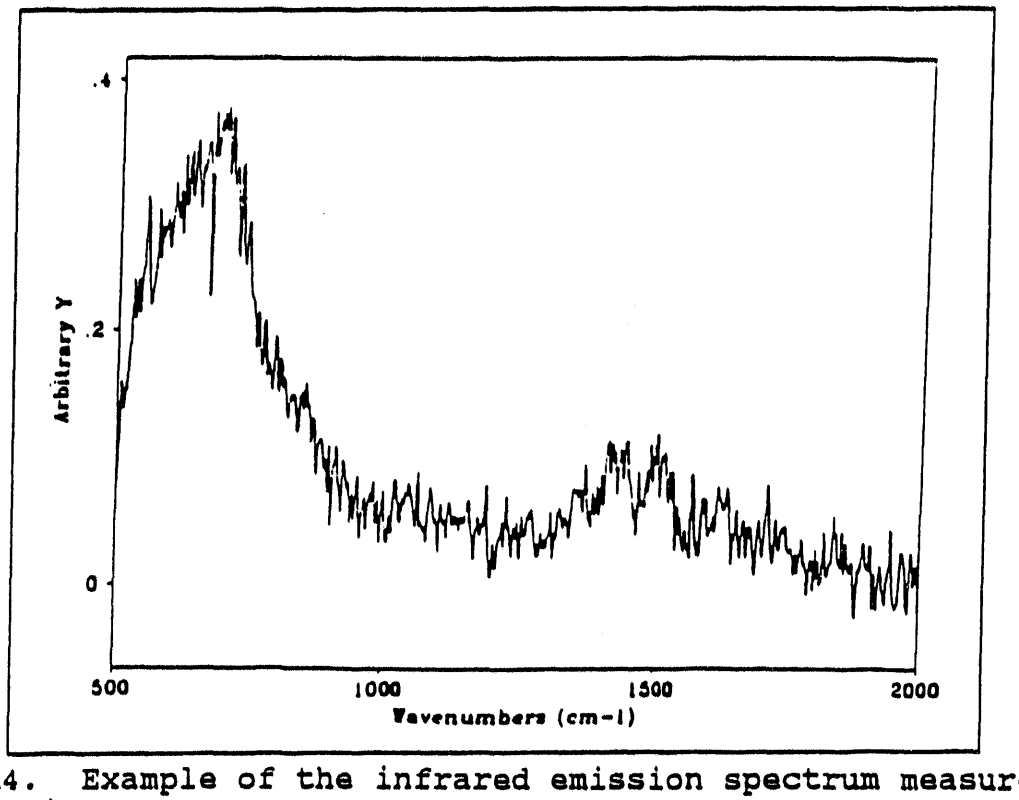


Figure A4. Example of the infrared emission spectrum measured by FIRS for cirrus clouds.

## APPENDIX B. DATA PRODUCTS FOR SELECTED IOPS

There were seven IOPs during the month-long ARM-91 field experiment (Table 2). Routine processed data products from the NOAA remote sensors are presented in this appendix for three of these cases. Wind profiler, RASS, and radiometer data are featured in these plots. The purpose is to more fully illustrate the kinds of data that can be obtained with the remote sensors, to compare their measurements with those of in situ sondes, and to highlight the superior temporal resolution of the remote profiling methods. The figures also demonstrate the consistency of the remote sensor measurements with one another and with the large-scale meteorological conditions documented by conventional upper air synoptic network of the NWS. Furthermore, the collection of figures provides a convenient starting point for detailed case study analyses. The three cases selected span the gamut of weather conditions sampled in ARM-91, ranging from cold frontal rain to clear skies.

### B.1. IOP #3: 28 FEBRUARY - 1 MARCH 1991 (VARIABLE CLOUDINESS)

This third ARM-91 IOP began with clear skies followed by broken to overcast altostratus and cirrus cloud cover over the project area. Figures B1-B3 show NWS surface, 700 mb, and 500 mb maps for selected times during the IOP. They show a weak ridge of high pressure over the Midwest and a weak trough entering western Colorado. The patterns aloft indicate veering winds and weak warm air advection over Colorado. At the surface there was south-southeasterly flow advecting warmer air into Colorado and a cold front moving southward through Montana.

Figures B4-B6 show time series of measurements obtained with WPL's microwave radiometer systems at Platteville, Denver, and Elbert. The surface meteorological observations at all three sites show a slight warming trend superimposed on the diurnal oscillation, a fairly steady rise of dewpoint temperature, and steadily falling pressure. The radiometer measurements of precipitable water vapor show an overall increase by a factor of 2-3 during the period, with the most rapid rise occurring around 1500 GMT on 28 February at Denver and Platteville and slightly earlier at Elbert, the most southerly station. The vertically integrated liquid water content measurements reveal the presence of water or mixed-phase clouds over Platteville for about 12 h starting at 1500 GMT on 28 February. Much smaller amounts of liquid were detected by the radiometers at Denver and Elbert during this period. The ceilometer measurements at Denver show that an altostratus cloud layer appeared near 3.5 km AGL at 1600 GMT on 28 February and lowered to about 1 km in the next 11 h. The infrared radiometer at Denver showed the cloud-base temperature had risen to about -10°C by the end of this 11-h period. The infrared radiometer data at Elbert show colder cloud

bases, indicating higher (or thinner) clouds, probably cirrus, were present there.

Figure B7 shows time series of precipitable water vapor measured by the three radiometers. These plots are annotated with radiosonde measurements obtained with NCAR CLASS sondes launched at Platteville and Elbert and the routine NWS launches at Denver. The computed PVW values shown for the radiosondes used the high-resolution, 6-s recording interval measurements. The CLASS surface measurements at Platteville and Elbert were apparently erroneous and have been replaced in the calculations by surface measurements at the nearby radiometer sites. The resulting agreement between radiometers and sondes is excellent, and small-scale details revealed by superior temporal resolution (2 min) of the radiometer data are evident.

The next five figures show time-height cross sections of wind data from various wind profilers operated in ARM-91. Figure B8 is a composite of data from WPL's 50 MHz profiler at Platteville and the 915 MHz high-power WPL profiler at Denver. Both the high and low sampling mode data are incorporated as well as data from a surface anemometer at Denver. The data shown have been passed through the automated time-height continuity editing algorithm of Wuertz and Weber (1989) to remove outlier points. Figure B9 shows the same data after being smoothed with the 4253HT median filter described by Velleman and Hoaglin (1981) and then linearly interpolated to a grid. The low-level data reveal a shift in the boundary layer flow from westerly to southerly winds; this layer grew from near the surface to almost 4 km MSL during the daylight hours (from 1400 GMT on 28 February to 0300 GMT on 1 March). Above 5 km there is clear depiction of a wave and its ridge axis passing the area at about 1500 GMT on 28 February. This is consistent with the synoptic situation shown in 500 mb map of Fig. B3. A jet stream core of 100 knots was evident in the profiler measurements near 250 mb at about 0700 GMT on 28 February.

The westerly component of the winds (in units of m $s^{-1}$) is shown in Fig. B10. The time-height location of the jet stream core is apparent. Figure B11 shows the southerly component speed pattern. The zero line clearly reveals the passage of the ridge aloft at 1200-1700 GMT on 28 February. The 1-h temporal resolution of the profiler data is excellent for revealing mesoscale features that would be lost in the standard NWS 12-h radiosonde data.

Figure B12 shows high-resolution wind data in the low levels measured by the Aeronomy Laboratory's 915 MHz boundary layer profiler. (Note that time increases toward the right for this wind diagram, unlike the others.) It shows quite variable height coverage during the period. Low-level circulations are revealed by this profiler that the other profilers missed because of their

higher minimum heights and coarser vertical resolution. For example, note the convergence between initial westerly and subsequent easterly flow in the lowest 0.5 km at about 0930 GMT on 28 February, and divergence in the same layer around 0100 GMT on 1 March.

Figures B13-B14 show skew-T log-P diagrams of temperature soundings obtained with RASS at Platteville and Denver and with CLASS radiosondes at Platteville for two times separated by 12 h during the IOP. The temperature agreement is very good. The weak warm air advection shown on the upper air synoptic weather maps is reflected in the slight warming detected by both RASS and CLASS in this 12 h interval. The CLASS sondes also show that the middle troposphere became much more moist; this is consistent with the radiometer data shown earlier. Time-height cross sections of temperature and potential temperature derived from the RASS measurements (augmented by surface in situ temperature measurements) are shown in Figs. B15 and B16, respectively. They show the history of an inversion near the surface that dissipated in the morning, at about 1800 GMT on 28 February. The temperature structure aloft shows the weak warming that occurred during the day.

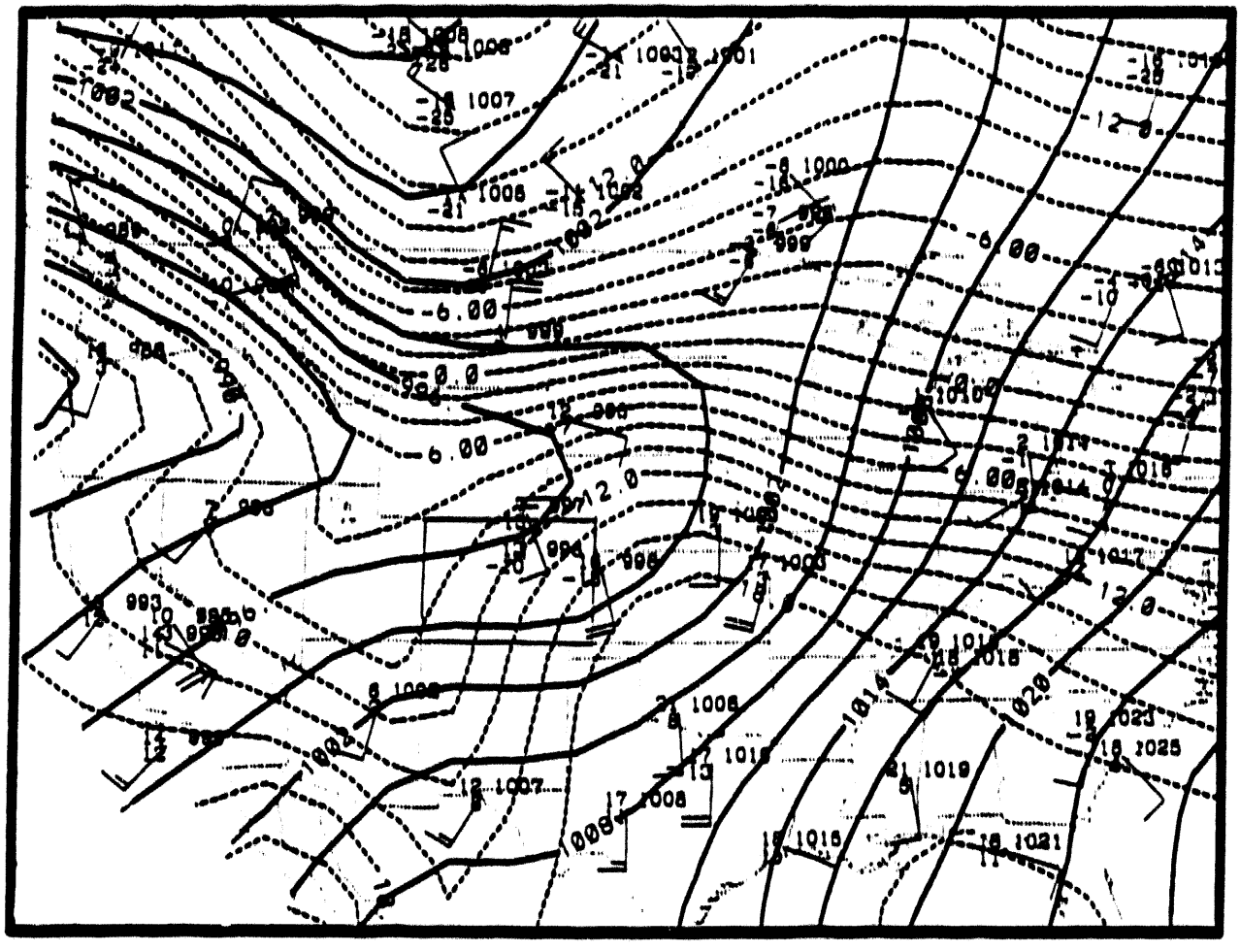

Surface
28-FEB-1991 2200 UTC

Figure B1. Surface weather map during IOP-3. Solid lines are isobars; dashed lines are isotherms.

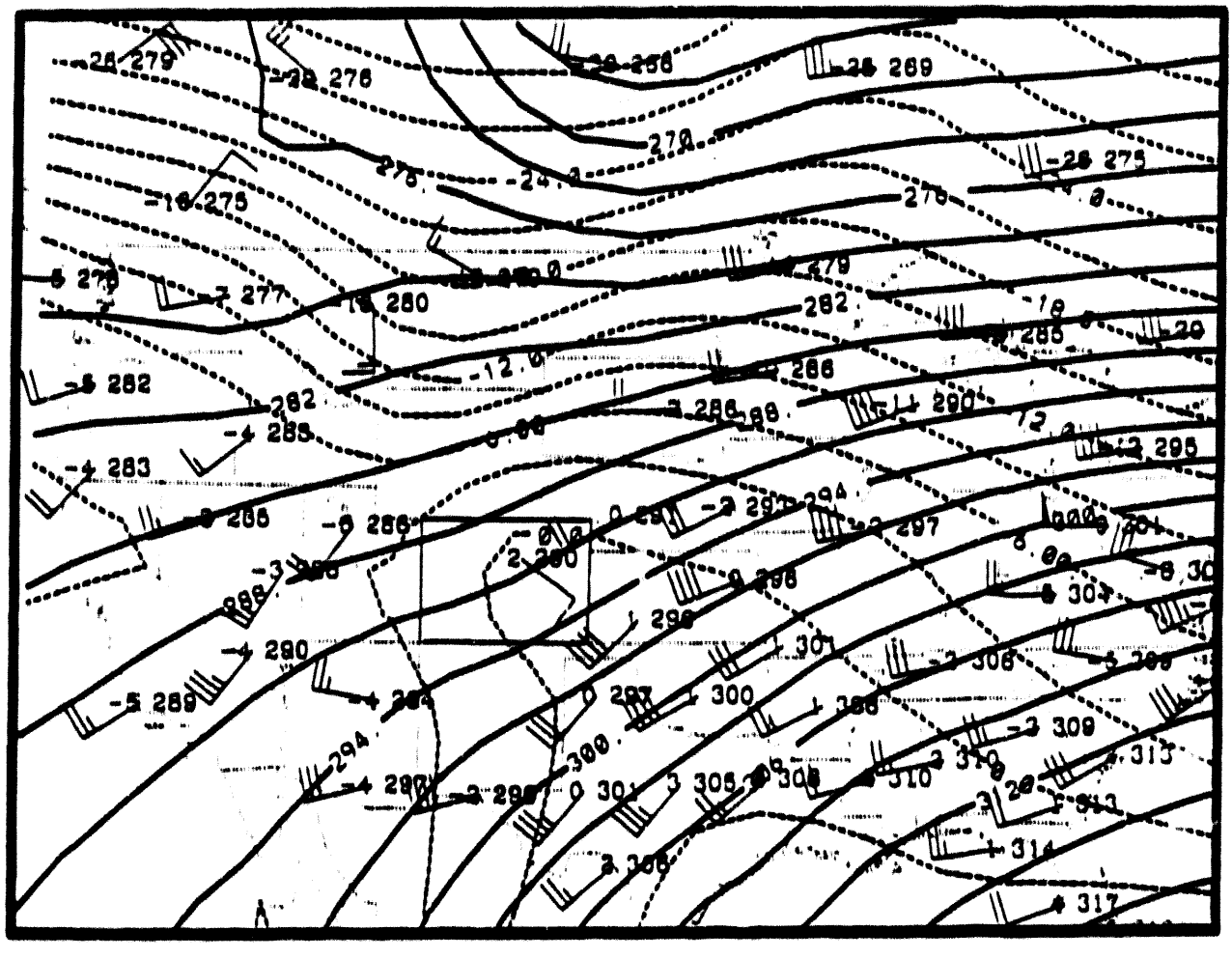

700 mb
0000 UTC 01-MAR-1991

Figure B2. A 700 mb map showing conditions aloft during IOP-3. Height contour lines are solid and isotherms are dashed.

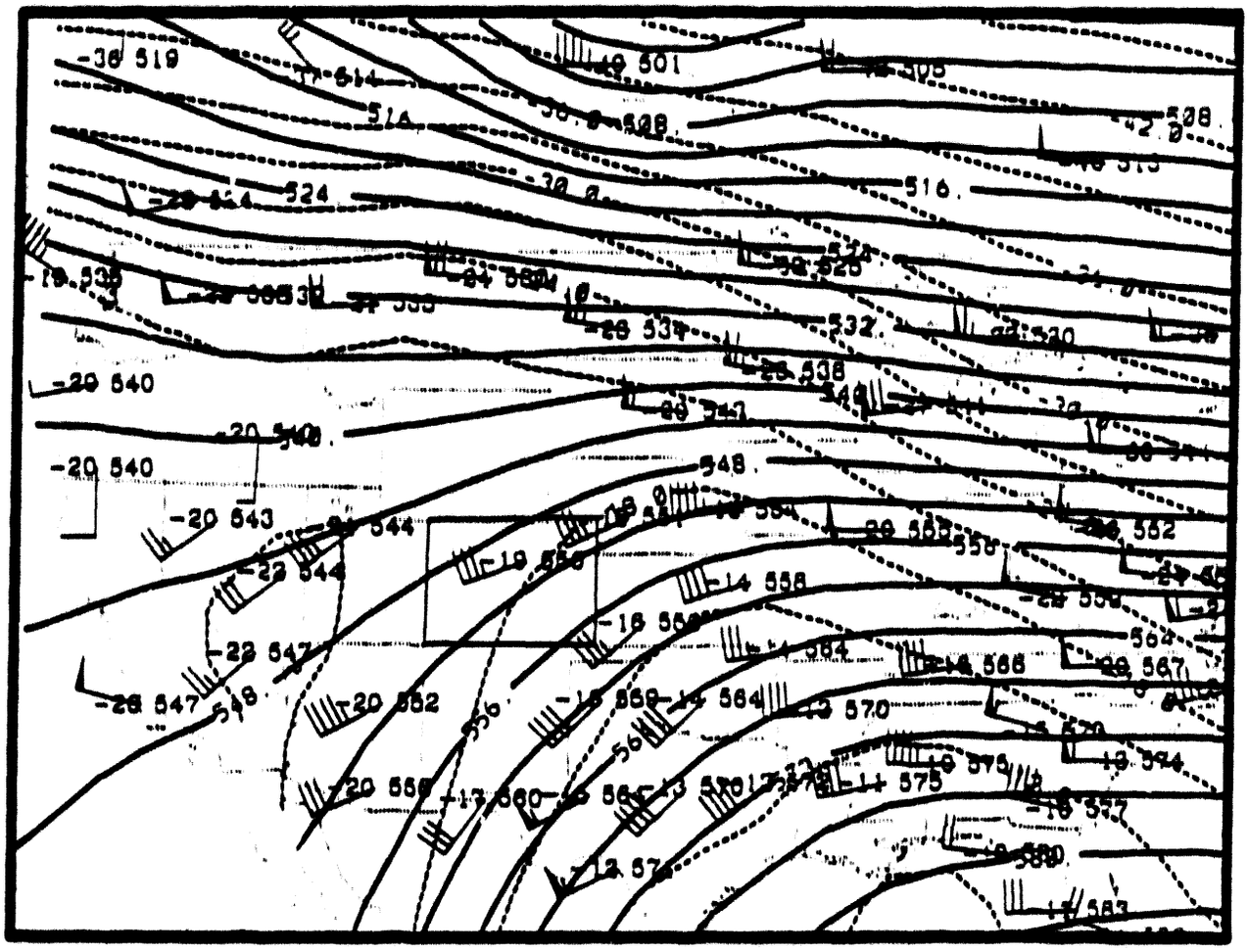

500 mb
0000 UTC 01-MAR-1991

Figure B3. A 500 mb map showing conditions aloft during IOP-3. Height contour lines are solid and isotherms are dashed.

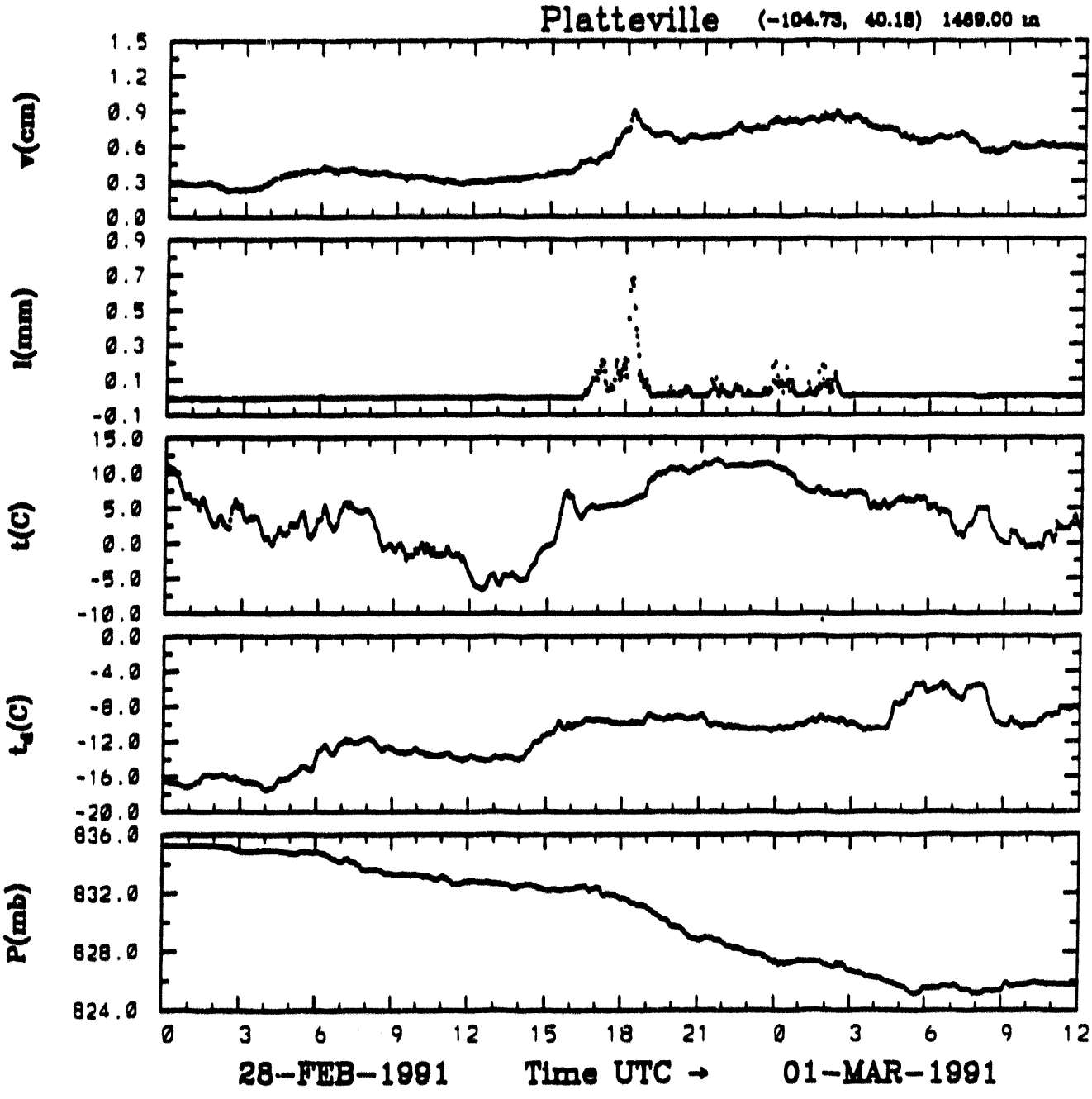


Figure B4. Data from the radiometer site at Platteville during IOP-3. Panels from top to bottom are: precipitable water vapor (v), path-integrated liquid water content (l), surface temperature (t), surface dewpoint temperature ($t_d$), and surface pressure (P).

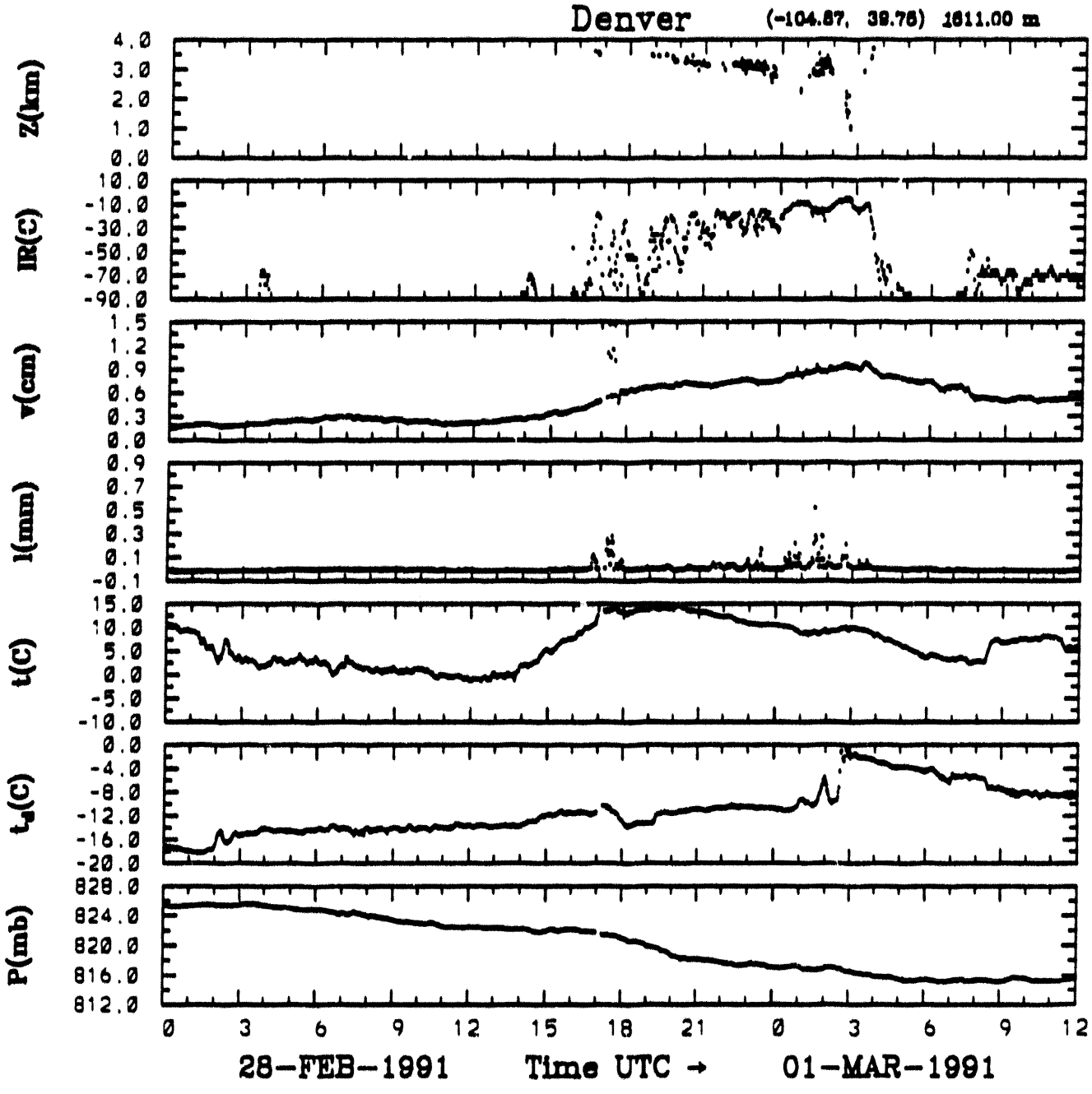


Figure B5. Data from the radiometer site at Denver for IOP-3. Panels from top to bottom are: cloud base height measured by ceilometer (Z), cloud base brightness temperature measured by infrared radiometer (IR), precipitable water vapor (v), path-integrated liquid water content (l), surface temperature (t), surface dewpoint temperature ($t_d$), and surface pressure (P).

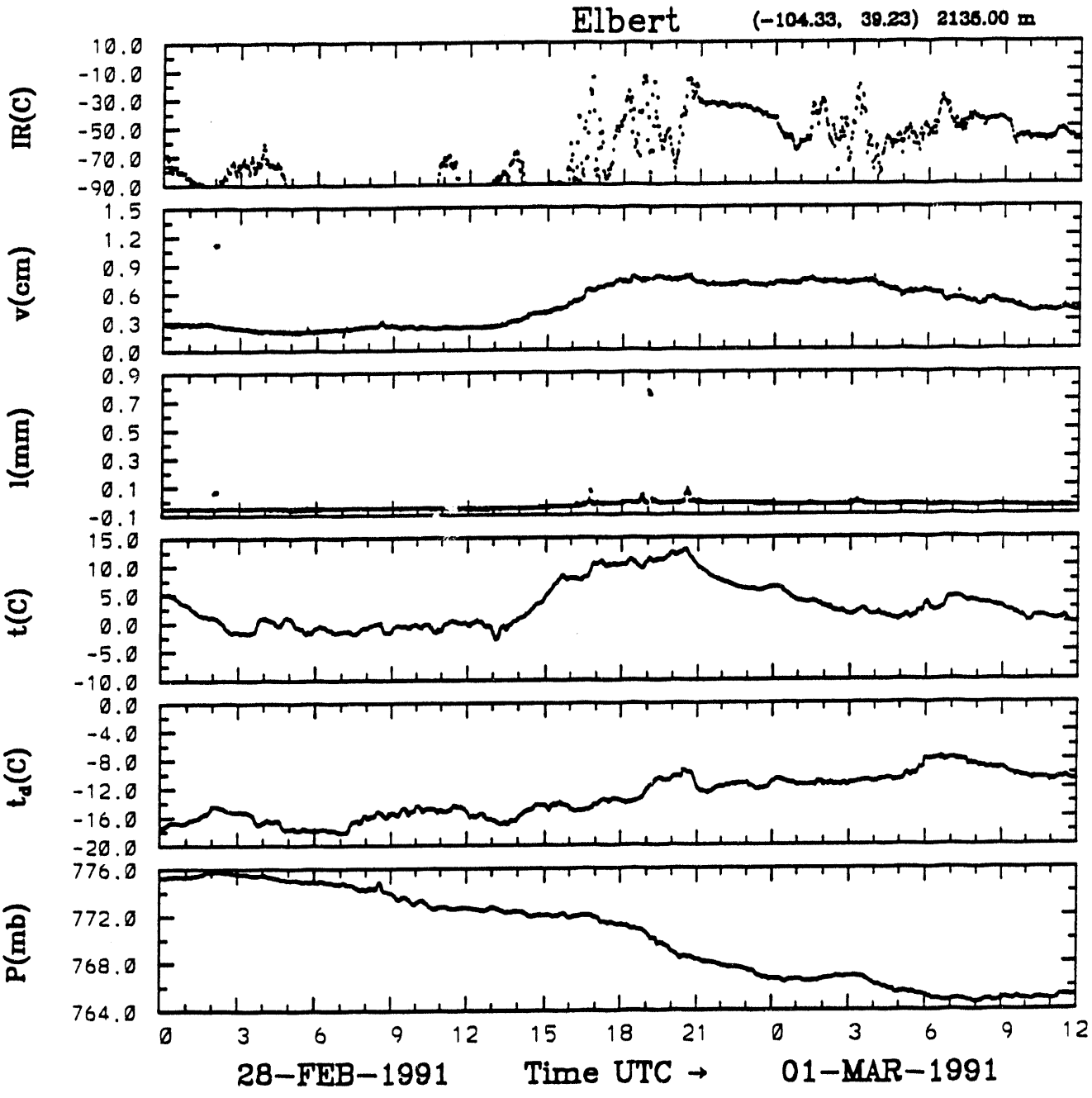


Figure B6. Data from the radiometer site at Elbert for IOP-3. Panels from top to bottom are: cloud base brightness temperature measured by infrared radiometer (IR), precipitable water vapor (v), path-integrated liquid water content (l), surface temperature (t), surface dew point temperature ($t_d$), surface pressure (P).

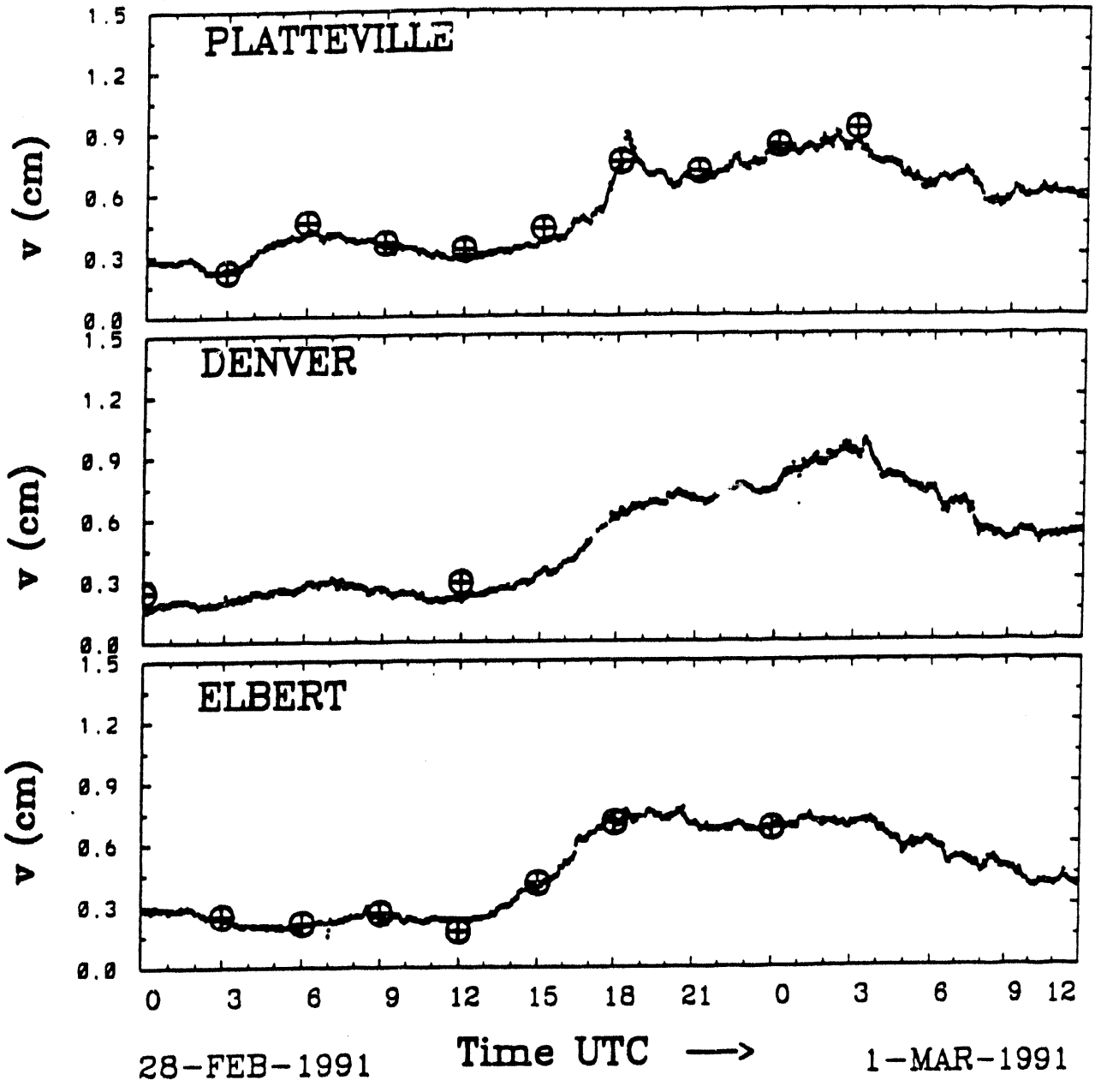


Figure B7. Precipitable water vapor measured by microwave radiometers (small dots) and radiosonde (circled crosses) at three sites during IOP-3.

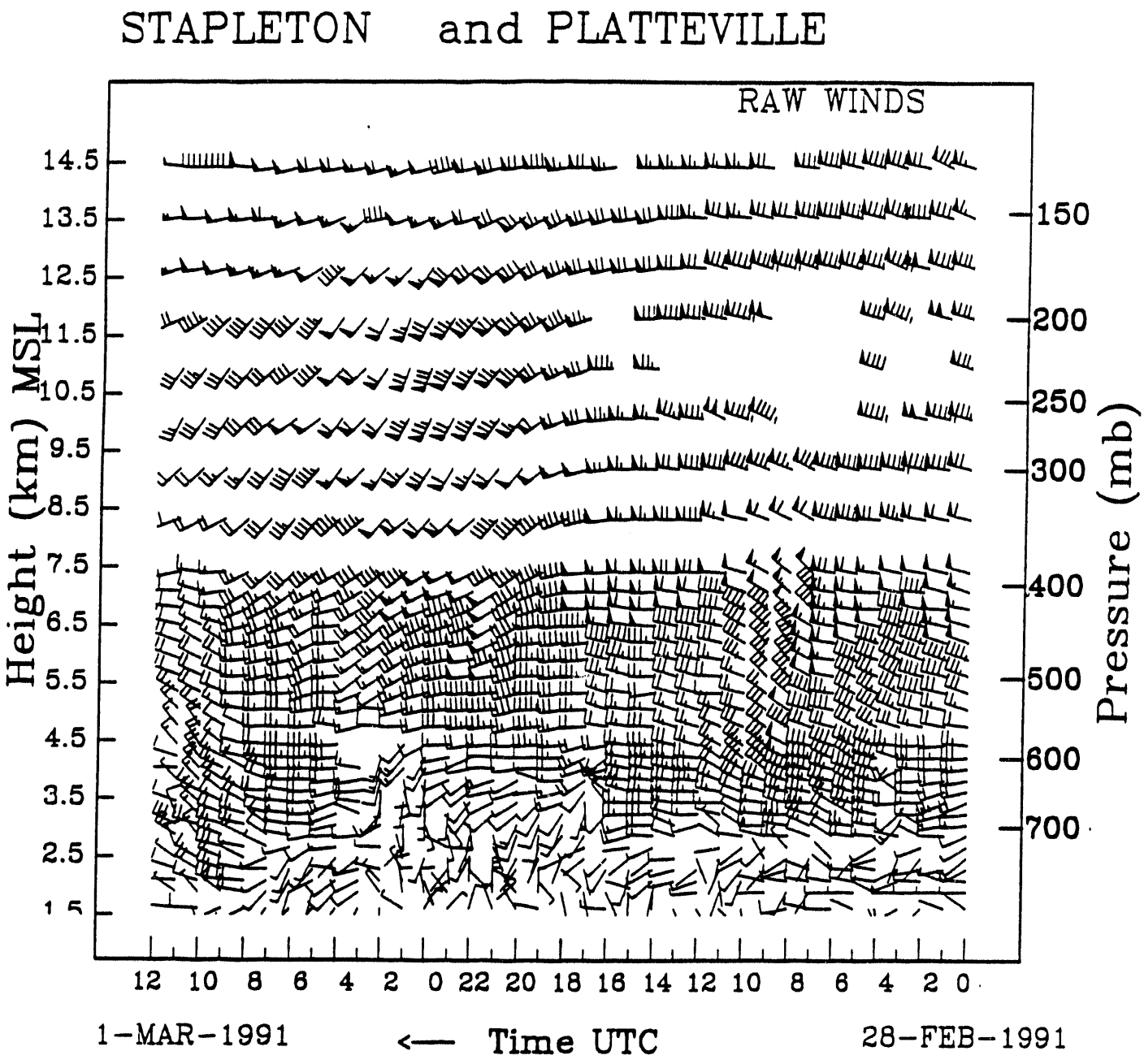


Figure B8. Time-height cross section of wind data composited from the 50 MHz wind profiler at Platteville and the high power 915 MHz wind profiler at Denver for IOP-3. Surface data are from an anemometer at Denver. Speed indicators are: short barb = 5 knots, long barb = 10 knots, flag = 50 knots.

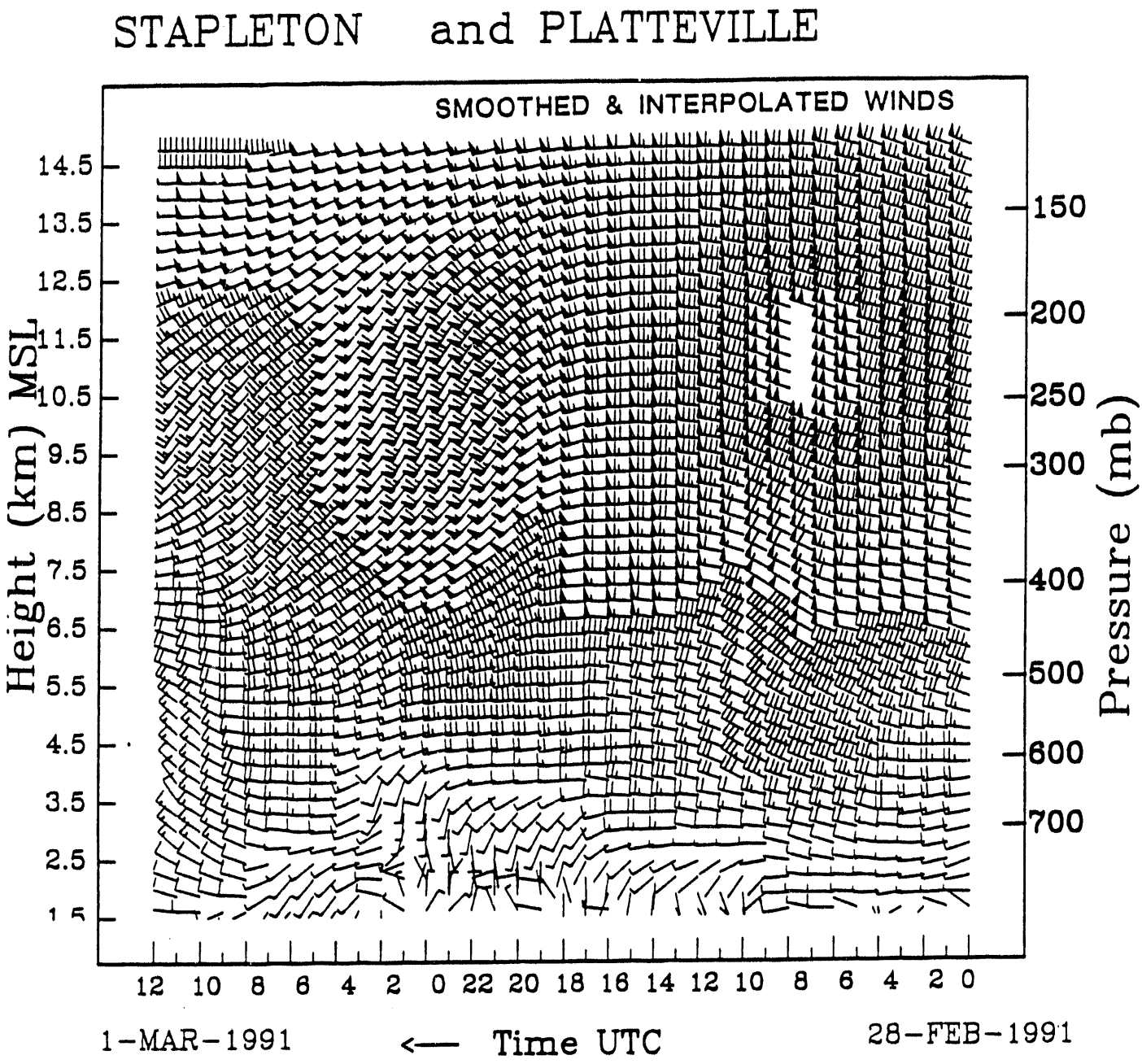


Figure B9. Wind data from the previous figure after smoothing and interpolation.

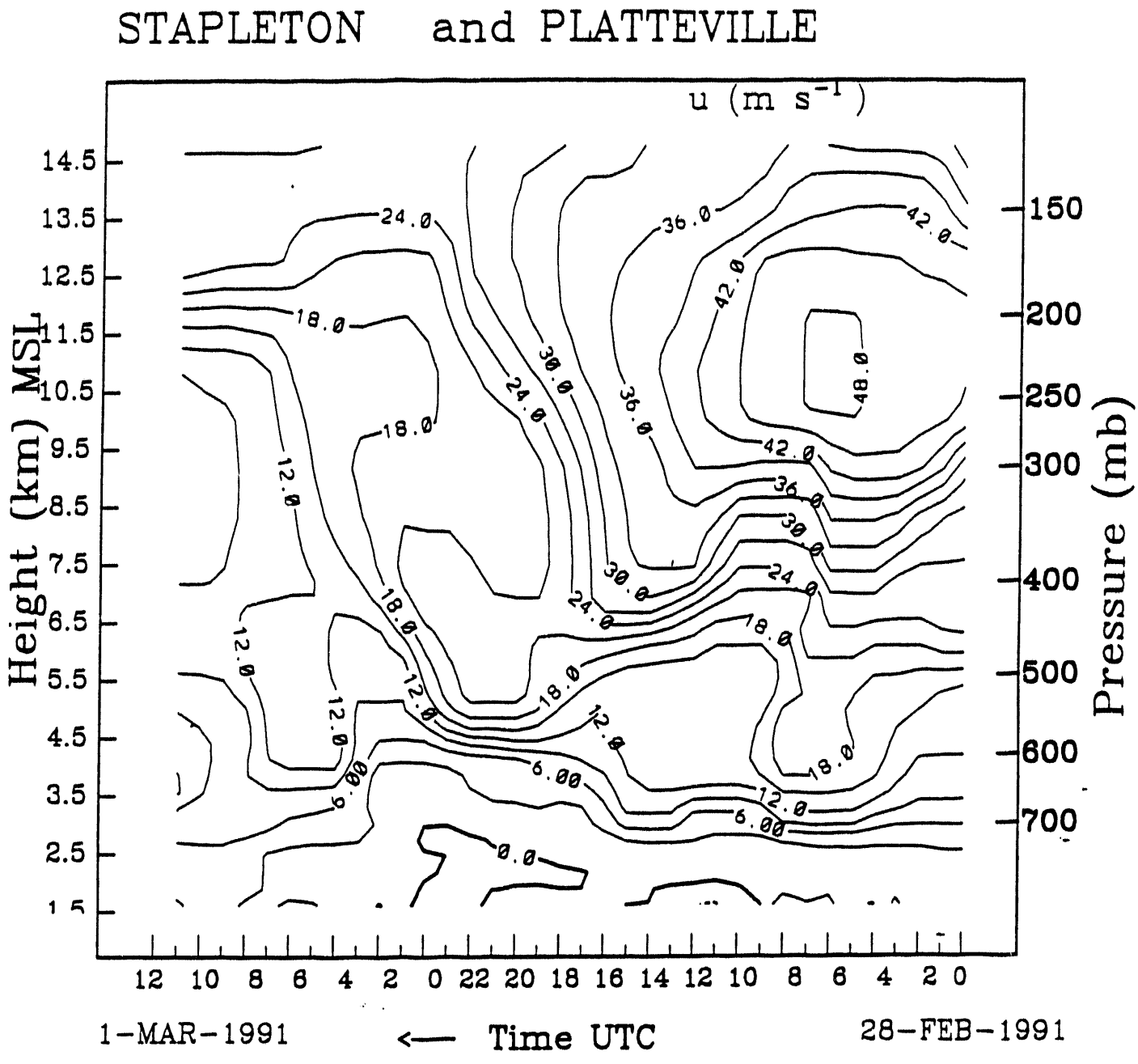


Figure B10. Time-height cross section of the westerly component of the wind data shown in the previous figure. Westerly component wind isotachs are positive (solid contours) and easterly are negative (dashed).

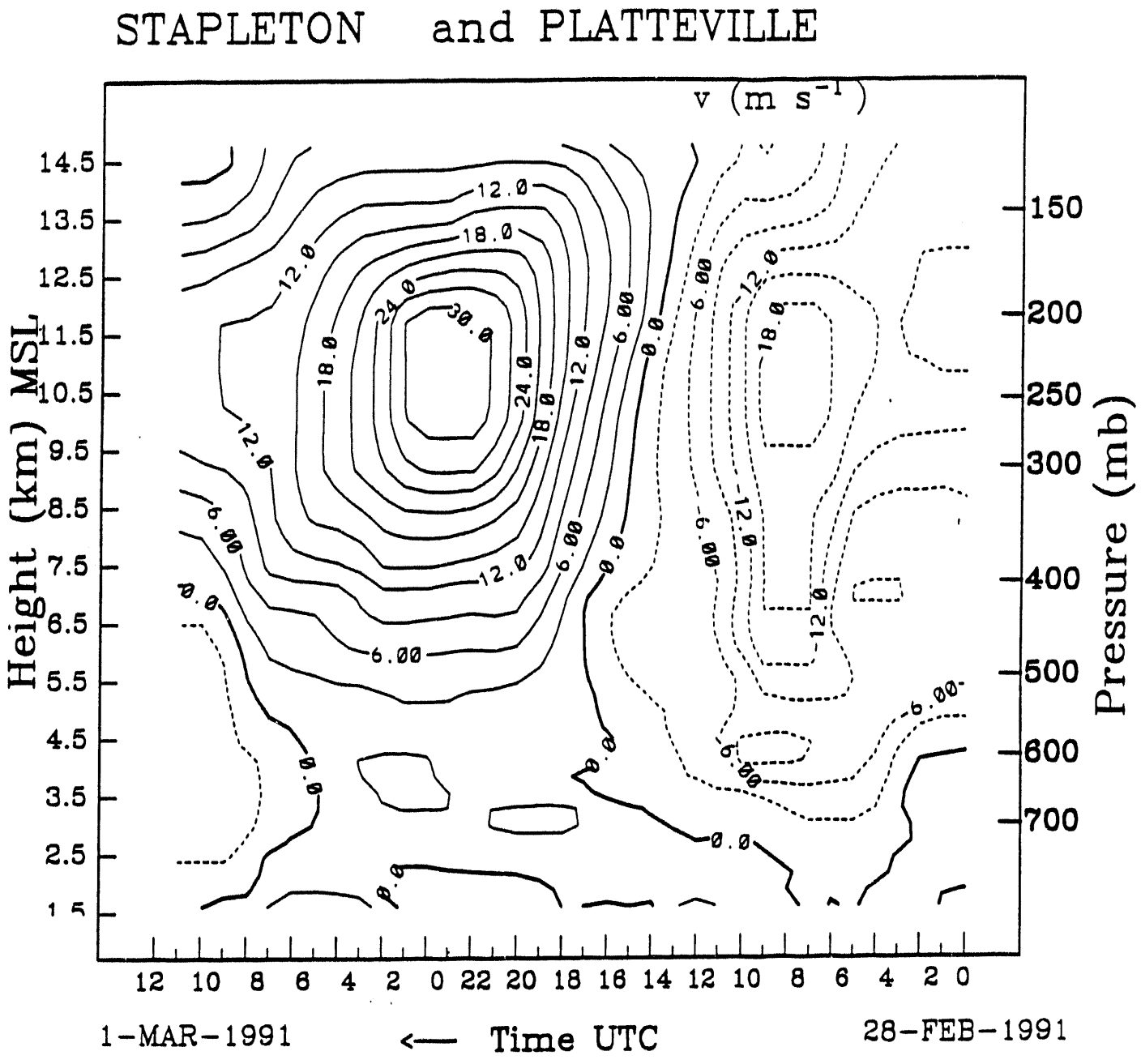


Figure B11. Time-height cross section of the southerly component of the wind data shown in the previous figures. Southerly component wind isotachs are positive (solid contours) and northerly are negative (dashed).

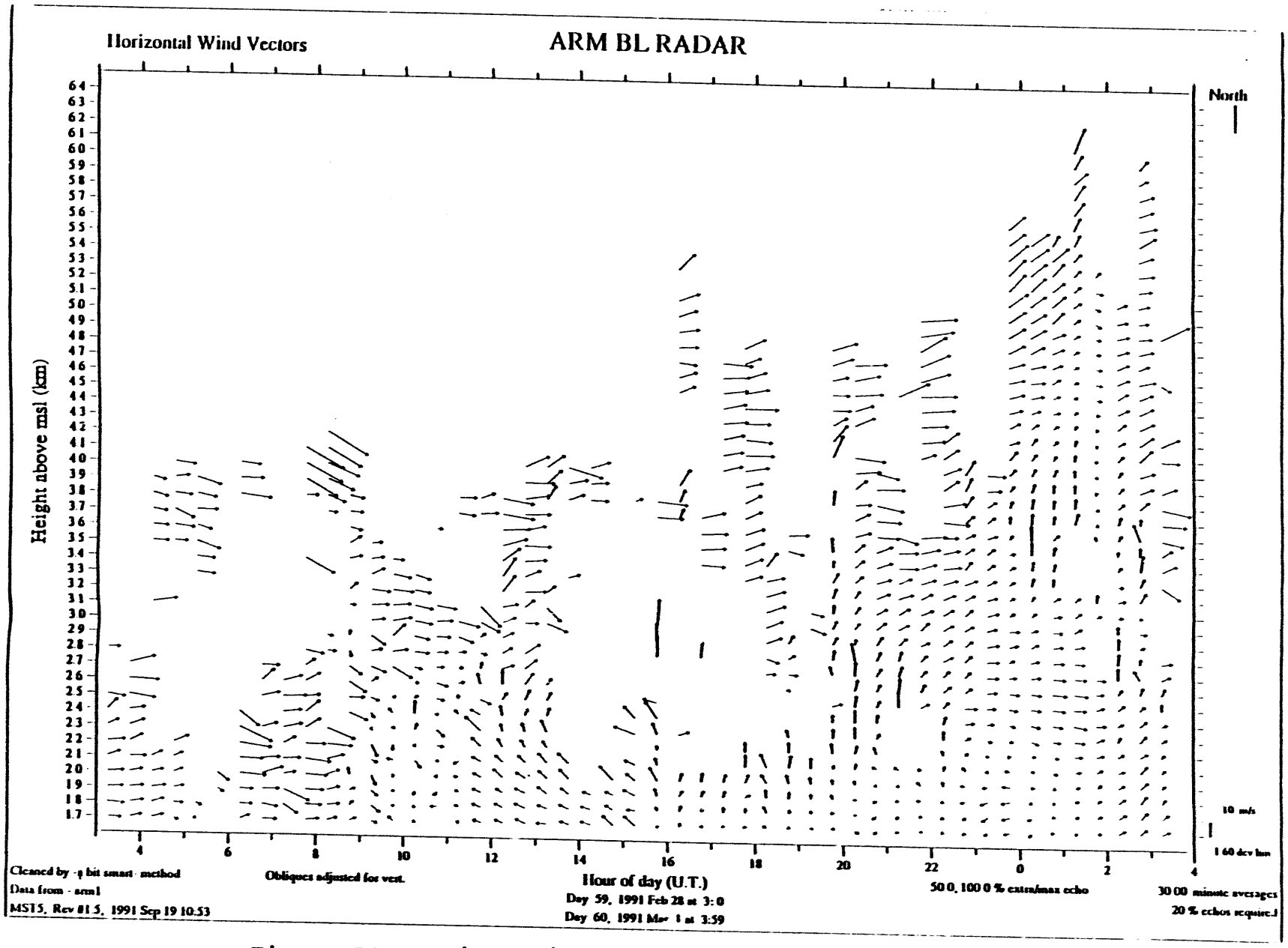


Figure B12. Time-height display of horizontal wind vectors measured by the boundary layer 915 MHz wind profiler at Platteville for IOP-3. The speed scale is shown at the lower right corner. Time increases toward the right.

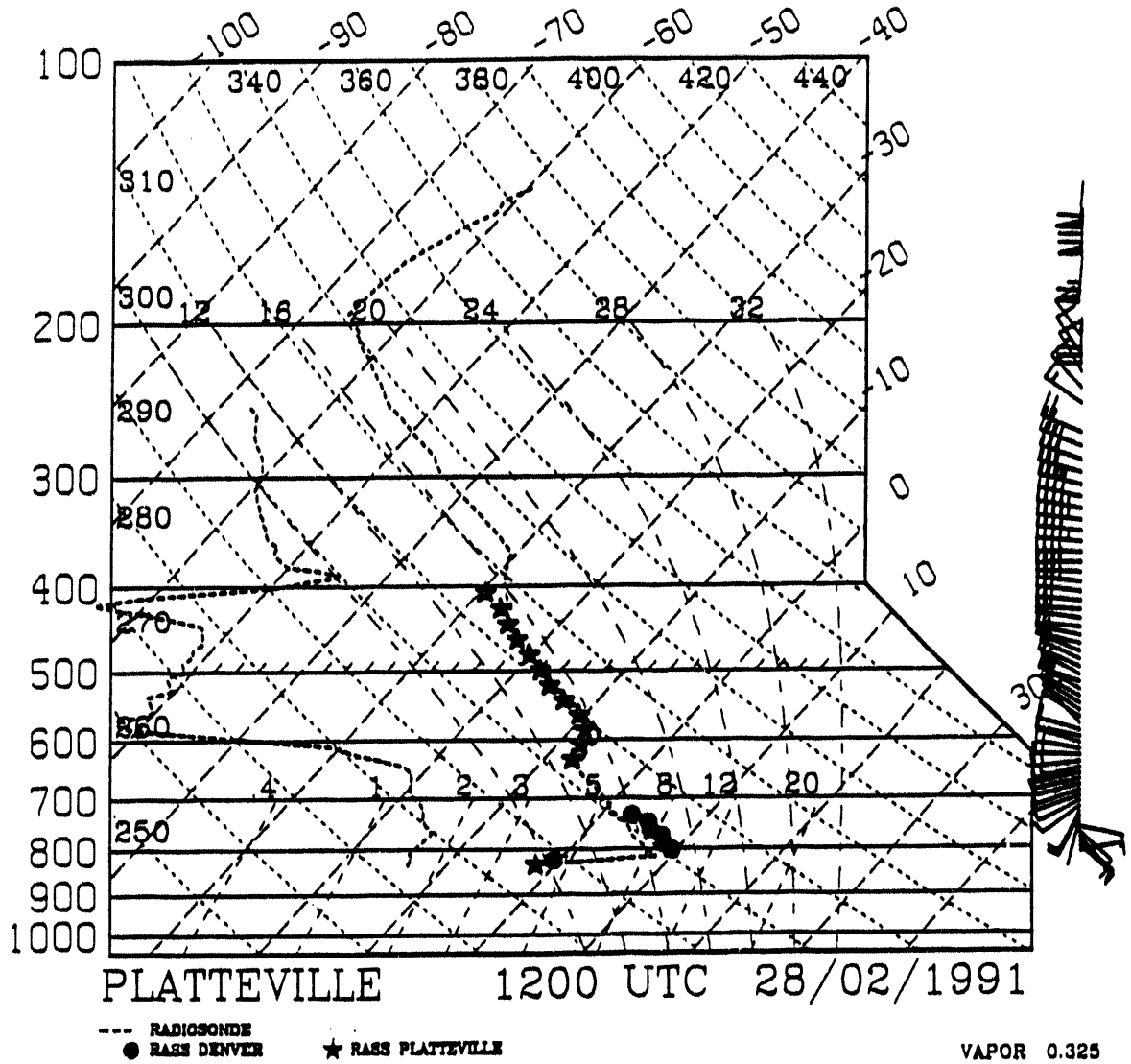


Figure B13. Temperature profiles measured by the 915 MHz RASS at Denver (solid dots) and 50 MHz RASS at Platteville (stars) for IOP-3. CLASS rawinsonde temperature and dewpoint data from Platteville are shown by the heavy dashed lines.

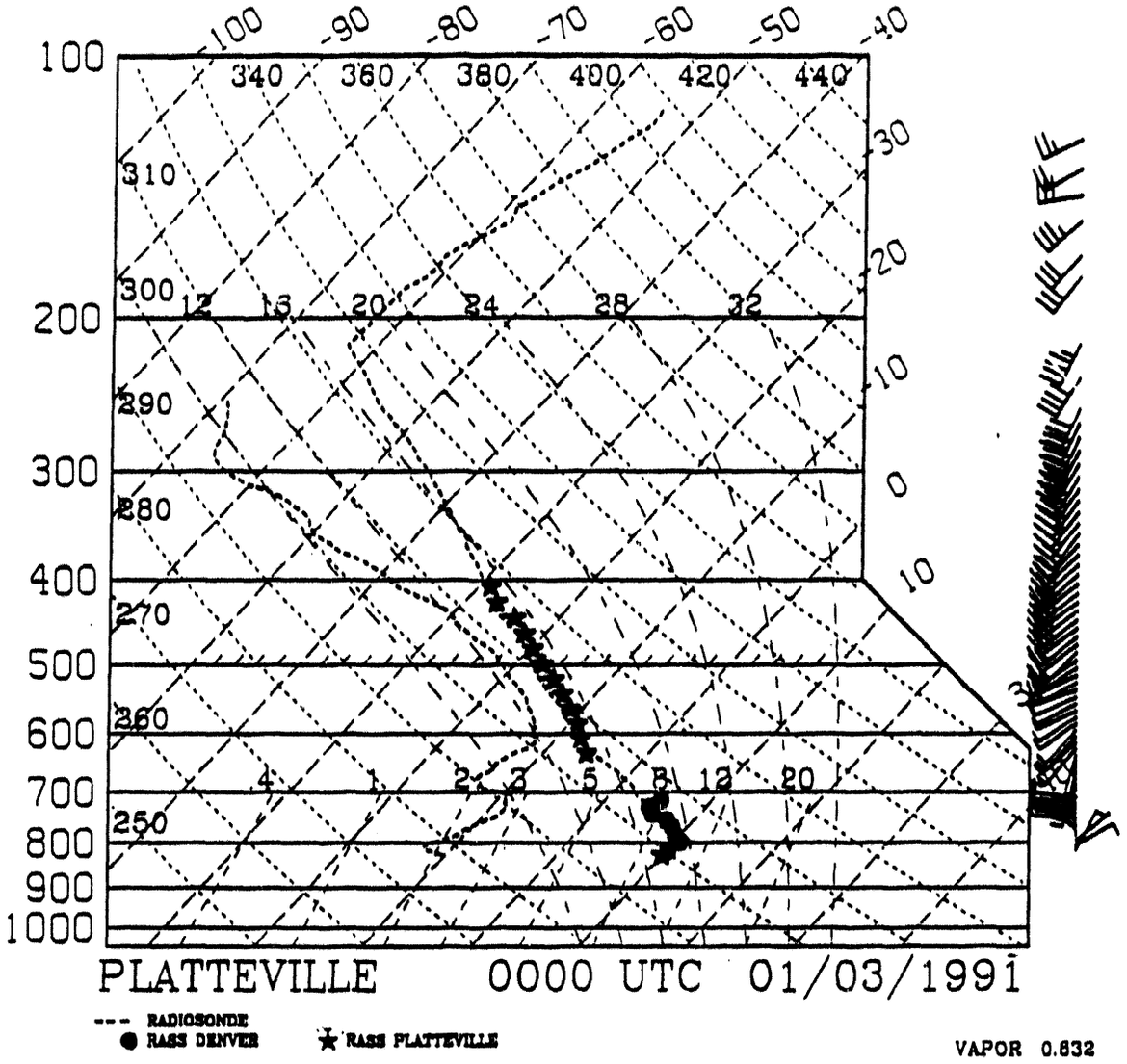


Figure B14. Same as for previous figure, except at a later time.

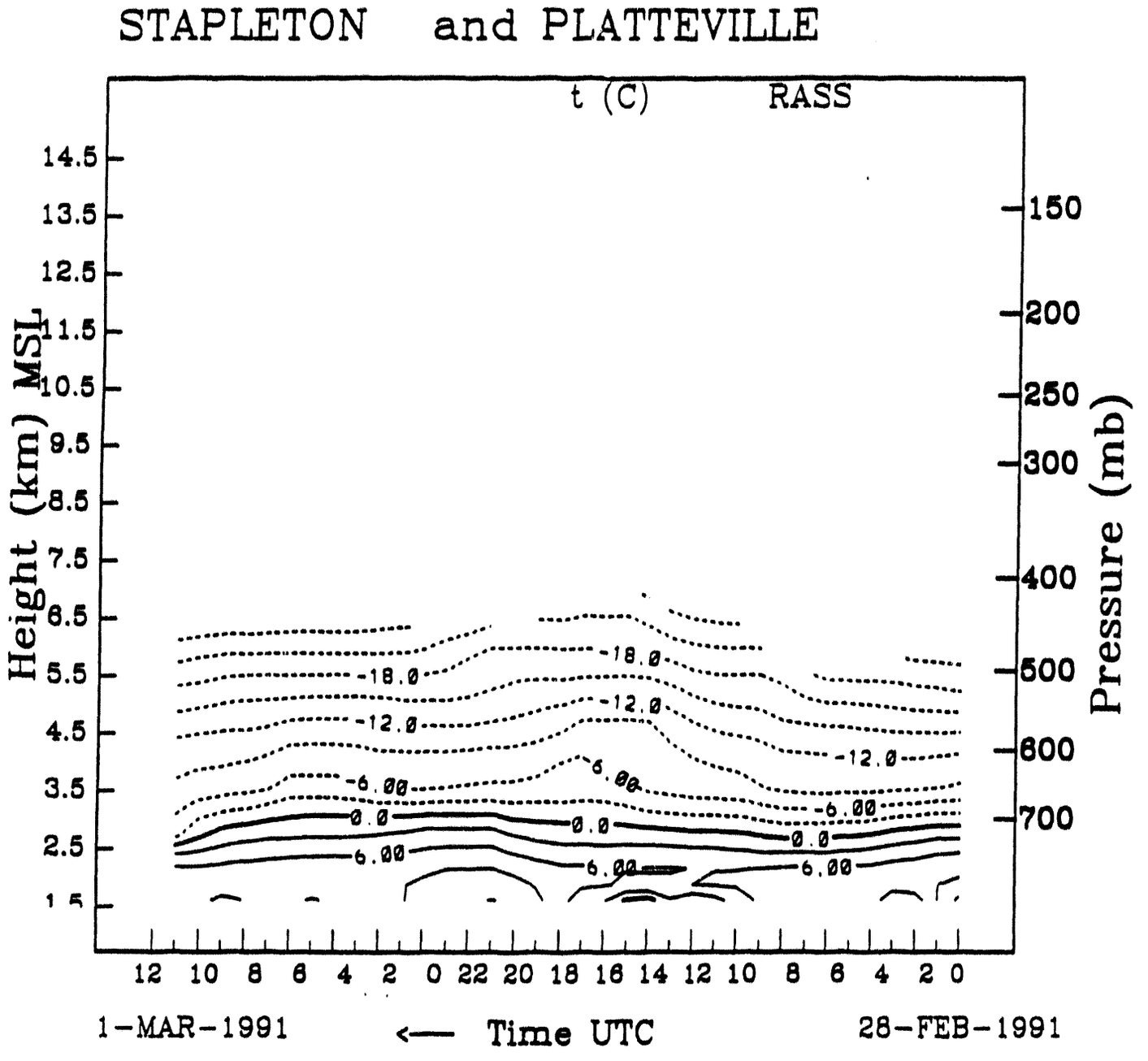


Figure B15. Time-height cross section of temperature from composite of RASS measurements at Denver and Platteville and using Denver surface temperature data during IOP-3. Temperatures above freezing are shown with solid isotherms and those below freezing have dashed isotherms.

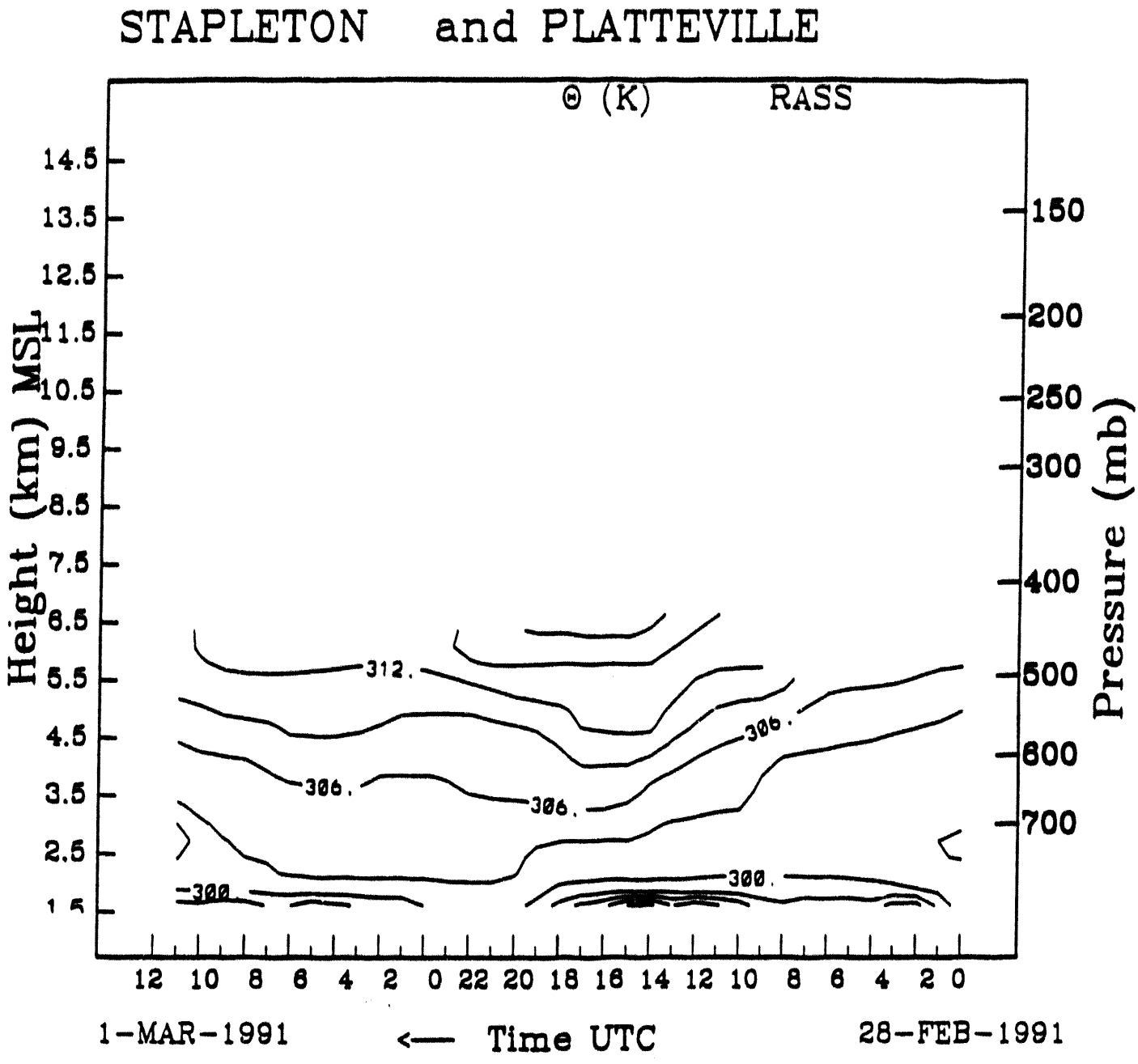


Figure B16. Time-height cross section of potential temperature derived from the RASS temperature data of the previous figure.

## B2. IOP #4: 5 MARCH - 7 MARCH 1991 (COLD FRONTAL RAIN)

The fourth IOP was conducted as a cold front swept southward through the region and brought low clouds and rain. Figures B17-B32 present the same sequence of data products that were shown for the previous case. The synoptic weather maps (Figs. B17-B19) show that a surface cold front extended from Wisconsin to Colorado. An upper air trough that tilted westward with altitude was passing over the High Plains and Rocky Mountains at 0000 GMT on 6 March. The winds backed with height, and strong cold air advection was occuring beneath 500 mb.

The radiometer system data (Figs. B20-B23) showed that the precipitable water vapor decreased steadily during the observation period at all three sites. High values of integrated liquid water content were detected near the time of frontal passage, and lower values occurred sporadically afterwards. The surface pressure and temperature data indicate the front passed on 5 March around 1800 GMT at Platteville, 2000 GMT at Denver, and 2100 GMT at Elbert. Low cloud bases were detected until late in the episode by the ceilometer and infrared radiometer at Denver and by the infrared radiometer at Elbert. As in the previous IOP, agreement between the radiometer and radiosonde-derived precipitable water vapor content was excellent.

The time-height cross sections of wind profiler data (Figs. B24-B27) do not include the high-altitude sampling mode data from the 50 MHz profiler for this case. The location of the frontal surface aloft is indicated on these cross sections by a line of sharp backing from westerly to more northerly flow. This boundary reached the low levels around 2000 GMT on 5 March and the 5 km MSL level by 0500 GMT on 6 March. The boundary layer profiler wind data (Fig. B28) extended almost 5 km above ground during precipitation early in the episode. However, the persistent northwesterly low-level winds indicated by this profiler are not consistent with those of the other profilers. The reason for the discrepancy is unknown.

The temperature profiles of Figs. B29-B30 show good agreement between the composite RASS from Platteville and Denver and the CLASS soundings at Platteville. The sonde dewpoint profiles show the drying aloft that occurred over 3 h; this supports the radiometer observations that showed a steady decrease of precipitable water vapor. The temperature time-height cross section (Fig. B31) shows the strong cooling that occurred at all levels until about 1700 GMT on 6 March. The location of the frontal boundary aloft is indicated by the large gradient of potential temperature near the 299° K contour in Fig. B32.

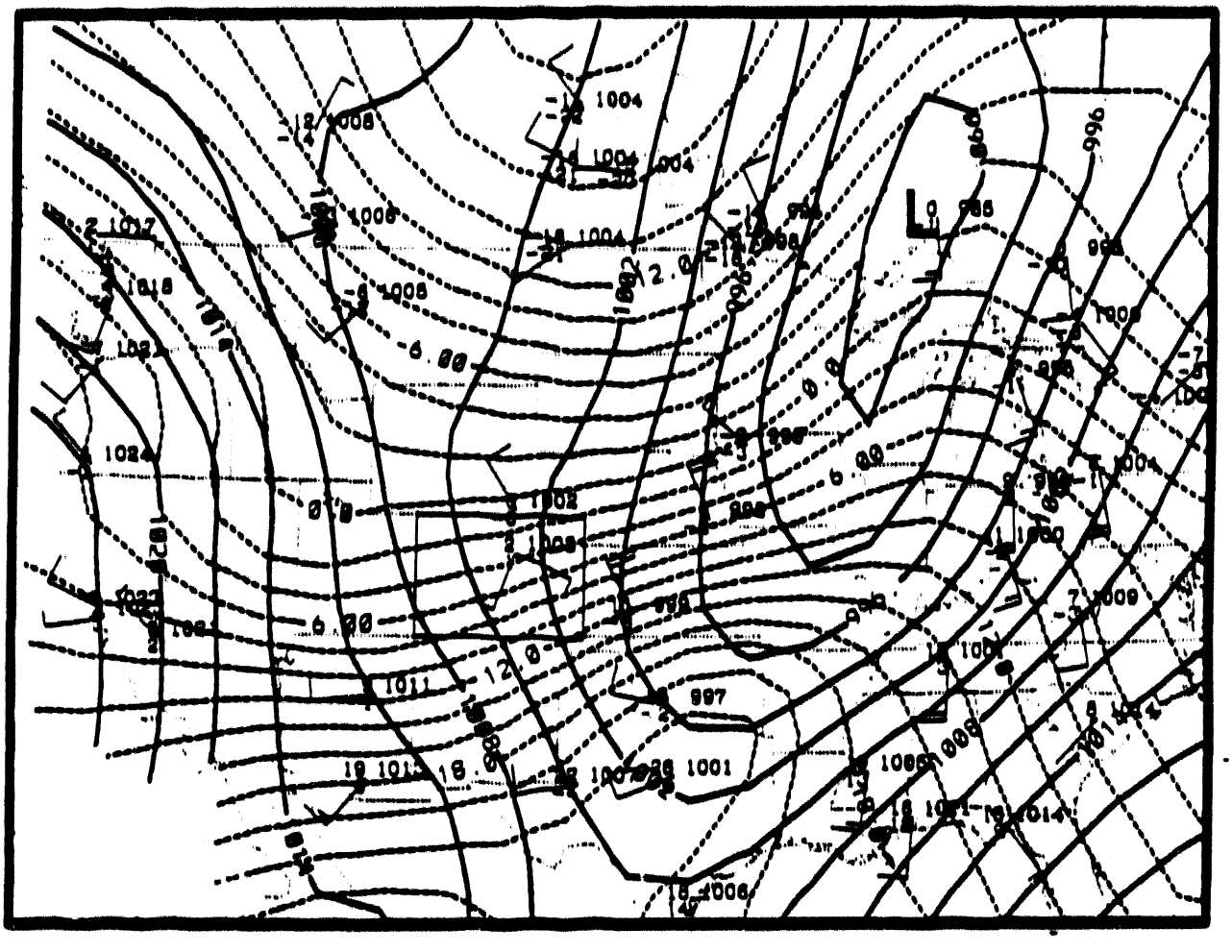

Surface
6-MAR-1991 0500 UTC

Figure B17. Surface weather map during IOP-4. Solid lines are isobars; dashed lines are isotherms.

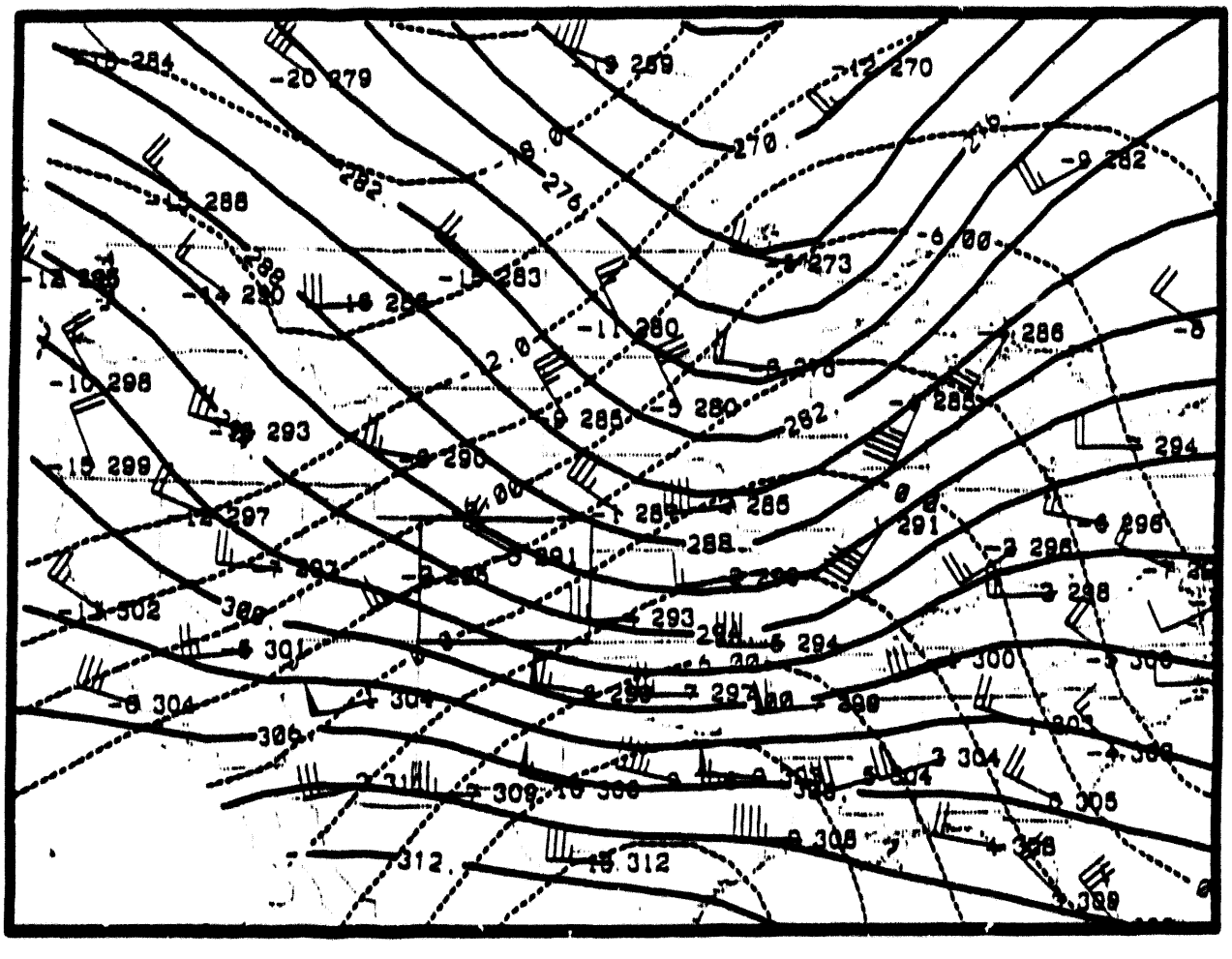

700 mb
0000 UTC 06-MAR-1991

Figure B18. A 700 mb map showing conditions aloft during IOP-4. Height contour lines are solid and isotherms are dashed.

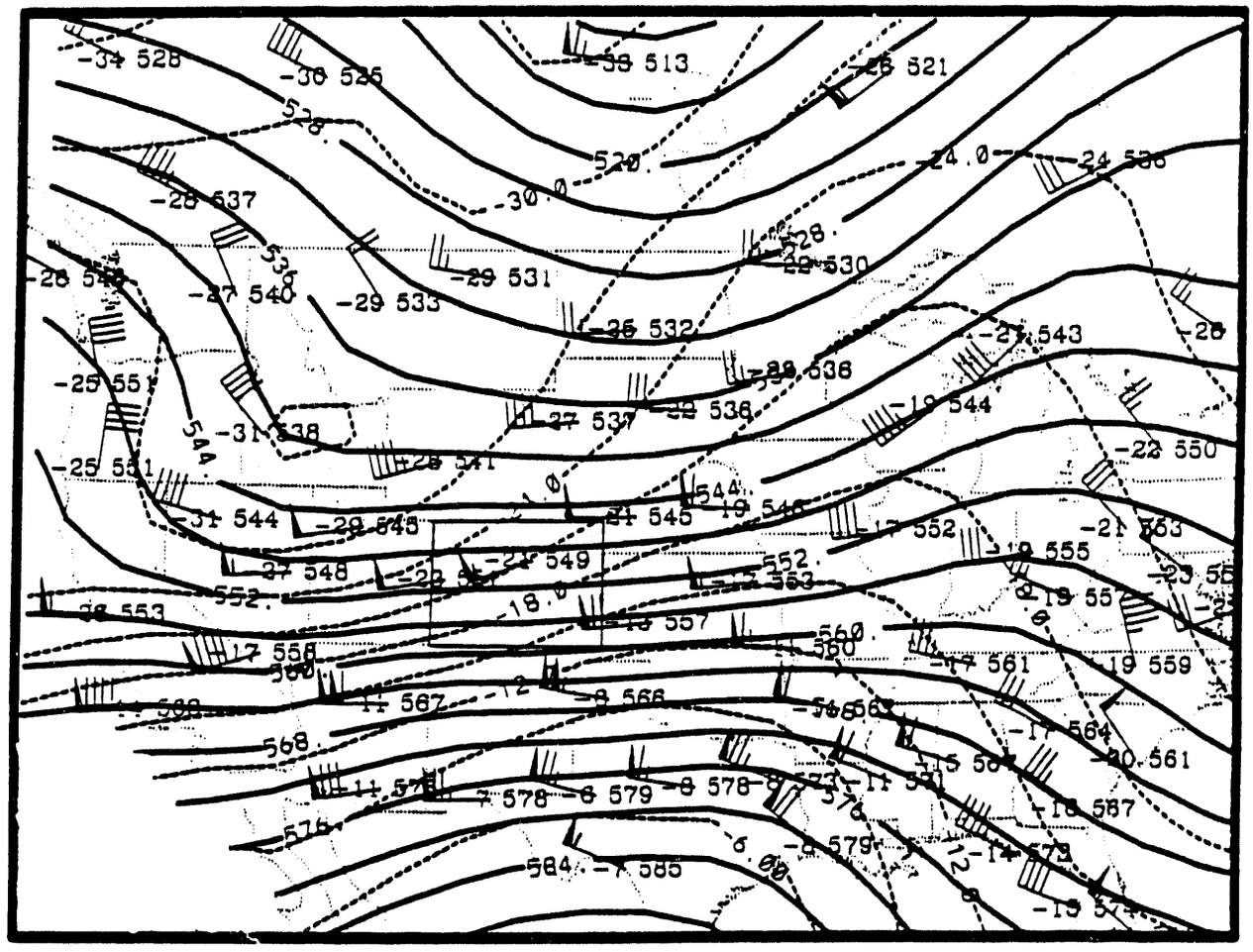

500 mb
0000 UTC 06-MAR-1991

Figure B19. A 500 mb map showing conditions aloft during IOP-4. Height contour lines are solid and isotherms are dashed.

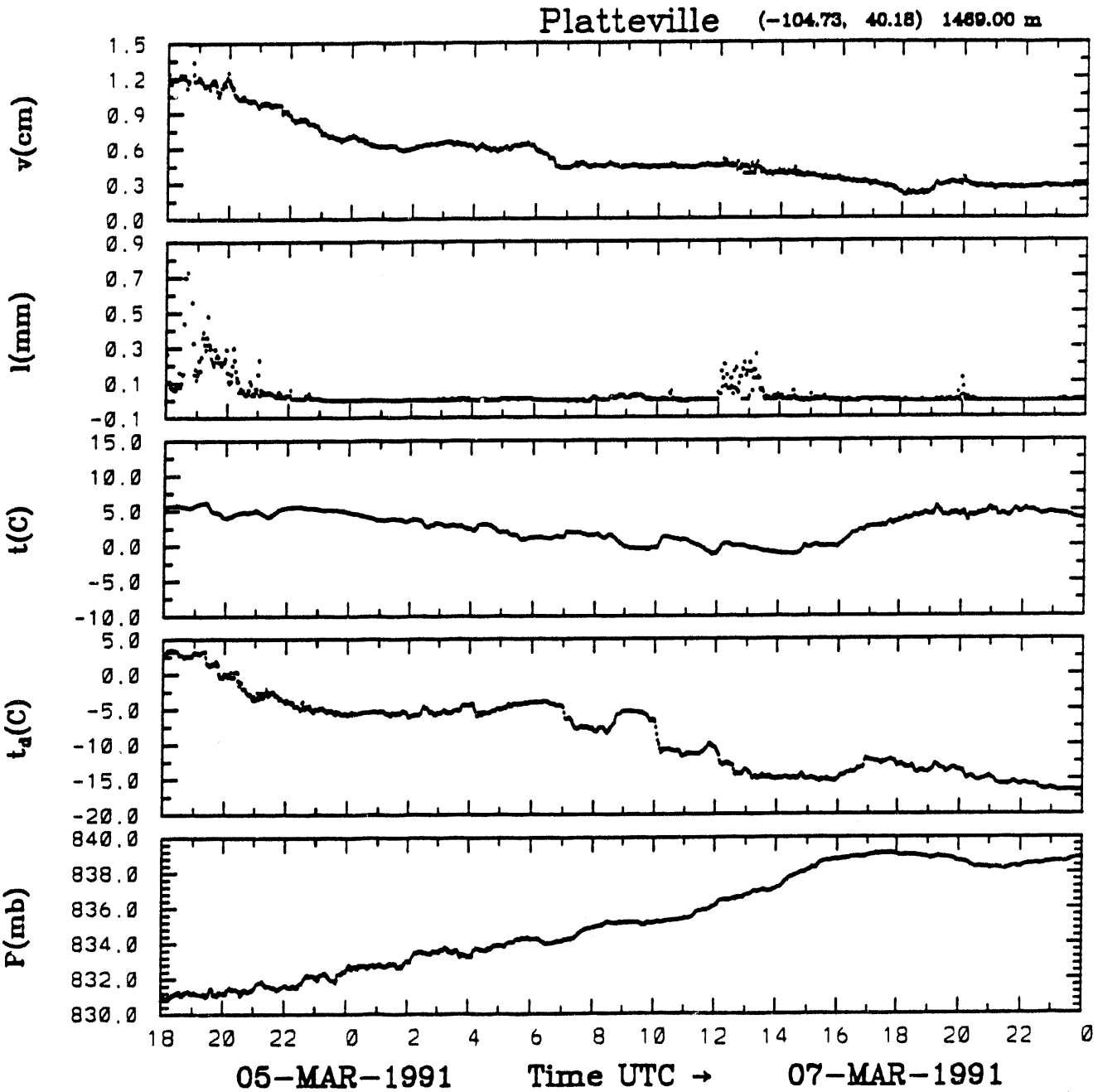


Figure B20. Data from the radiometer site at Platteville during IOP-4. Panels from top to bottom are: precipitable water vapor (v), path-integrated liquid water content (l), surface temperature (t), surface dewpoint temperature ($t_d$), surface pressure (P).

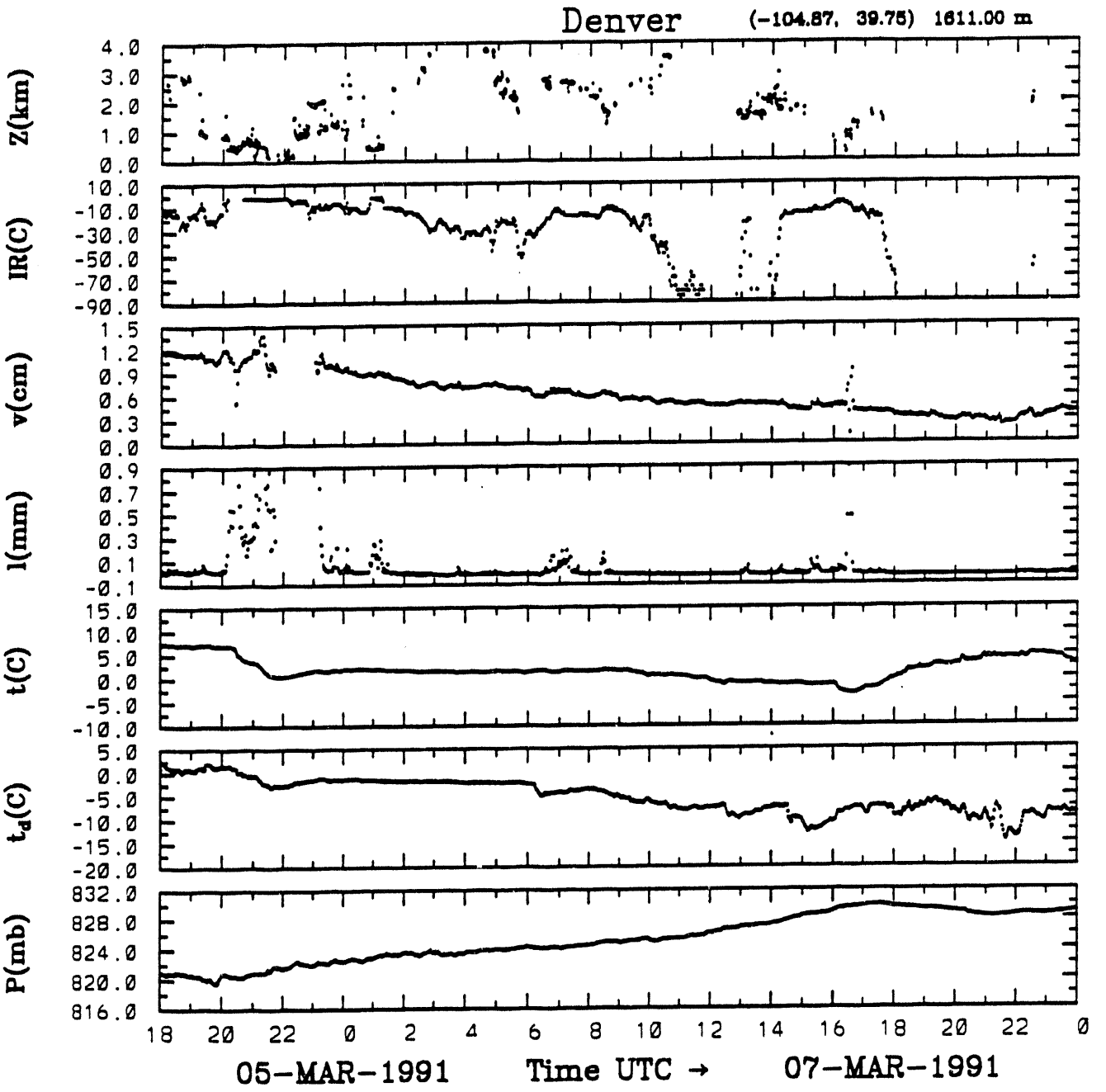


Figure B21. Data from the radiometer site at Denver for IOP-4. Panels from top to bottom are: cloud base height measured by ceilometer (Z), cloud base brightness temperature measured by infrared radiometer (IR), precipitable water vapor (v), path-integrated liquid water content (l), surface temperature (t), surface dewpoint temperature ($t_d$), surface pressure (P).

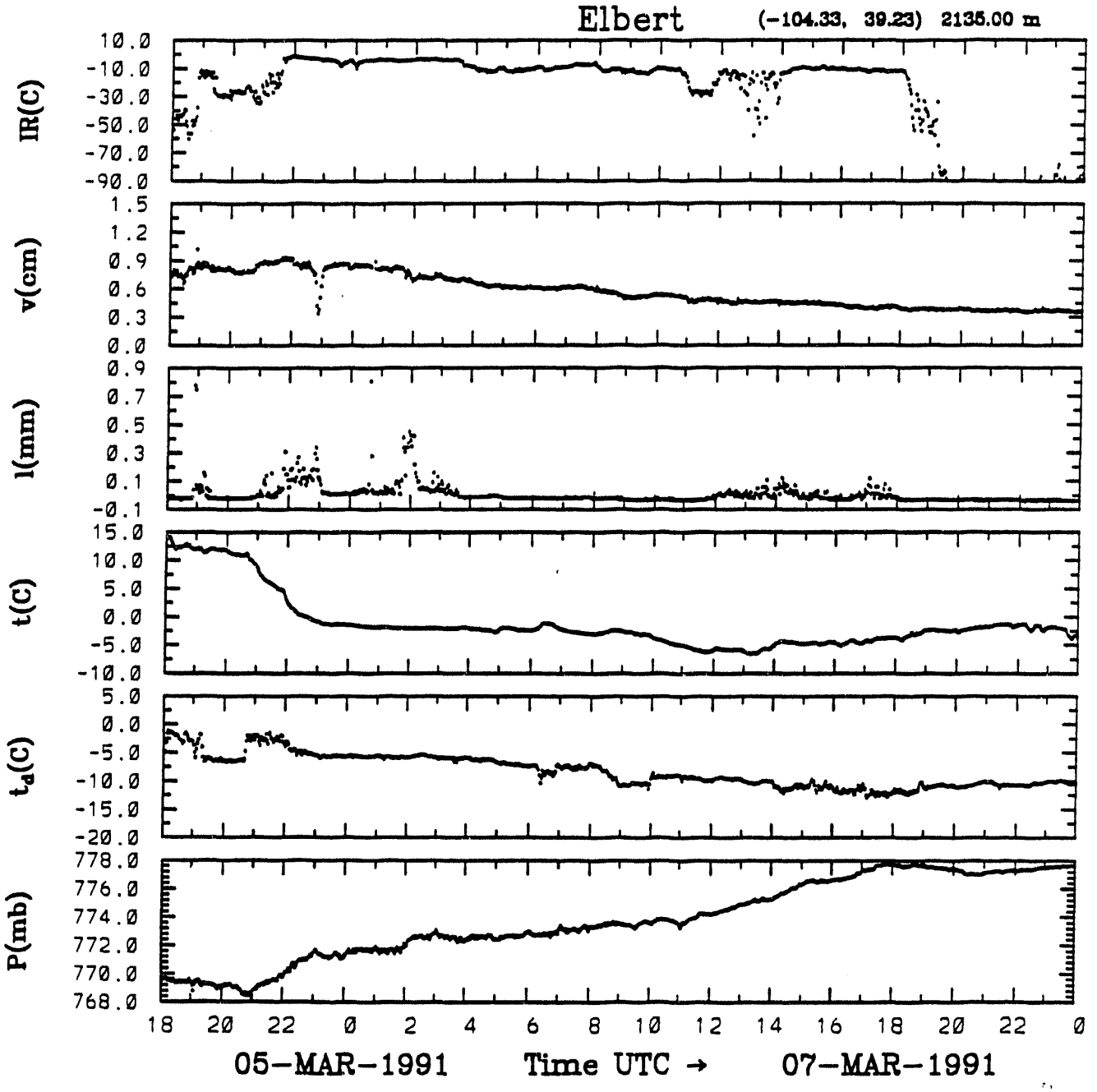


Figure B22. Data from the radiometer site at Elbert for IOP-4. Panels from top to bottom are: cloud base brightness temperature measured by infrared radiometer (IR), precipitable water vapor (v), path-integrated liquid water content (l), surface temperature (t), surface dew point temperature ($t_d$), surface pressure (P).

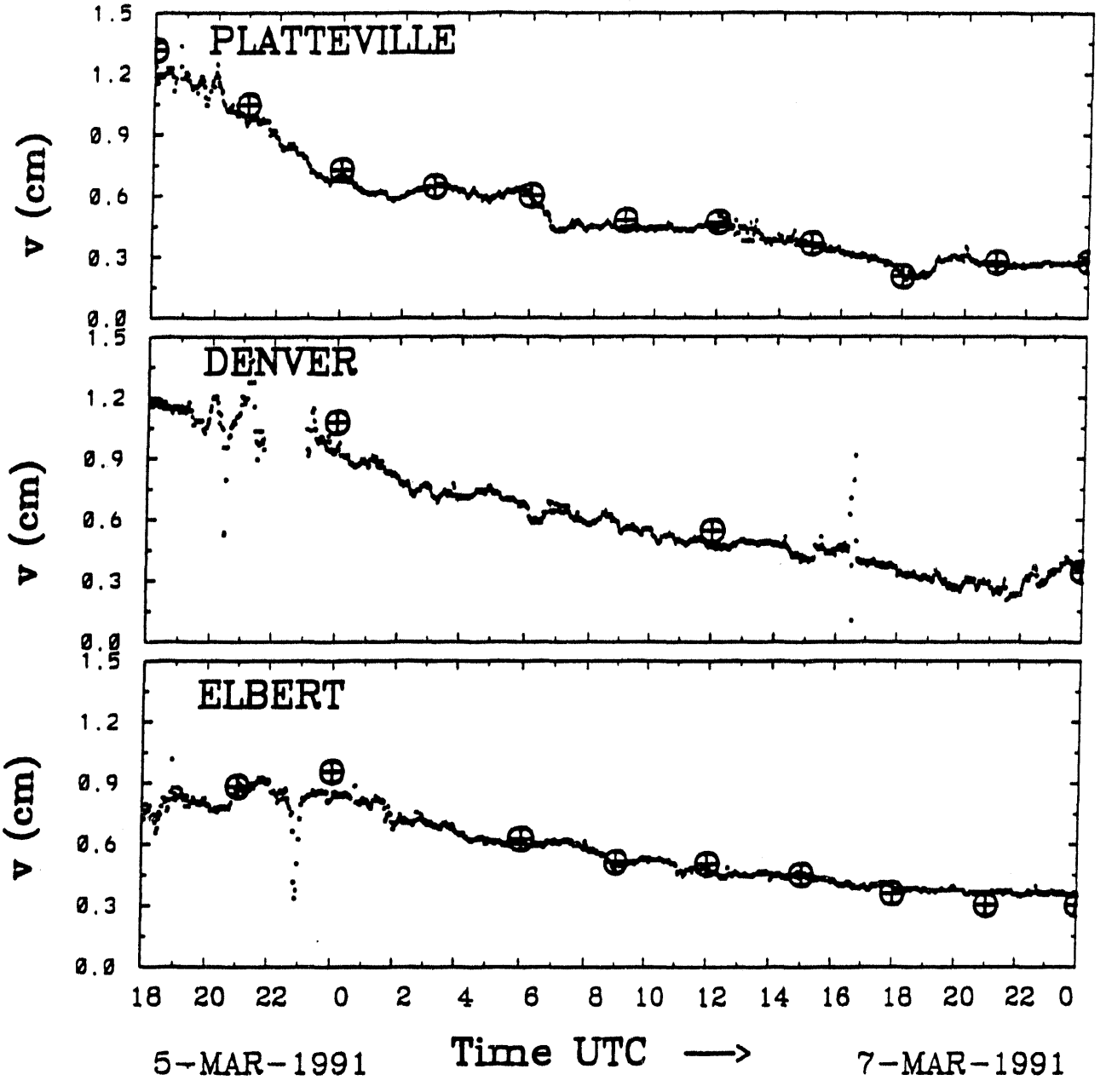


Figure B23. Precipitable water vapor measured by microwave radiometers (small dots) and radiosonde (circled crosses) at three sites during IOP-4.

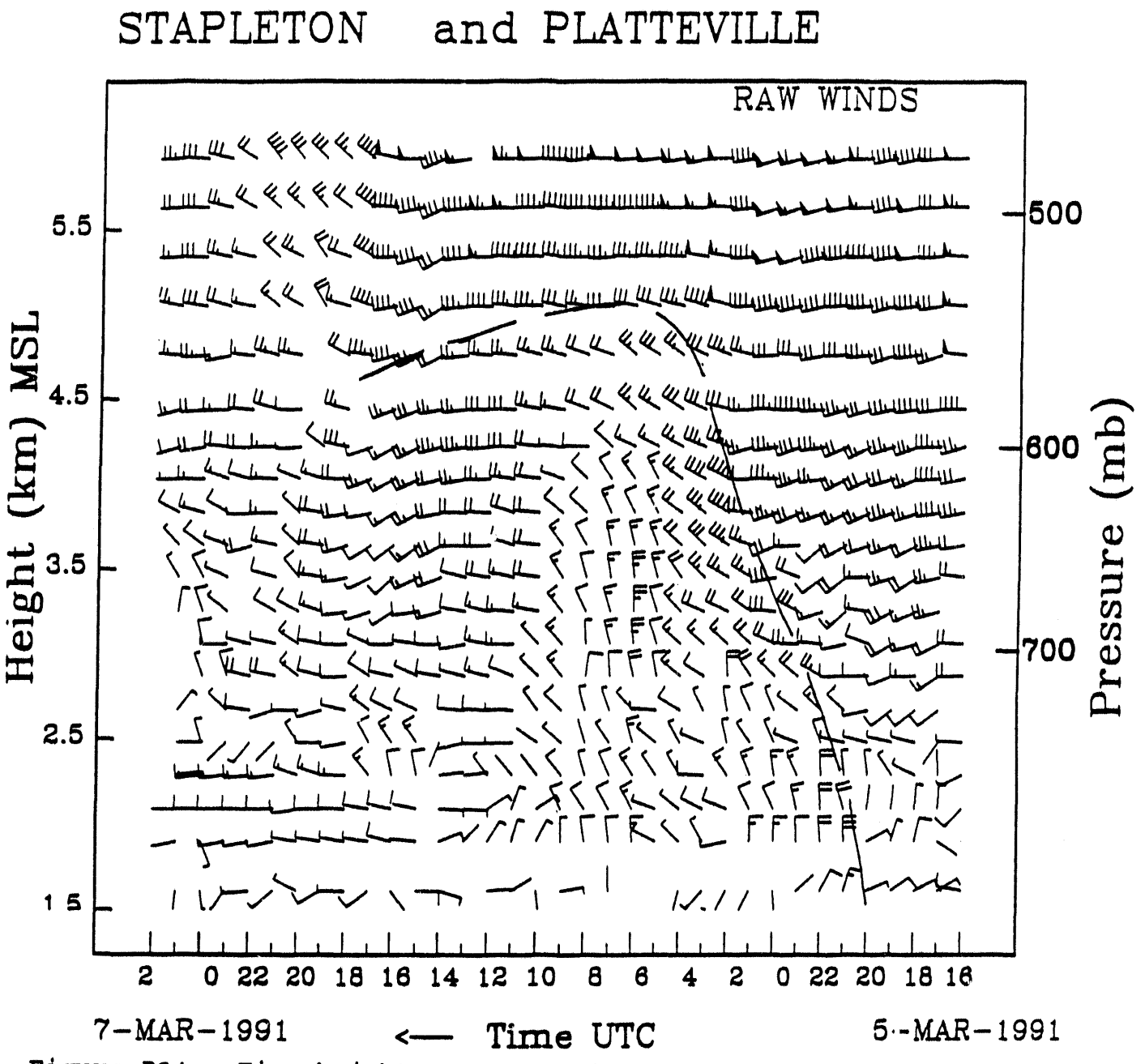


Figure B24. Time-height cross section of wind data composited from the 50 MHz wind profiler at Platteville and the high power 915 MHz wind profiler at Denver for IOP-4. Surface data are from an anemometer at Denver. Speed indicators are: short barb = 5 knots, long barb = 10 knots, flag = 50 knots. Dashed line shows approximate location of cold front boundary aloft.

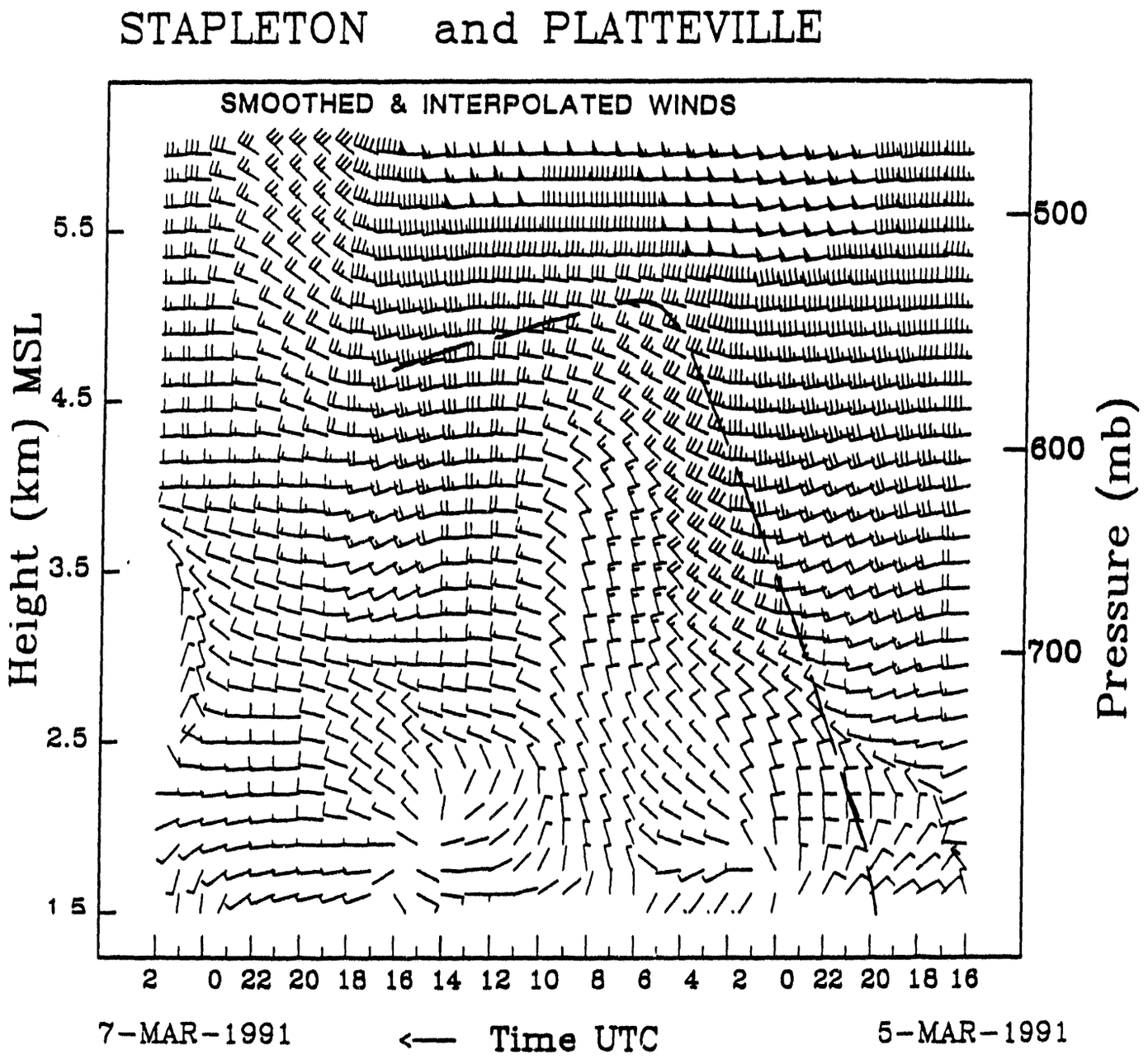


Figure B25. Wind data from the previous figure after smoothing and interpolation.

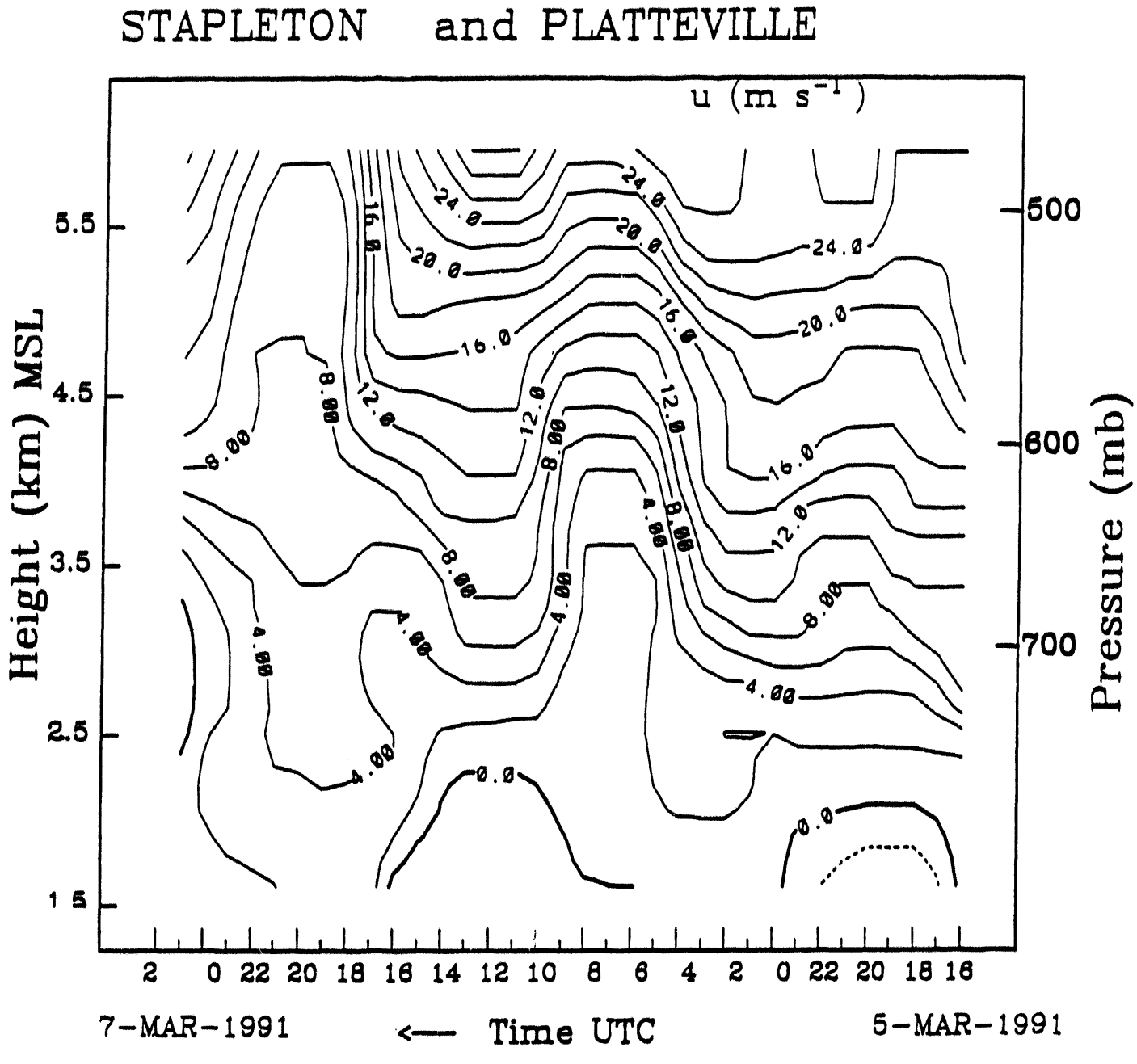


Figure B26. Time-height cross section of the westerly component of the wind data shown in the previous figure. Westerly component wind isotachs are positive (solid contours) and easterly are negative (dashed).

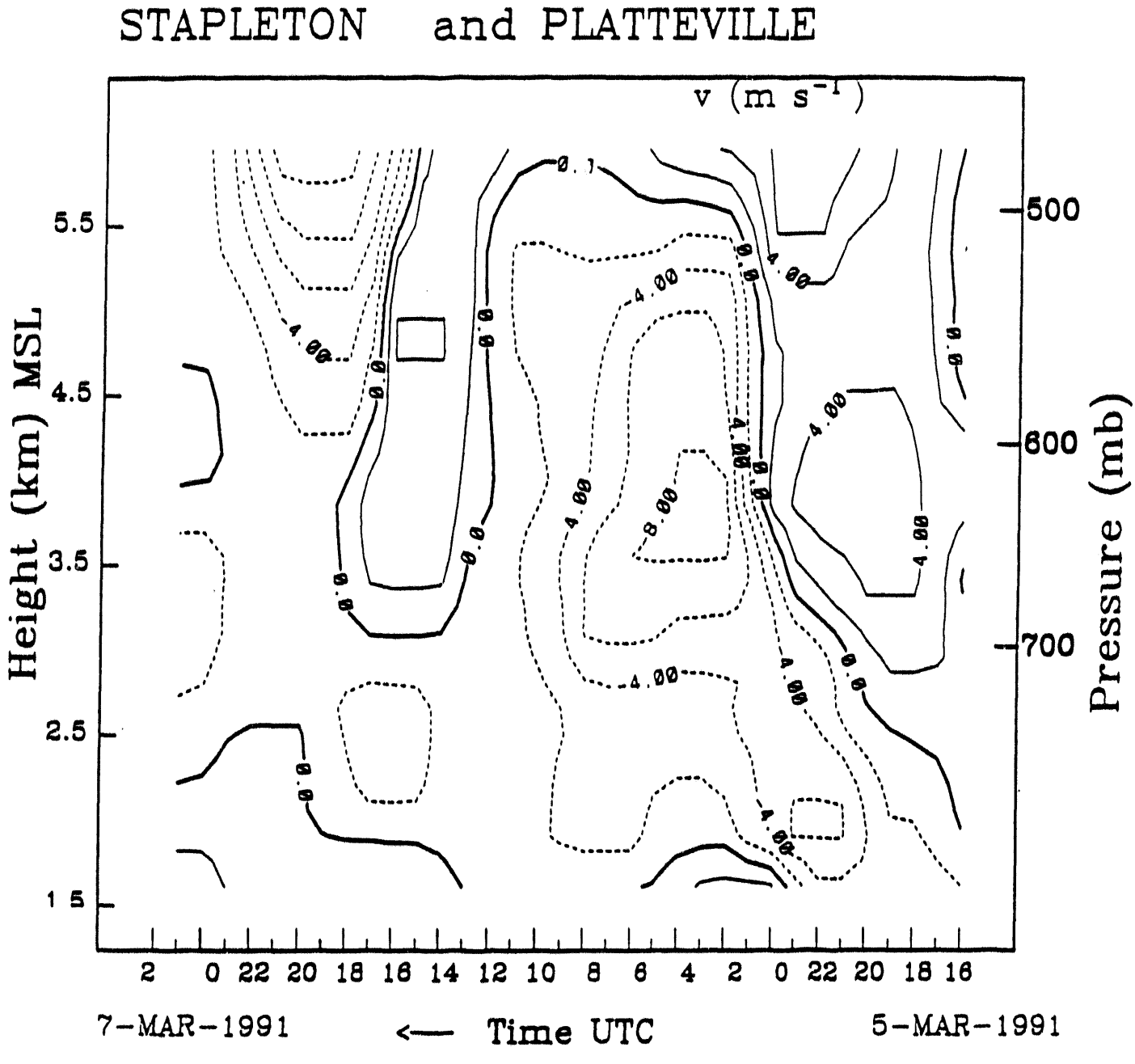


Figure B27. Time-height cross section of the southerly component of the wind data shown in the previous figures. Southerly component wind isotachs are positive (solid contours) and northerly are negative (dashed).

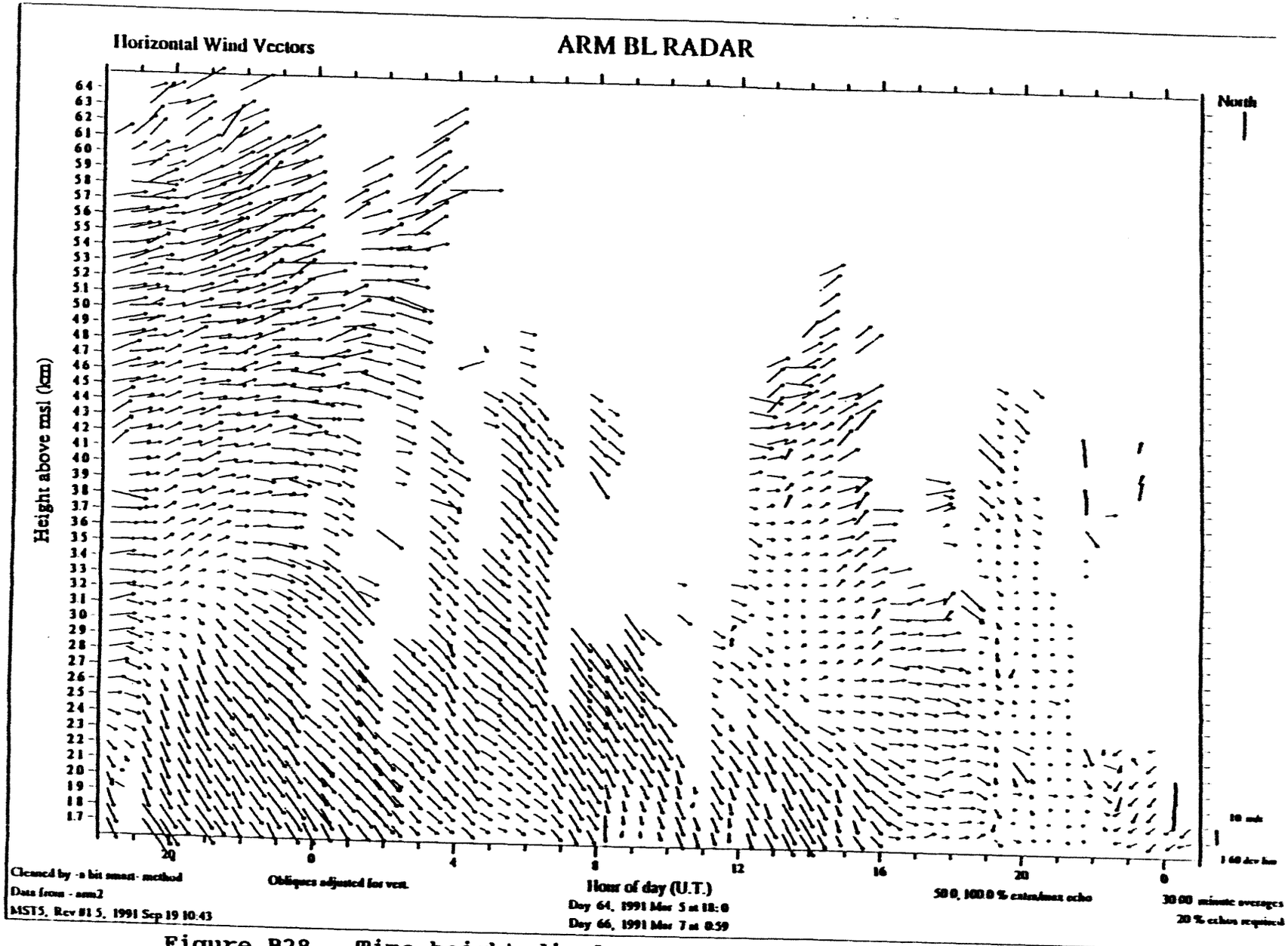


Figure B28. Time-height display of horizontal wind vectors measured by the boundary layer 915 MHz wind profiler at Platteville for IOP-4. The speed scale is shown at the lower right corner. Time increases toward the right.

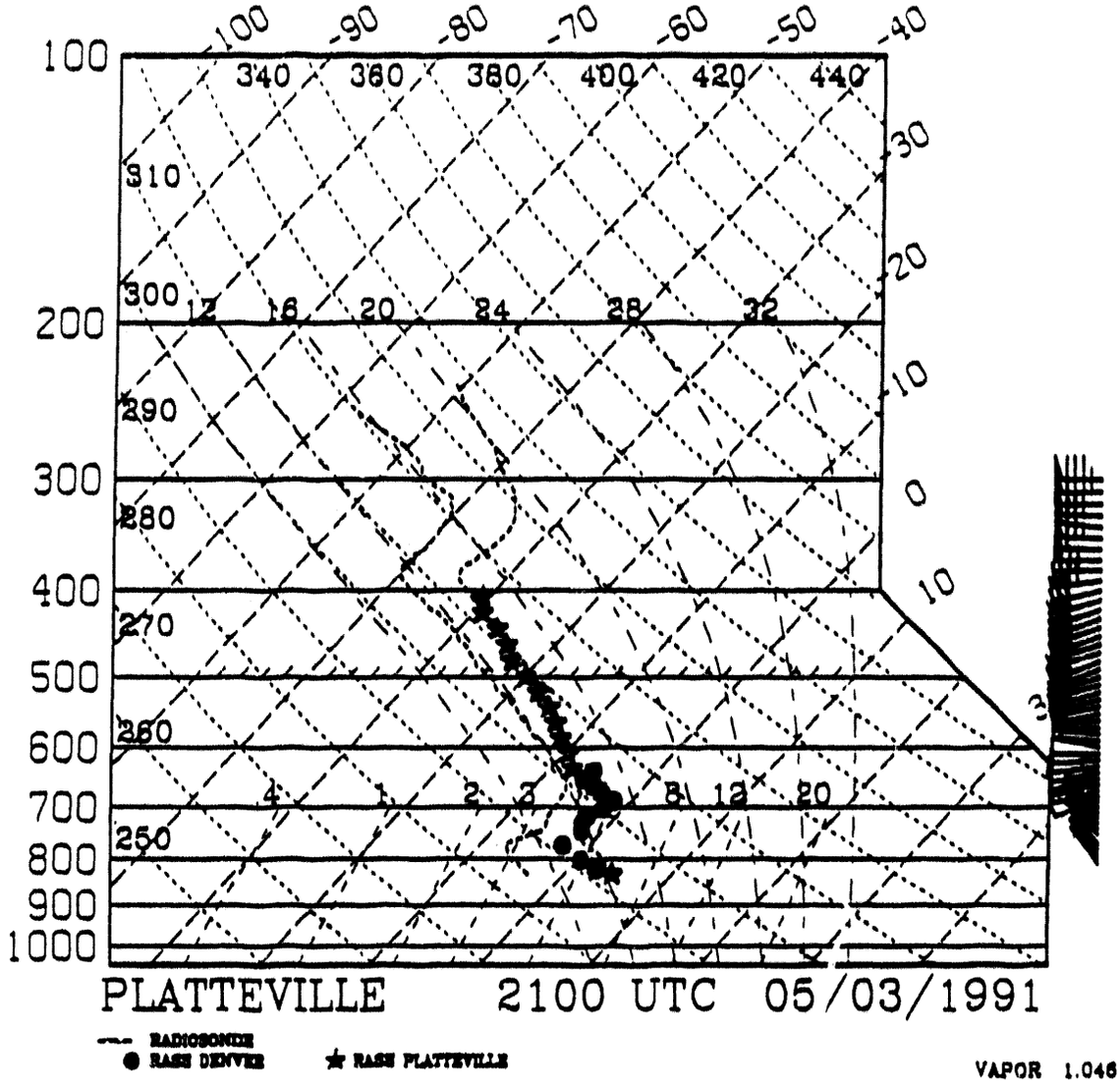


Figure B29. Temperature profiles measured by the 915 MHz RASS at Denver (solid dots) and 50 MHz RASS at Platteville (stars) for IOP-4. CLASS rawinsonde temperature and dewpoint data from Platteville are shown by the heavy dashed lines.

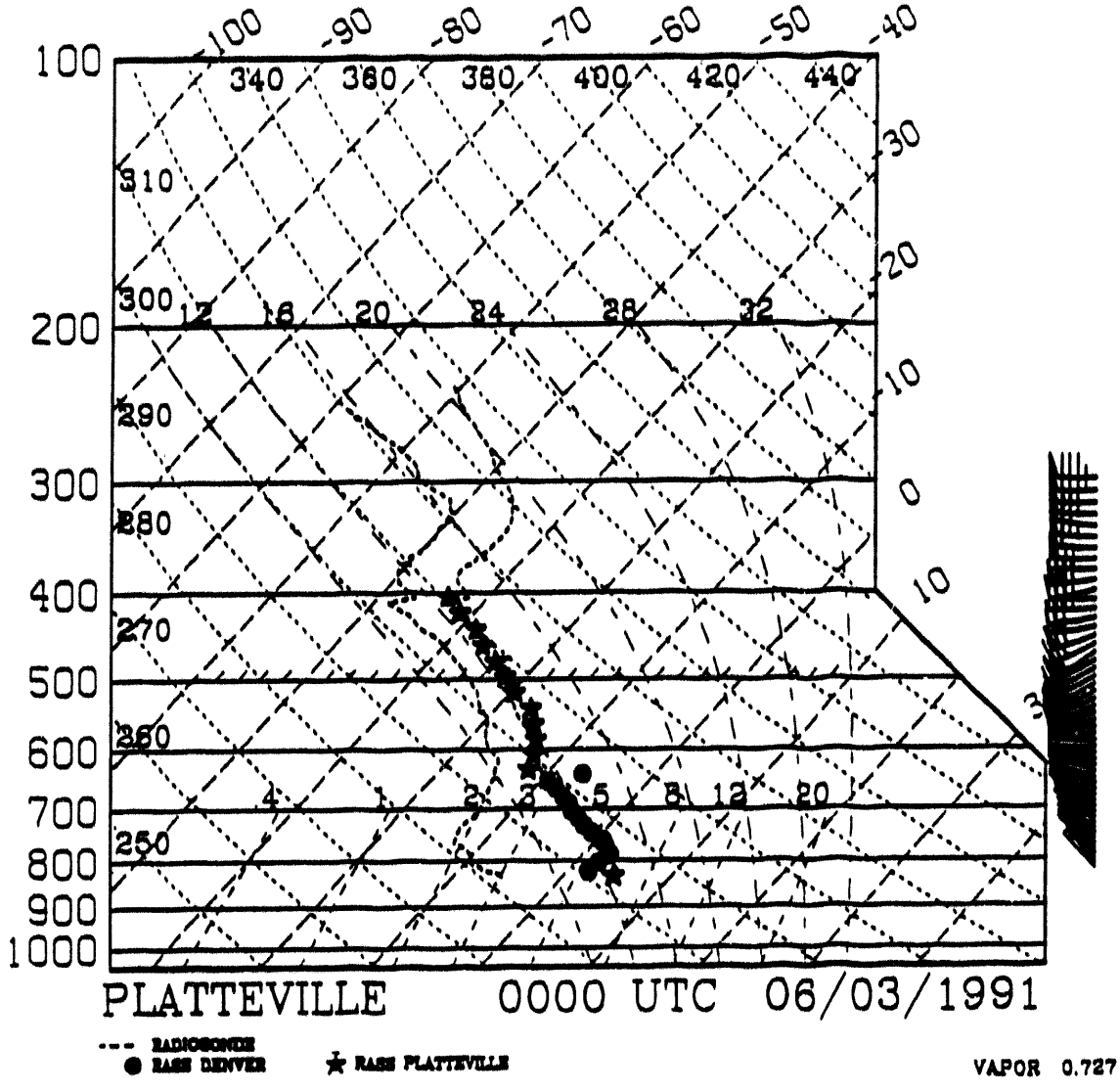


Figure B30. Same as for previous figure, except at a later time.

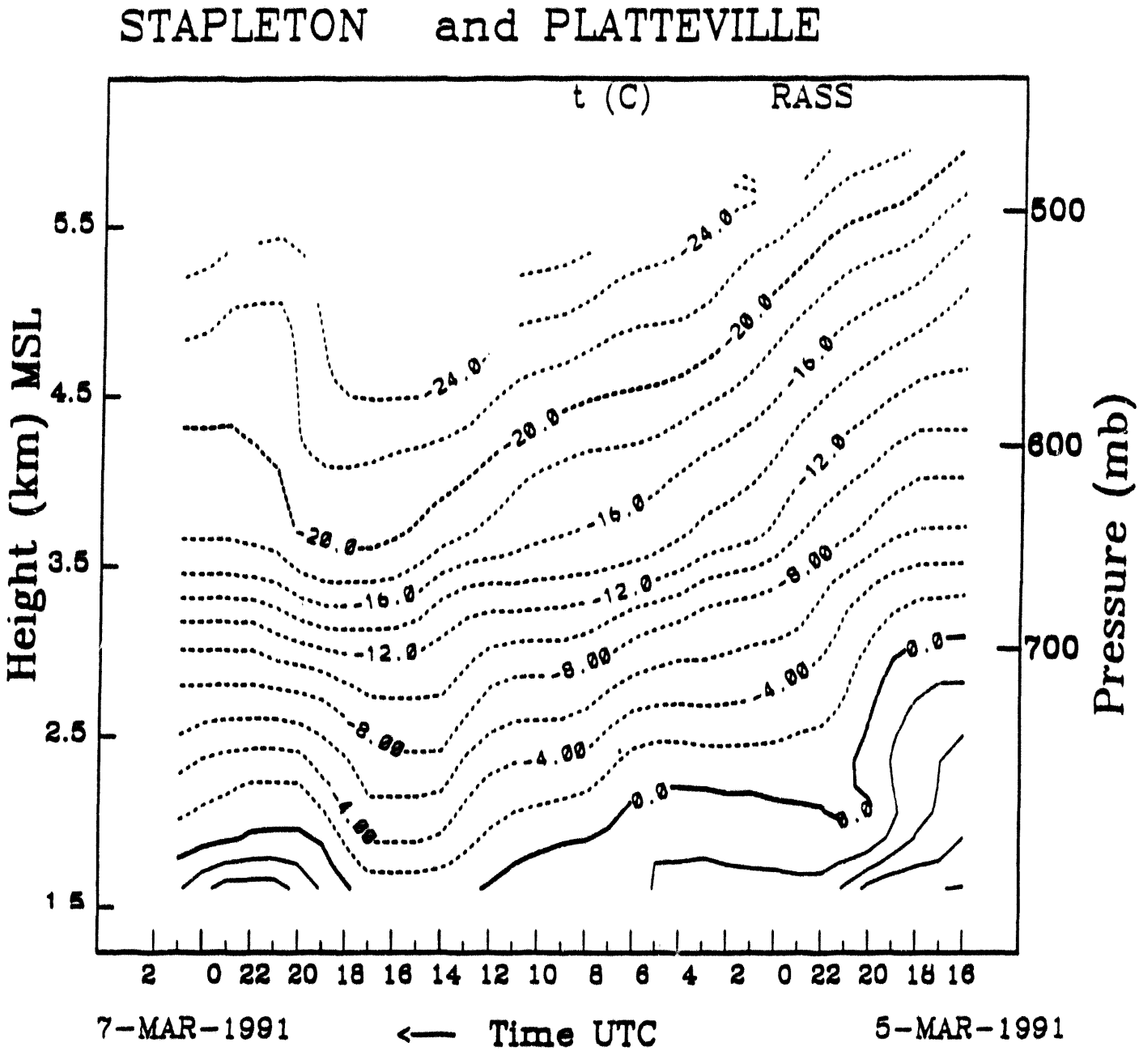


Figure B31. Time-height cross section of temperature from composite of RASS measurements at Denver and Platteville and using Denver surface temperature data during IOP-4. Temperatures above freezing are shown with solid isotherms and those below freezing have dashed isotherms.

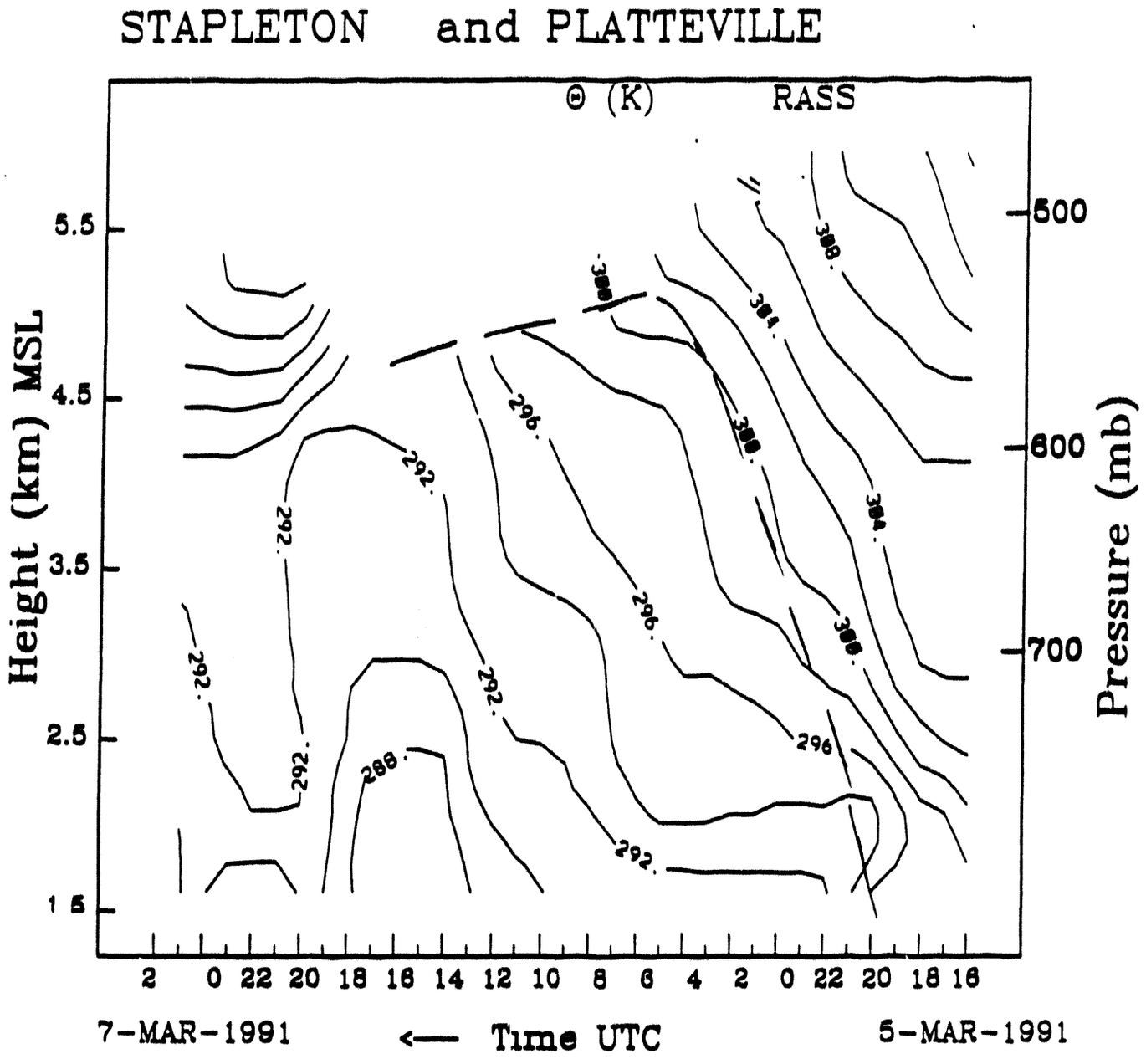


Figure B32. Time-height cross section of potential temperature derived from the RASS temperature data of the previous figure. Dashed line shows approximate location of the cold front boundary aloft.

## B3. IOP #5: 8 MARCH - 9 MARCH 1991 (CLEAR SKIES)

The fifth IOP was a case of almost cloudless skies. Figures B33-B48 present the same sequence of data products that were shown for IOPs #3 and #4.

The synoptic weather maps (Figs. B33-B35) show that a dome of high pressure was located over southeastern Colorado, and a strong ridge was moving into the western part of the state. The radiometer site data (Figs. B36-B38) show the building surface pressure and a strong diurnal temperature cycle under the clear sky conditions. Except for a brief period near the beginning of the observations, the precipitable water vapor measured by the radiometers was much lower than in the other two IOPs. The presence of cloud was detected at Platteville and Elbert only before 0000 GMT on 9 March. Clear skies prevailed thereafter. The precipitable water vapor comparisons between radiometers and radiosondes (Fig. B39) are not quite as good in these very dry conditions as they were for the other two IOPs.

The time-height cross sections of wind profiler data (Figs. B40-B43) are consistent with the synoptic weather situation. This time, the low-level wind data of the 915 MHz boundary layer profiler (Fig. B44) are in good agreement with those of the other profilers. RASS temperature profiles (Figs. B45-B46) again show excellent agreement with radiosonde data. Time-height cross sections of temperature and potential temperature (Figs. B47-B48) show the gradual warming aloft by subsidence and the diurnal temperature cycle near the surface.

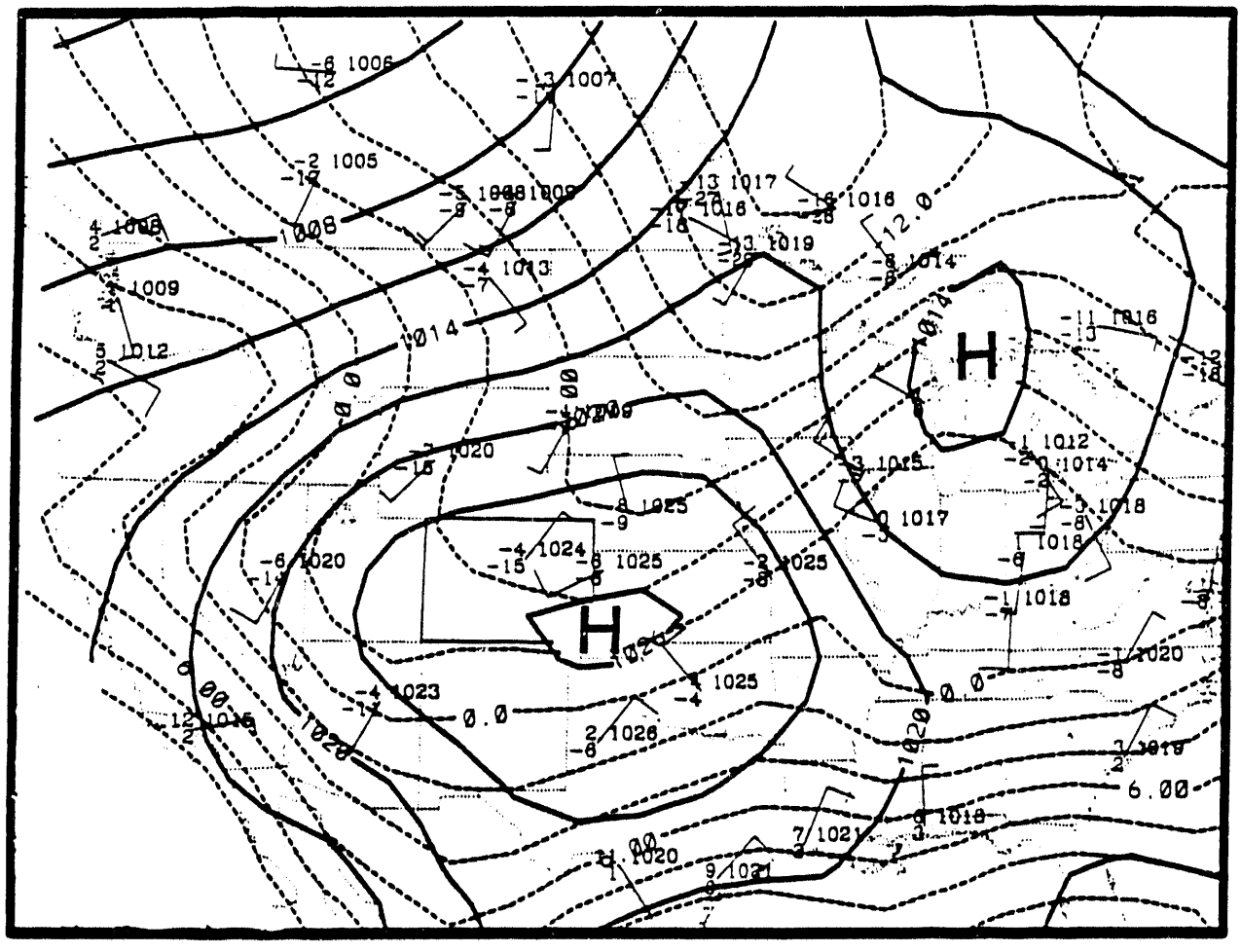


Surface
9-MAR-1991 1200 UTC

Figure B33. Surface weather map during IOP-5. Solid lines are isobars; dashed lines are isotherms.

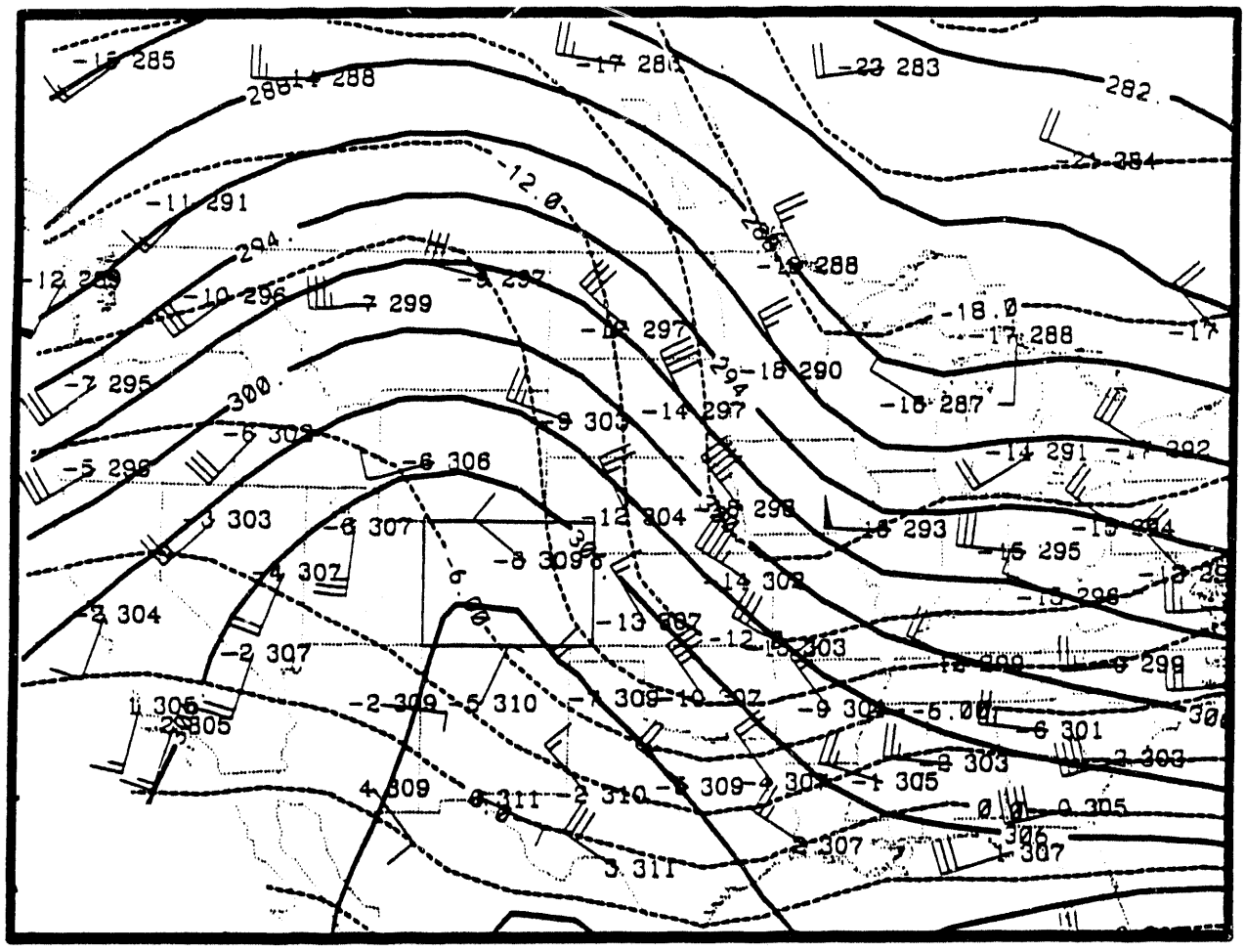

700 mb
1200 UTC 09-MAR-1991

Figure B34. A 700 mb map showing conditions aloft during IOP-5. Height contour lines are solid and isotherms are dashed.

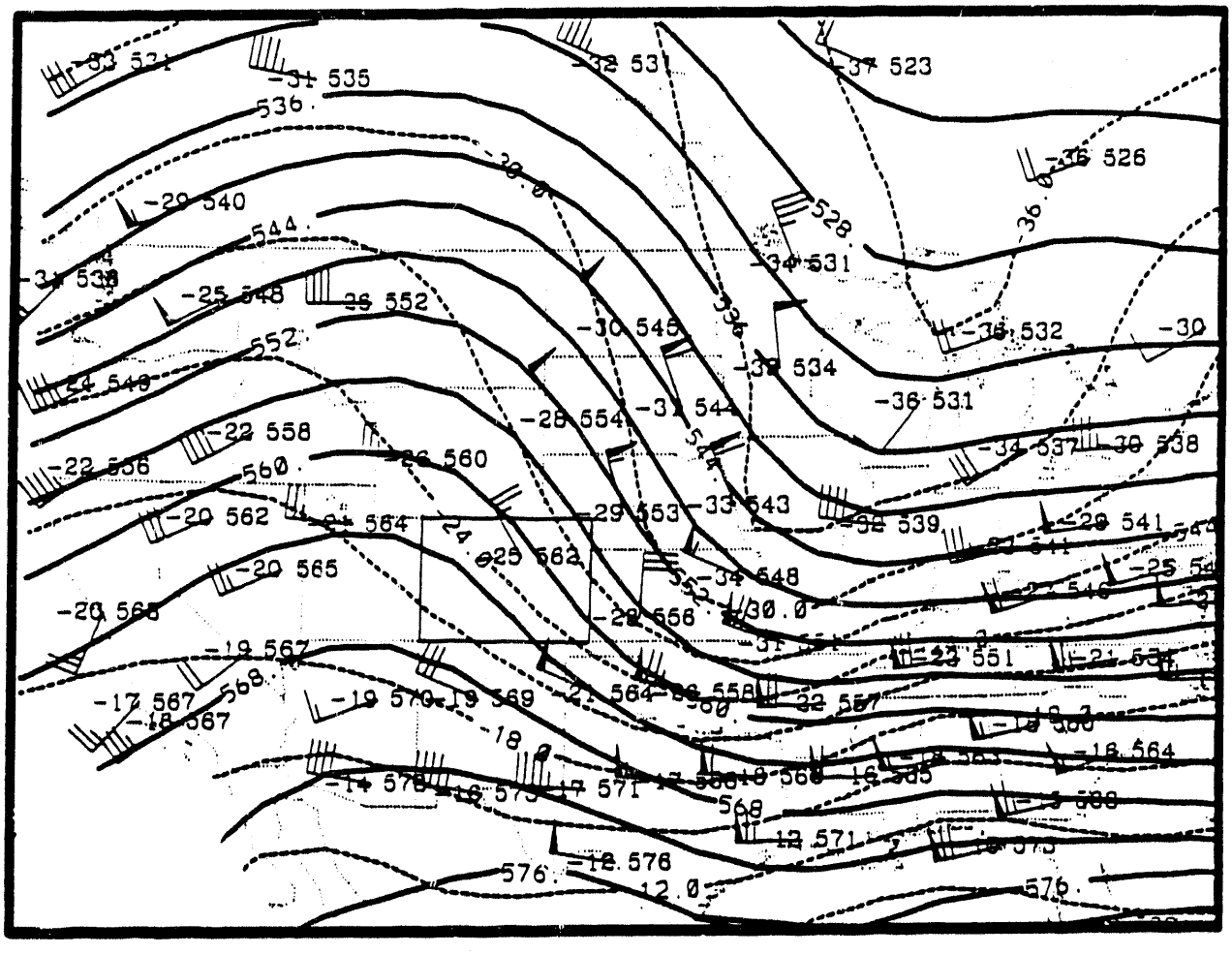

500 mb
1200 UTC 09-MAR-1991

Figure B35. A 500 mb map showing conditions aloft during IOP-5. Height contour lines are solid and isotherms are dashed.

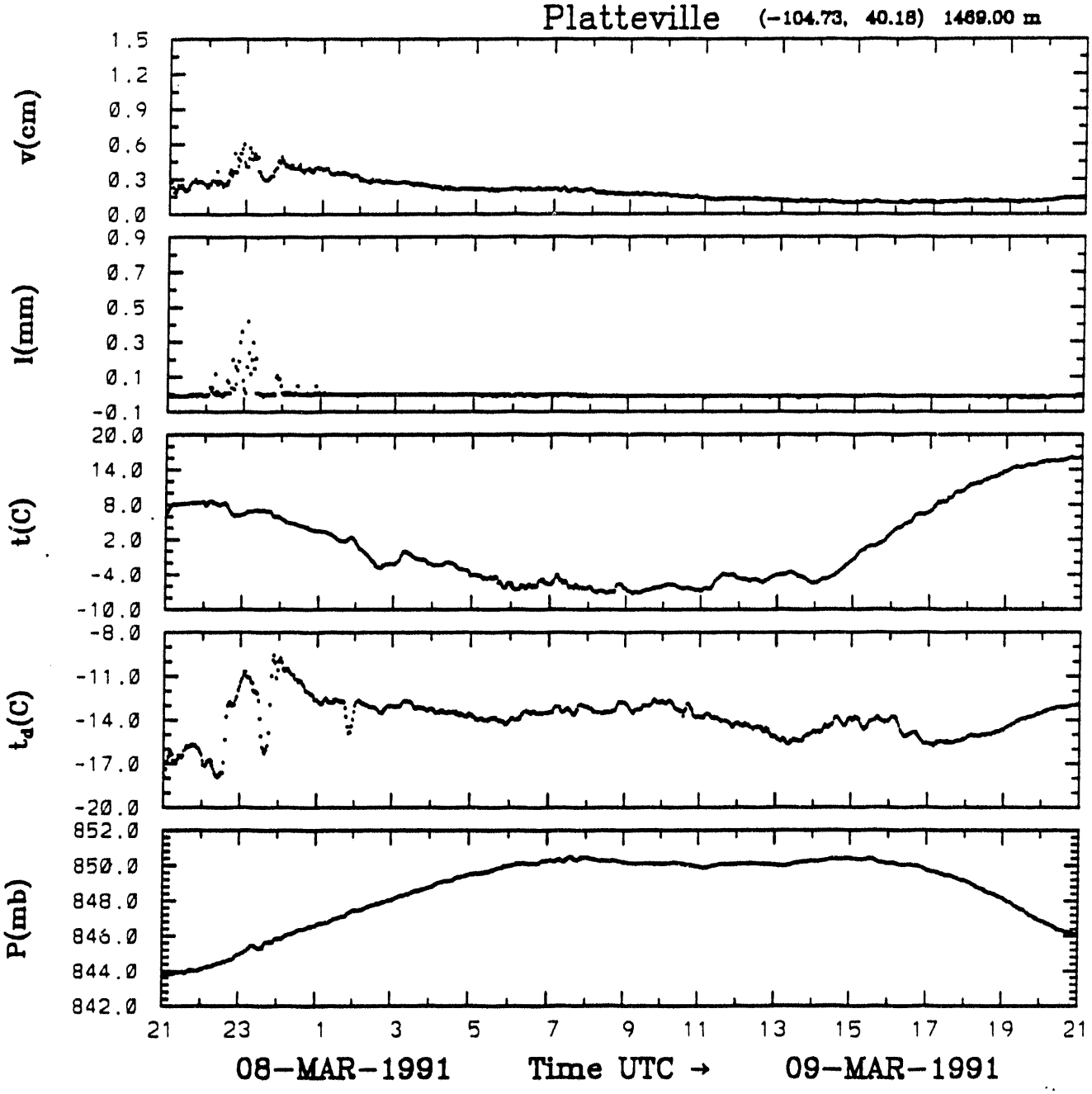


Figure B36. Data from the radiometer site at Platteville during IOP-5. Panels from top to bottom are: precipitable water vapor (v), path-integrated liquid water content (l), surface temperature (t), surface dewpoint temperature ($t_d$), surface pressure (P).

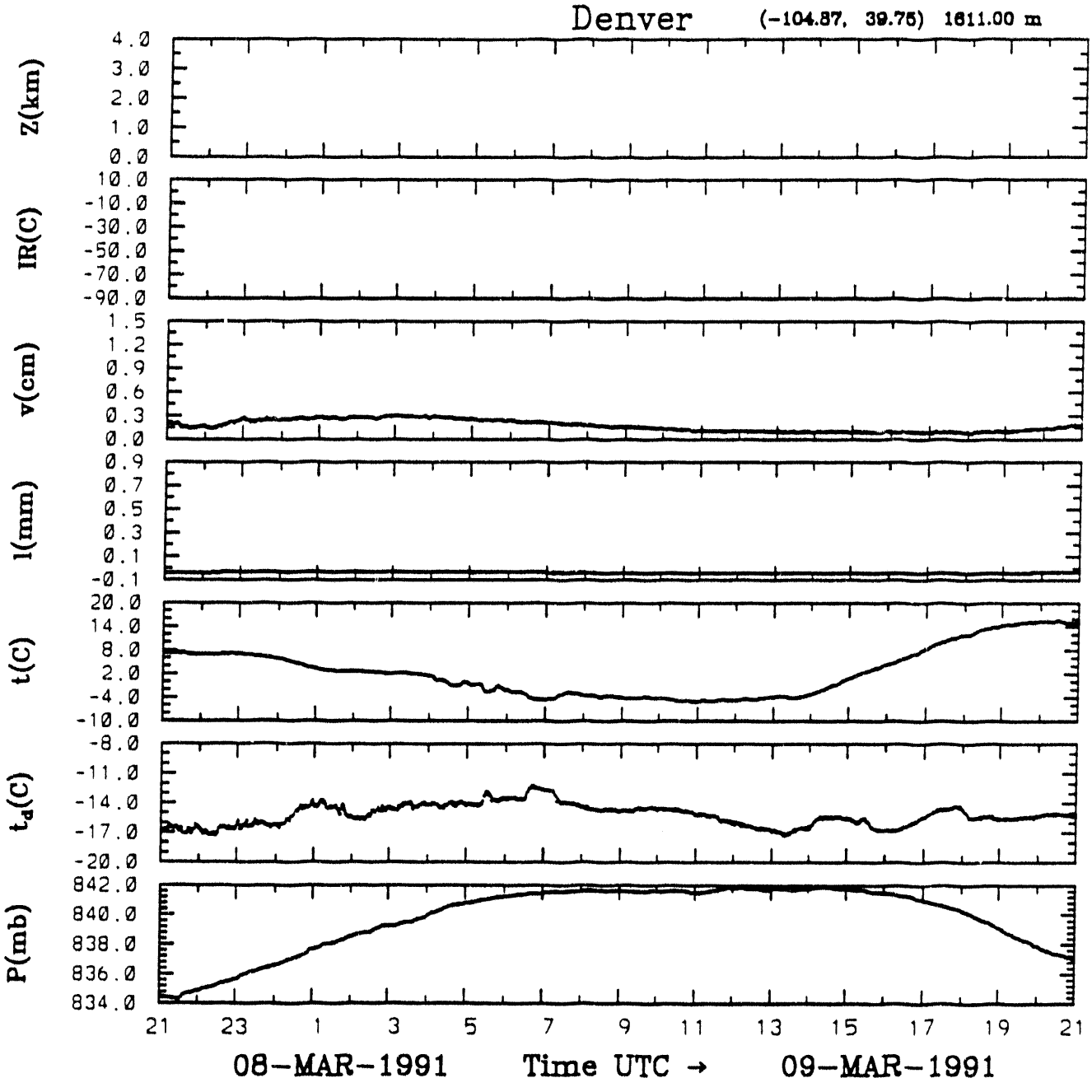


Figure B37. Data from the radiometer site at Denver for IOP-5. Panels from top to bottom are: cloud base height measured by ceilometer (Z), cloud base brightness temperature measured by infrared radiometer (IR), precipitable water vapor (v), path-integrated liquid water content (l), surface temperature (t), surface dewpoint temperature ($t_d$), surface pressure (P).

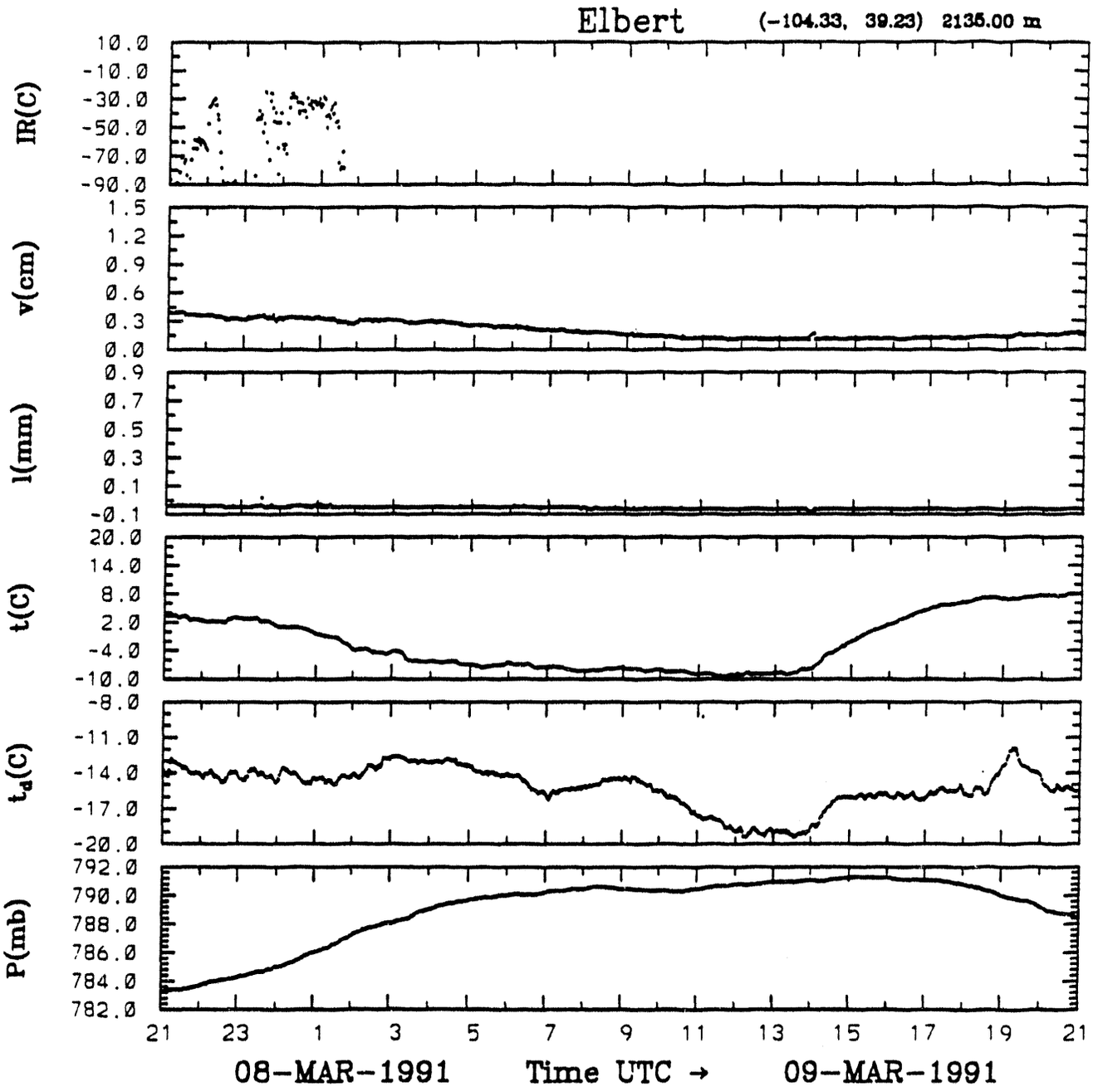


Figure B38. Data from the radiometer site at Elbert for IOP-5. Panels from top to bottom are: cloud base brightness temperature measured by infrared radiometer (IR), precipitable water vapor (v), path-integrated liquid water content (l), surface temperature (t), surface dewpoint temperature ($t_d$), surface pressure (P).

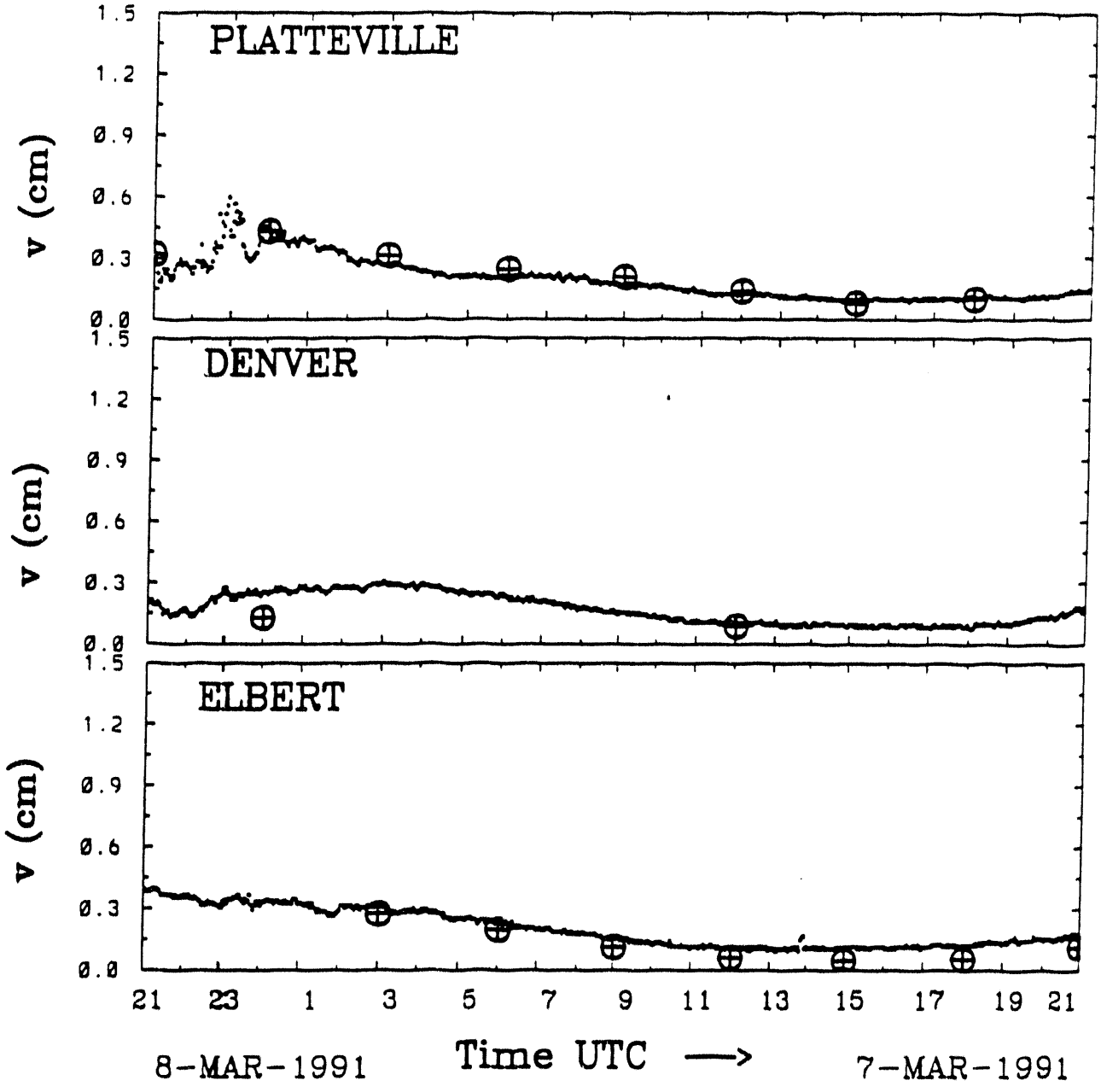


Figure B39. Precipitable water vapor measured by microwave radiometers (small dots) and radiosonde (circled crosses) at three sites during IOP-5.

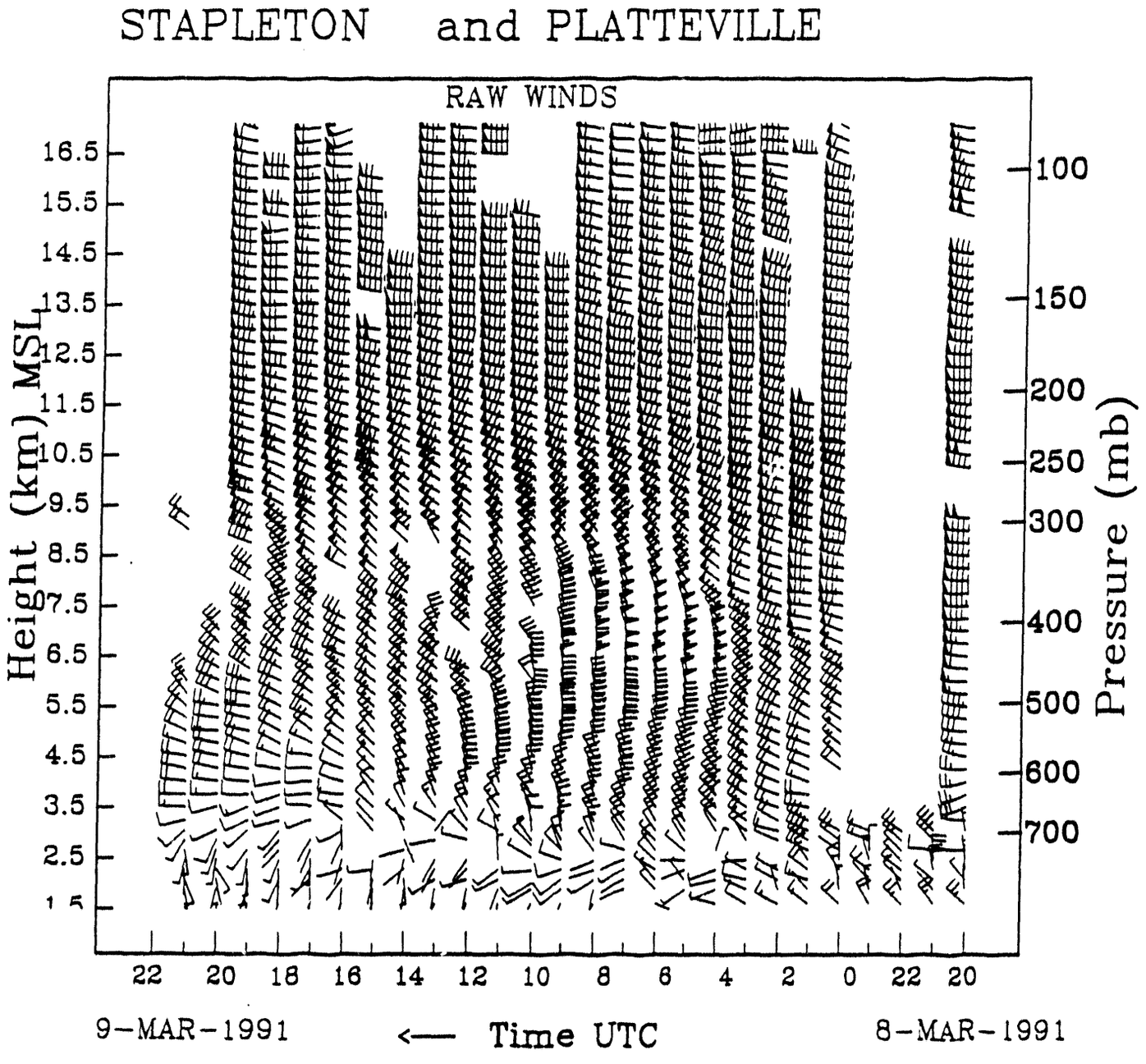


Figure B40. Time-height cross section of wind data composited from the 50 MHz wind profiler at Platteville and the high power 915 MHz wind profiler at Denver for IOP-5. Surface data are from an anemometer at Denver. Speed indicators are: short barb = 5 knots, long barb = 10 knots, flag = 50 knots.

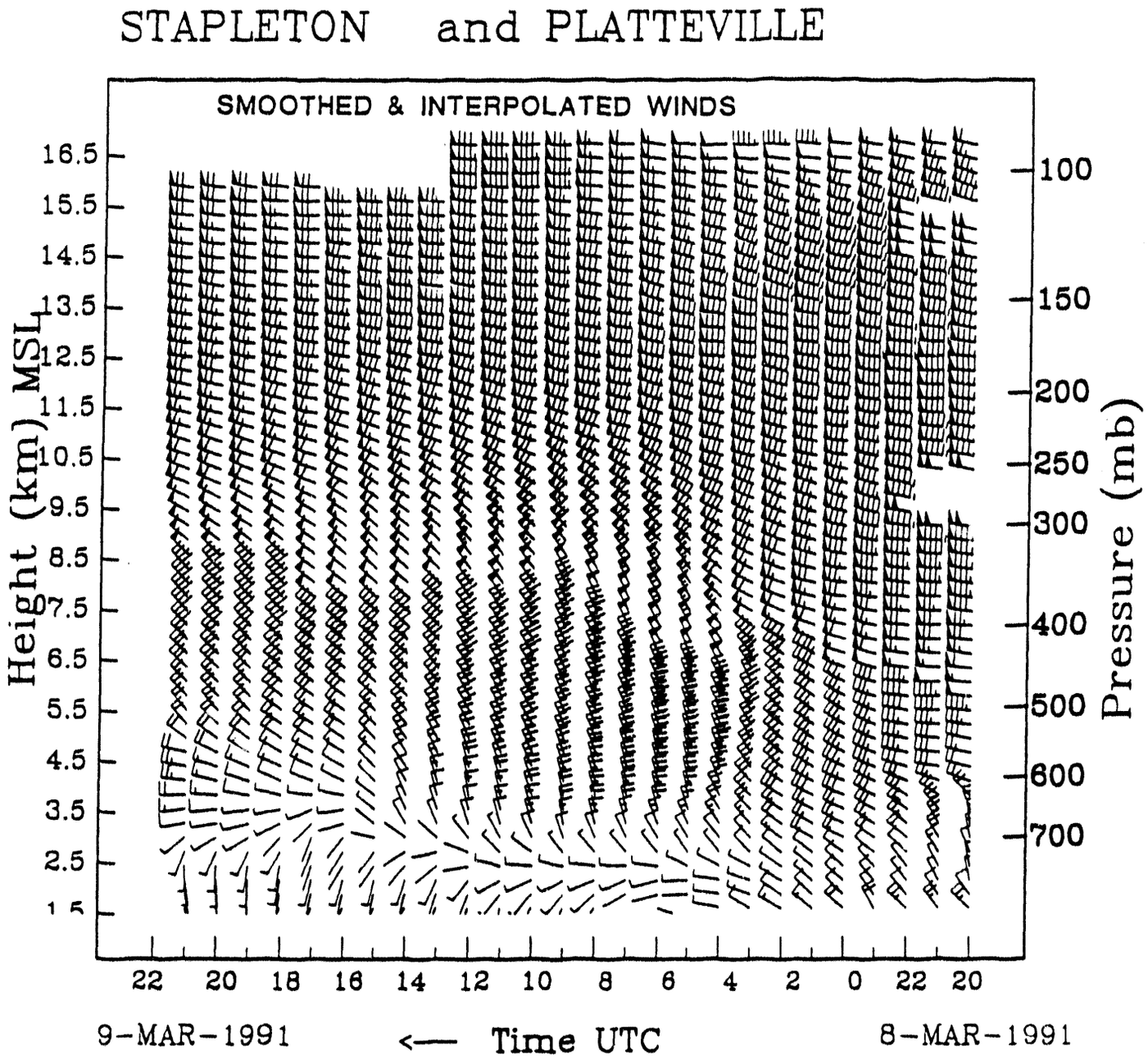


Figure B41. Wind data from the previous figure after smoothing and interpolation.

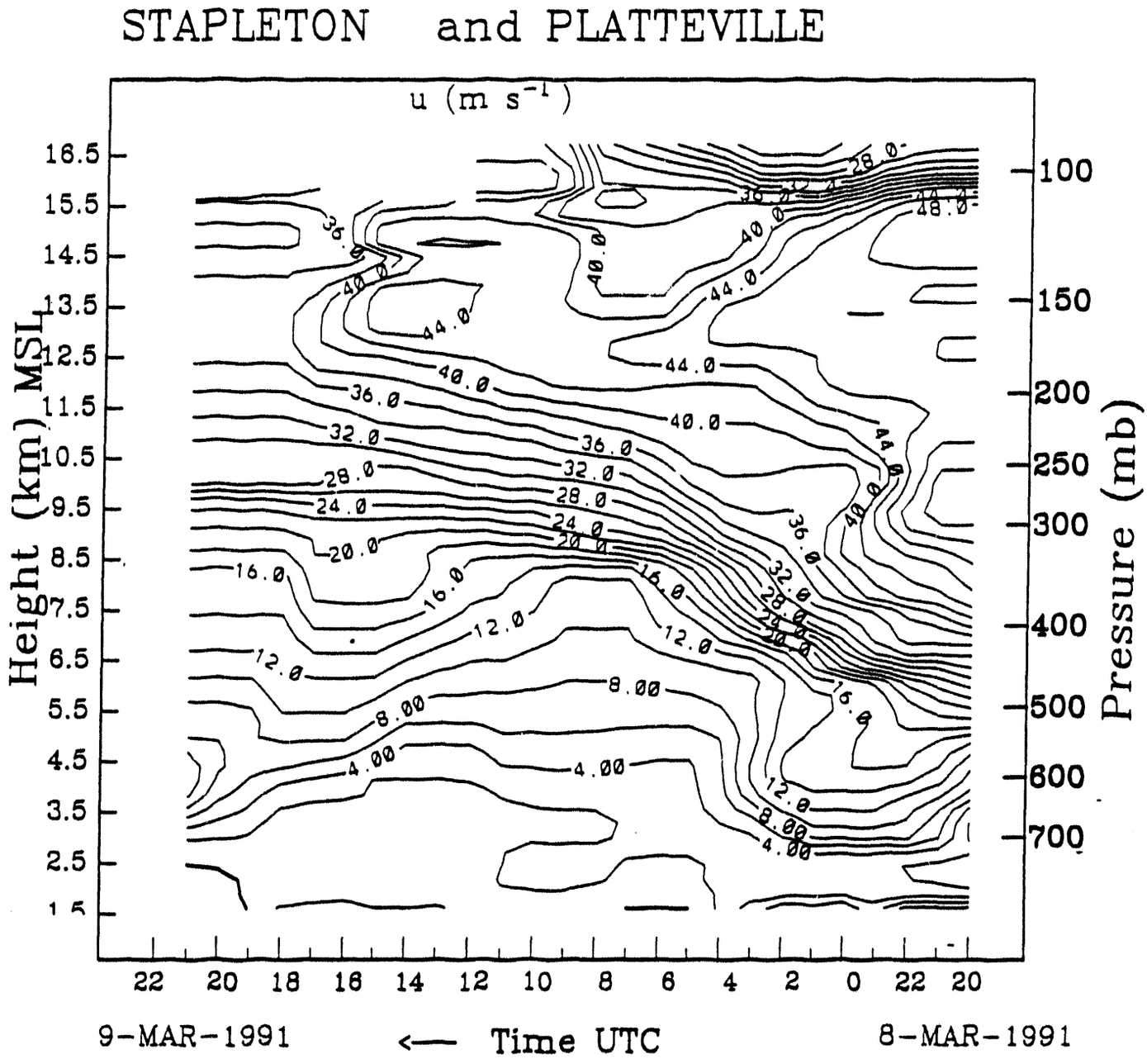


Figure B42. Time-height cross section of the westerly component of the wind data shown in the previous figure. Westerly component wind isotachs are positive (solid contours) and easterly are negative (dashed).

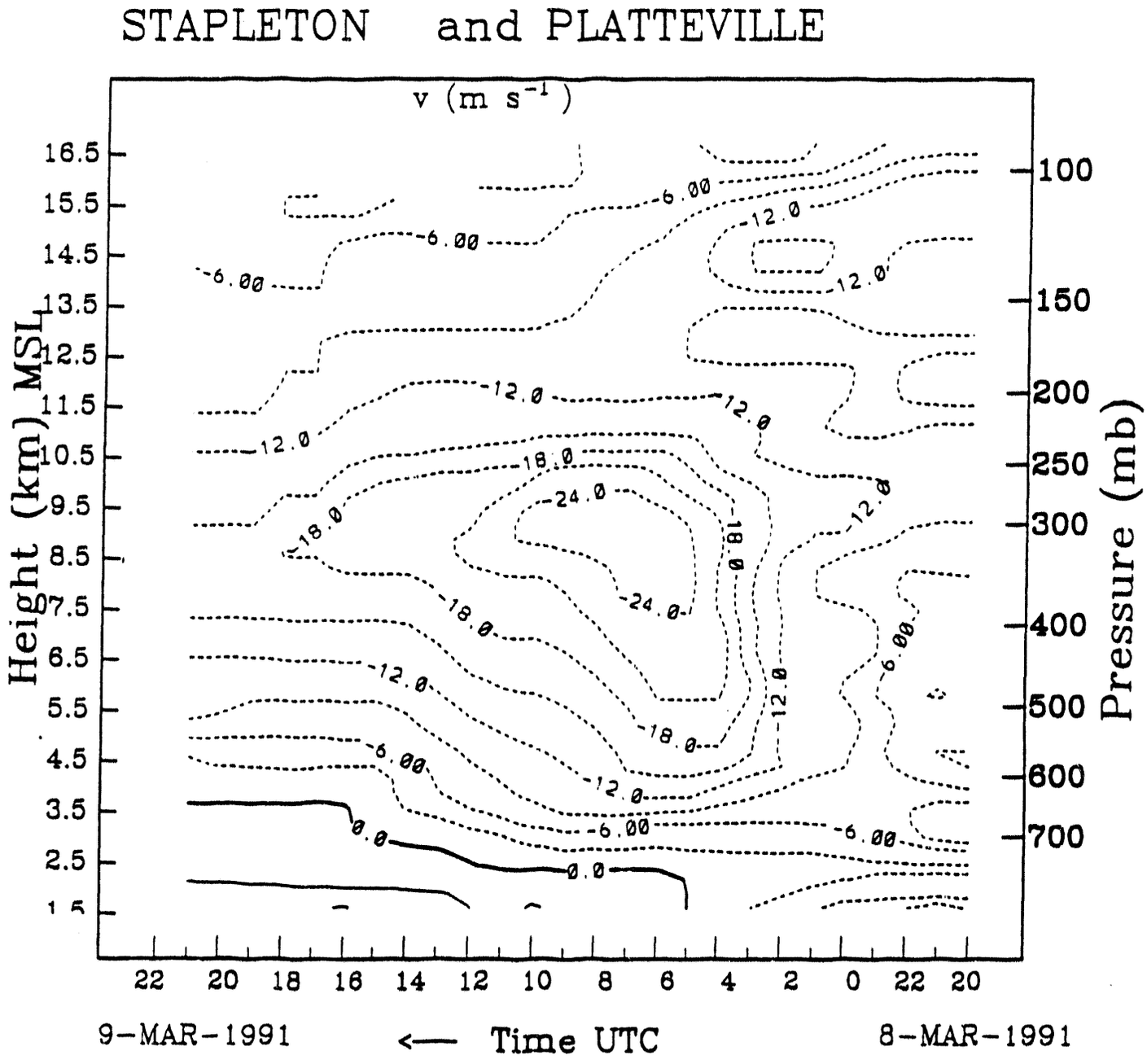


Figure B43. Time-height cross section of the southerly component of the wind data shown in the previous figures. Southerly component wind isotachs are positive (solid contours) and northerly are negative (dashed).

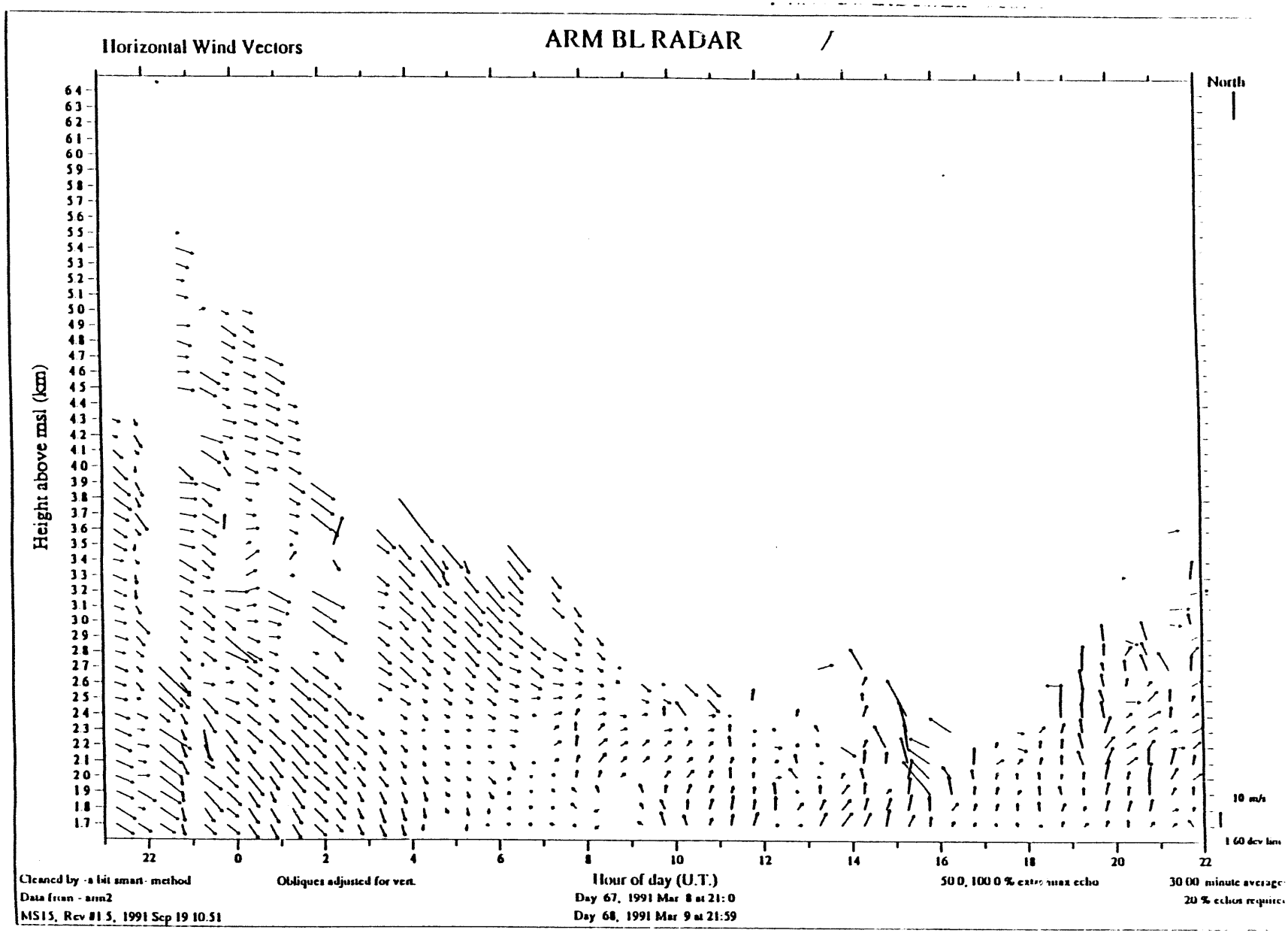


Figure B44. Time-height display of horizontal wind vectors measured by the boundary layer 915 MHz wind profiler at Platteville for IOP-5. The speed scale is shown at the lower right corner. Time increases toward the right.

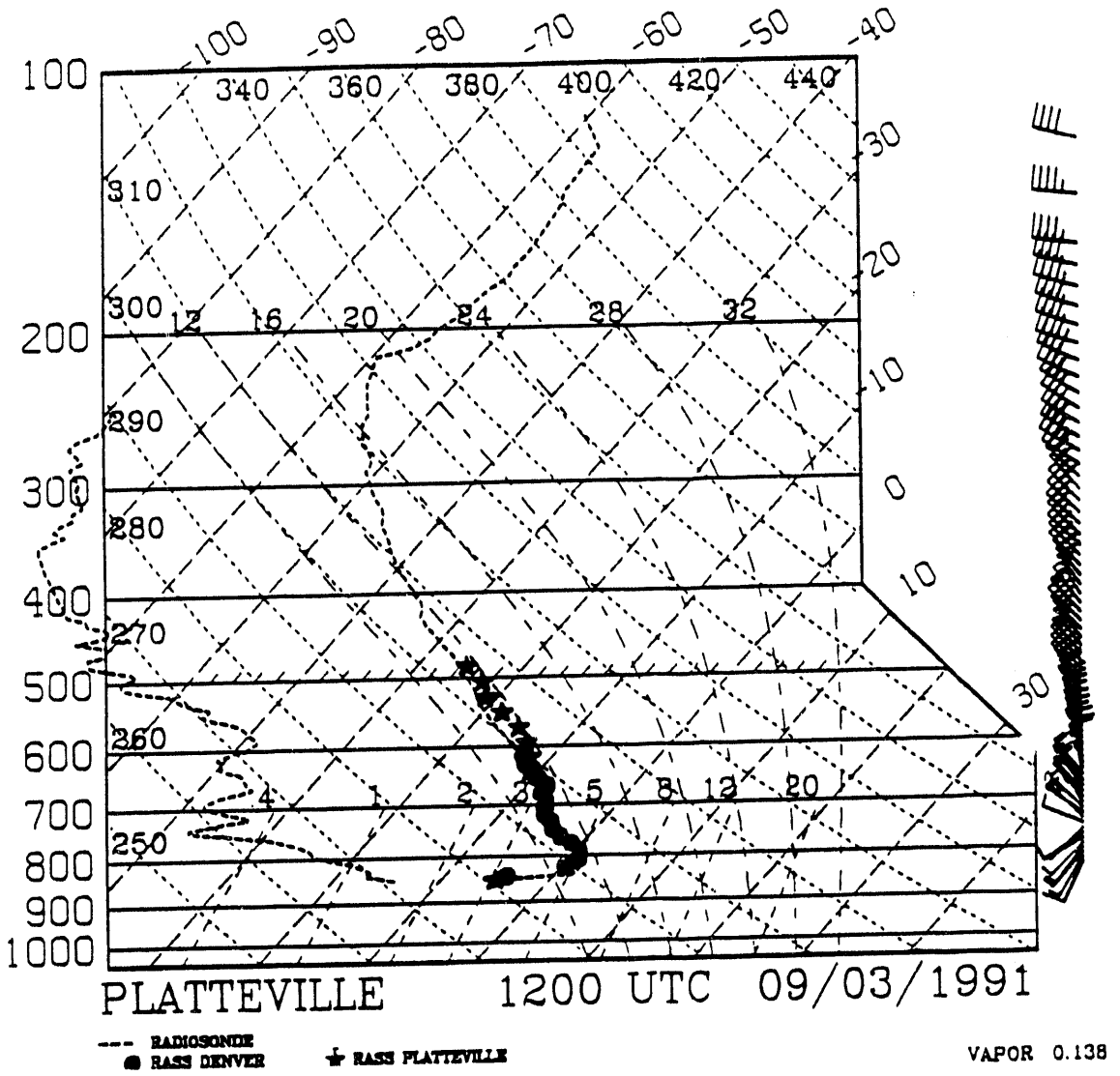


Figure B45. Temperature profiles measured by the 915 MHz RASS at Denver (solid dots) and 50 MHz RASS at Platteville (stars) for IOP-5. CLASS rawinsonde temperature and dewpoint data from Platteville are shown by the heavy dashed lines.

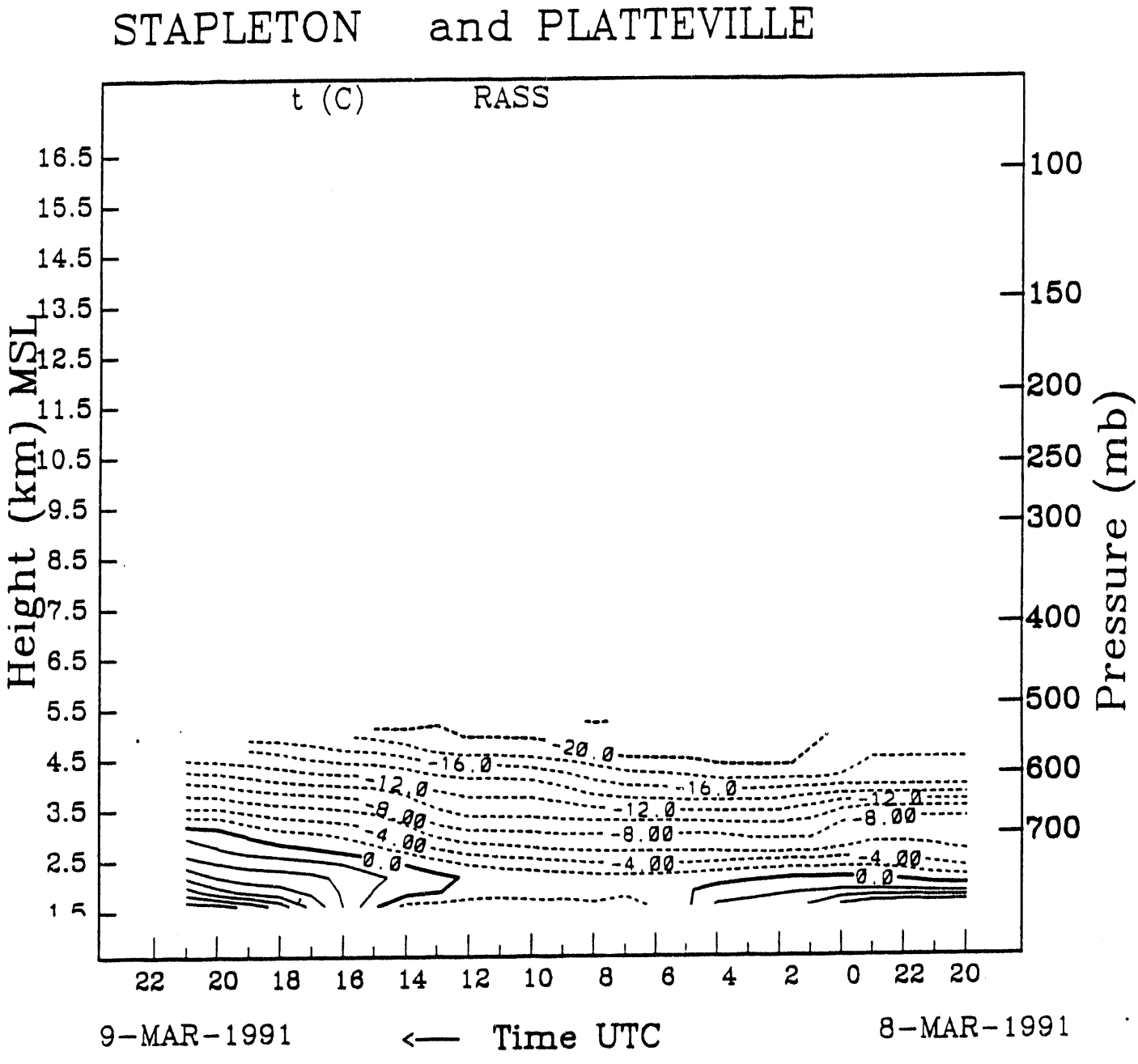


Figure B47. Time-height cross section of temperature from composite of RASS measurements at Denver and Platteville and using Denver surface temperature data during IOP-5. Temperatures above freezing are shown with solid isotherms and those below freezing have dashed isotherms.

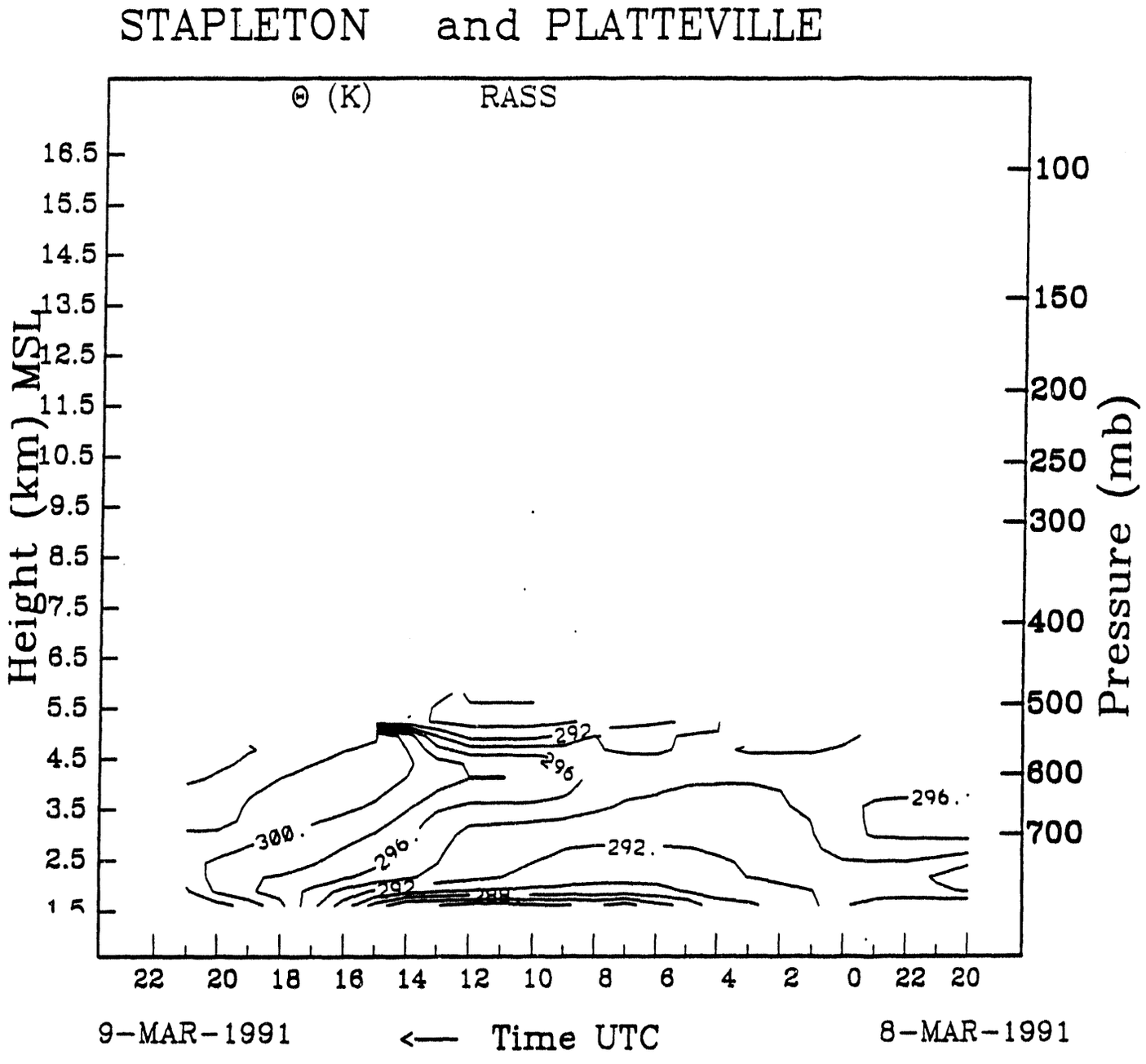


Figure B48. Time-height cross section of potential temperature derived from the RASS temperature data of the previous figure.

# END

# DATE FILMED

11/30/93